JYVÄSKYLÄ STUDIES IN BIOLOGICAL AND ENVIRONMENTAL SCIENCE
211

Satu Pekkala

Functional Characterization of Carbamoyl Phosphate Synthetase I Deficiency and Identification of the Binding Site for Enzyme Activator

JYVÄSKYLÄN YLIOPISTO

JYVÄSKYLÄ STUDIES IN BIOLOGICAL AND ENVIRONMENTAL SCIENCE 211

Satu Pekkala

Functional Characterization of Carbamoyl Phosphate Synthetase I Deficiency and Identification of the Binding Site for Enzyme Activator

Esitetään Jyväskylän yliopiston matemaattis-luonnontieteellisen tiedekunnan suostumuksella
julkisesti tarkastettavaksi Jyväskylän yliopiston Ylistönrinteellä salissa YAA303
elokuun 13. päivänä 2010 kello 12.

Academic dissertation to be publicly discussed, by permission of
the Faculty of Mathematics and Science of the University of Jyväskylä,
in Ylistönrinne, hall YAA303 on August 13, 2010 at 12 o'clock noon.

UNIVERSITY OF JYVÄSKYLÄ

JYVÄSKYLÄ 2010

Functional Characterization of Carbamoyl Phosphate Synthetase I Deficiency and Identification of the Binding Site for Enzyme Activator

JYVÄSKYLÄ STUDIES IN BIOLOGICAL AND ENVIRONMENTAL SCIENCE 211

Satu Pekkala

Functional Characterization of Carbamoyl Phosphate Synthetase I Deficiency and Identification of the Binding Site for Enzyme Activator

UNIVERSITY OF JYVÄSKYLÄ

JYVÄSKYLÄ 2010

Editors
Varpu Marjomäki
Department of Biological and Environmental Science
Pekka Olsbo, Sini Rainivaara
Publishing Unit, University Library of Jyväskylä

Jyväskylä Studies in Biological and Environmental Science

Cover picture by Satu Pekkala

URN:ISBN:978-951-39-8045-0
ISBN 978-951-39-8045-0 (PDF)
ISSN 1456-9701

ISBN 978-951-39-3946-5
ISSN 1456-9701

Jyväskylä University Printing House, Jyväskylä 2010

ABSTRACT

Pekkala, Satu
Functional characterization of carbamoyl phosphate synthetase I deficiency and identification of the binding site for enzyme activator
Jyväskylä: University of Jyväskylä
(Jyväskylä Studies in Biological and Environmental Science,
ISSN 1456-9701; 211)
ISBN 978-951-39-3946-5
Yhteenveto: Karbamyylifosfaatti syntetaasi I:n puutteen patologian toiminallinen karakterisaatio ja entsyymin aktivaattorin sitoutumiskohdan identifikaatio
Diss.

Carbamoyl phosphate synthetase I deficiency (CPSID), an autosomal, recessively inherited error of the urea cycle, causes life-threatening hyperammonemia. CPSI is a multidomain 1464-residue mitochondrial matrix protein of liver that synthesizes carbamoyl phosphate (CP) and is allosterically activated by N-acetyl-L-glutamate (NAG).

In this study, we have characterized the pathogenicity and the functional impact of eleven missense mutations of CPSI, which was done by producing the recombinant CPSI in insect cells, introducing the desired mutations to the protein by site-directed mutagenesis and by studying the effects of mutations on the stability and function of CPSI. Four mutations completely abolished CP synthesis. All the remainder mutations except one, which corresponds to CPSI polymorphism, decreased CP synthesis and, in addition, two of them rendered the enzyme much less stable. The results validate the use of rat recombinant CPSI as a pathogenicity testing model for human CPSID, support the causality of the mutations, and identify the derangements caused by several of the mutated residues.

We have also identified the binding site for the enzyme activator, NAG. We selected various amino acid residues for mutagenesis basing on the known binding site of allosteric effectors of homologous CPS of *Escherichia coli* and produced the mutant enzyme forms in insect cells. Several of the mutated residues clearly affected the activation of CPSI by NAG and seem to be implicated in allosteric signal transmission too. The crystalline structure of a fragment of the CPSI regulatory domain also enabled the screening for the cavities within the structure and docking of NAG into the structure.

Keywords: Carbamoyl phosphate synthetase I (CPSI); CPSI deficiency (CPSID); N-acetyl-L-glutamate (NAG); site-directed mutagenesis.

Satu Pekkala, University of Jyväskylä, Department of Biological and Environmental Science, P.O. Box 35, FI-40014 University of Jyväskylä, Finland

Author's address Satu Pekkala
Centro de Investigación Príncipe Félipe
Avenida Autopista del Saler 16
46013 Valencia, Spain
satupekkala@yahoo.com

Supervisors Doctor Javier Cervera
Centro de Investigación Príncipe Félipe
Avenida Autopista del Saler 16
46013 Valencia, Spain

Professor Jaana Bamford
Departement of Biological and Environmental Science
P.O. Box 35
FI-40014 University of Jyväskylä
Jyväskylä, Finland

Reviewers Dosent Tomi Airenne
Abo Akademi, Department of Biosciences and Biochemistry
Biocity, Tykistönkatu 6
FI-20520 Turku, Finland

Professor Kari Keinänen
Department of Biosciences
Division of Biochemistry
P.O. Box 56
FI-00014 University of Helsinki
Helsinki, Finland

Opponent Professor Markku Kulomaa
Institute of Medical Technology
University of Tampere
Biokatu 6
FI-33014 University of Tampere
Tampere, Finland

CONTENTS

LIST OF ORIGINAL PUBLICATIONS

The thesis is based on the following original papers, which will be referred to in the text by their Roman numerals I-III. In addition, some unpublished results are presented.

I was responsible for setting up the insect cell expression and production system for CPSI used in all the original papers. I also performed completely the characterization of the recombinant protein and its comparison with the native CPSI from rat liver.

The greatest part of the site-directed mutagenesis of the present study was made by me, but Dr. Igor Yefimenko (at present in CNIO, Madrid, Spain) helped me with two of the mutants, which he also produced leaving the production of the rest of the mutants as my responsibility.

I performed all the characterization of the mutant enzyme forms with the aid of Dr. Ana Martinez (Centro de Investigación Príncipe Félipe, Valencia, Spain). I participated in protein modeling and docking experiments, which were done by more experienced Dr. Belen Barcelona and Dr. José Gallego (Centro de Investigación Príncipe Félipe, Valencia, Spain).

I made or adapted all the figures and tables of this thesis. I wrote the original articles together with Dr. Javier Cervera and Dr. Vicente Rubio.

I Pekkala, S., Martinez, A. I., Barcelona, B., Gallego, J., Bendala, E., Yefimenko, I., Rubio, V. & Cervera, J. 2009. Structural insight on the control of urea synthesis: identification of the binding site for N-acetyl-L-glutamate, the essential allosteric activator of mitochondrial carbamoyl phosphate synthetase. Biochemical Journal 424, 211-220.

II Pekkala, S., Martinez, A. I., Barcelona, B., Yefimenko, I., Finckh, U., Rubio, V., Cervera, J. 2010. Understanding carbamoyl-phosphate synthetase I (CPS1) deficiency by using expression studies and structure-based analysis. Human Mutation 31(7): 801–808.

III Pekkala, S., Martinez, A. I., Barcelona, B. & Cervera, J. 2010. Towards understanding of allosteric signal transmission in carbamoylphosphate synthetase I. Manuscript.

ABBREVIATIONS

3-D	three dimensional
ADP	adenosine diphosphate
AMPPNP	5'-adenylyl-beta, gamma-imidodiphosphate
ATP	adenosine triphosphate
CAD	multienzymatic complex formed by carbamoyl phosphate synthetase II, aspartate transcarbamoylase and dihydroorotase
ClNAG	chloro-acetylglutamate
CP	carbamoyl phosphate
CPS	carbamoyl phosphate synthetase
CPSI	carbamoyl phosphate synthetase I
CPSID	carbamoyl phosphate synthetase I deficiency
DMSO	dimethyl sulfoxide
DTT	dithiotreitol
IMP	inosine monophosphate
K_a	activation constant
K_d	dissociation constant
K_m	affinity constant (Michaelis-Menten)
kDa	kilodalton
m.o.i	multiplicity of infection
MGS	methylglyoxyl synthase
NAβpheG	N-acetyl-β-phenylglutamate
NAG	N-acetyl-L-glutamate
NAGS	N-acetyl-L-glutamate synthase
NADH	nicotinamide adenine dinucleotide hydroxyl
NADP	nicotinamide adinine dinucleotide phosphate
NO	nitric oxide
ORN	ornithine
OTC	ornithine transcarbamoylase
PBS	phosphate-buffered saline
PrPP	phosphoribosyl pyrophosphate
SDS-Page	sodium dodecyl sulfate polyacrylamide gel electrophoresis
Sf	*Spodoptera frugiperda*
UDP	uridine diphosphate
UMP	uridine monophosphate
UTP	uridinetriphosphate

1 INTRODUCTION

Carbamoyl phosphate synthetases (CPS) are enzymes that catalyze one of the most remarkable biochemical reaction, which is the formation of carbamoylphosphate (CP) from two molecules of ATP, bicarbonate and either glutamine or ammonia (Jones & Lipmann 1960, Meister 1989). The CP formed in the reaction can be destined to the biosynthesis of pyrimidines or to produce arginine and/or urea. The CPS family includes prokaryotic CPS, which in the case of *E. coli* is a single protein functioning in both biosynthetic routes mentioned above; two eukaryotic CPS: cytosolic CPSII that is responsible of *de novo* production of pyrimidines, and mitochondrial CPSI, the rate-limiting enzyme that catalyzes the first committed step of the urea cycle and the subject of this study; and CPSIII, which is an evolutionary intermediate between the prokaryotic CPS and the CPSI of higher organisms.

The urea cycle, located mostly in the mitochondria of hepatocytes, involves a series of biochemical steps in which waste nitrogen produced by protein metabolism, is removed from the blood and converted to urea. Normally, the urea is transferred into the urine and removed from the body. In urea cycle disorders, the nitrogen accumulates in the form of ammonia, a highly toxic substance, which is not removed from the body resulting in hyperammonemia, encephalopathy and respiratory alkalosis (Brusilow & Horwich 2001). Urea cycle disorders are included in the category of inborn errors of metabolism. Because many cases of urea cycle disorders remain undiagnosed and/or infants born with the disorders die without a definitive diagnosis, the exact incidence of these cases is unknown and underestimated. For CPSI deficiency it has been estimated to be for example 1/62000 in USA (Brusilow & Maestri 1996), and 1/539000 in Finland (Keskinen et al. 2008).

The diagnosis of a urea cycle disorder is based on the evaluation of clinical, biochemical, and molecular data, which some times can be misleading since different metabolic diseases can cause similar symptoms, or the molecular mutational data can be confounded with normally existing genetic

polymorphisms (Summar et al. 2003). It is therefore important to have other systems to specifically characterize and functionally test the disease-causing agents, such as missense mutations.

The only known 3-D structures of the CPS family are that of *Escherichia coli* (PDB 1jdb) and the 20 kDa C-terminal domain of human CPSI (PDB 2yvq) produced in a cell-free sytem. The binding site of the very essential allosteric activator of CPSI, N-acetyl-L-glutamate (NAG), has remained unknown, while the allosteric site of bacterial CPS is well characterized. Thus, we undertook the challenge to express and characterize recombinant CPSI, and finally succeeded in the task by using baculovirus expression system and Sf9 insect cells and identified the binding site for the enzyme activator.

In this doctoral thesis, the CPS protein family is reviewed by means of their function, structure and regulation. Then the urea cycle and its disorders are described focusing mainly on the CPSI deficiency. We produced mutant forms of CPSI bearing specific mutations that have been detected in patients with CPSI deficiency and studied the effects of the mutations on the protein. We evaluated the recombinant expression system as a suitable method to confirm the pathogenicity of the clinical mutations of patients with CPSI deficiency. One of the main aims was also to identify the binding site for NAG basing on the known allosteric site of CPS of *E. coli*, design and produce mutant forms of CPSI and study their effects on the activation of the enzyme by NAG. We also identified a cavity in the crystal structure of the C-terminal domain of CPSI that can accommodate a NAG molecule, a result, which is in accordance with the CPSI mutant activity studies.

In addition, we produced and analyzed mutant CPSI forms, which were assumed to have the transmission of the allosteric signal perturbed. Finally, we constructed a 3-D molecular model of CPSI to better interpret the results of the enzyme activity studies.

2 REVIEW OF THE LITERATURE

2.1 Carbamoyl phosphate synthetases

The carbamoyl phosphate synthetases (CPSs) are enzymes that catalyze the formation of carbamoyl phosphate and, depending on the organism and their function, use either ammonia or glutamine as the source of nitrogen, and always bicarbonate and two molecules of ATP (Jones & Lipmann 1960, Anderson & Meister 1965, 1966, Ratner 1973). The final product of the reaction, carbamoyl phosphate (CP), can be destined to two separate biosynthetic routes. CP can react with aspartate in the reaction catalyzed by aspartate transcarbamoylase for the subsequent *de novo* synthesis of pyrimidines, or it can react with ornithine, the reaction being catalyzed by ornithine transcarbamoylase. Citrulline formed in the reaction can be used for the synthesis of both arginine and/or urea.

In the eukaryotic systems there are two distinct forms of CPS. The mitochondrial CPSI participates in both arginine biosynthesis and the urea cycle and is the rate-limiting enzyme that catalyzes the first committed step of the urea cycle, which is responsible for the removal of waste nitrogen produced by protein metabolism. CPSI is mainly expressed in liver cells of ureotelic species and in small amounts in the epithelial cells of the small intestine (Christoffels et al. 2000). Tissue-specificity of *CPS1* gene expression is achieved because of a specific hormone-dependent far-upstream enhancer (Christoffels et al 1995, 1996, 2000). However, an isoform of CPSI (Gene Bank AY317138) has been found to be highly expressed in human testis and probably serves for high arginine requirement during the spermiogenic process. This isoform is produced as splicing variant from *CPS1* gene. In a contrary to liver CPSI with 1464 amino acids, the putative protein contains 1049 amino acid residues and lacks the N-terminal domain (Huo et al 2005).

A cytosolic species, CPSII, is involved in pyrimidine biosynthesis. CPSII occurs as large multienzymatic complex along with aspartate transcarbamoylase and dihydroorotase (Coleman et al. 1977, Jones 1980) and is

expressed in all type of cells and tissues. The mitochondrial and cytosolic forms require free ammonia and glutamine, respectively, as nitrogen donoring substrates. *E. coli* employs only one dual CPS for both metabolic pathways and this molecular species utilizes glutamine as the source of nitrogen (Meister 1989). Bacilli resemble more the eukaryotes in producing two carbamoyl phosphate synthetases, one for arginine biosynthesis and the other for pyrimidine production (Paulus & Switzer 1979).

The prokaryotic CPS is a heterodimer composed of 40 kDa small subunit and 120 kDa large subunit that are encoded by two different genes, *carA* and *carB*, respectively (Mergeay et al. 1974). In the ureotelic CPSI these two domains are fused resulting in a 160 kDa large polypeptide. As is the case for many mitochondrial proteins that are encoded by nuclear genes, CPSI is synthesized as a precursor 5000-6000 daltons larger than the final product. The precursor protein has a mitochondrial targeting signal peptide, which after the transport to the mitochondria is cleaved by specific proteolysis and the remaining protein is called the mature CPSI (Nguyen et al. 1986).

The third major group of carbamoyl phosphate synthetases, CPSIII, utilizes the amide group of glutamine as the nitrogen-donating substrate like CPSII. These CPSs are found in invertebrates (Trammel & Campbell 1970, 1971) and in some fish species (Anderson 1976, 1980, Mommsen & Walsh 1989). The properties of CPSIII are very similar to those of CPSI since it is NAG-dependent, and ammonia at high and non-physiological concentrations can replace glutamine as the nitrogen-donoring substrate. Alignment of amino acid sequences of CPSIII with rat and frog CPSI and hamster CPSII shows that CPSIII is more closely related to CPSI, and uncovers that CPSIII found in invertebrates and fish species represents an intermediate in evolution of ancestral glutamine-dependent CPSII toward the ammonia-dependent CPSI in ureotelic vertebrates (Hong et al. 1994). However, all the CPS are able to use ammonia as substrate to catalyze the formation of CP, though their affinity for ammonia varies.

2.1.1 The stages of the CPS reaction

The reaction of the synthesis of CP from the substrates bicarbonate, ATP-Mg^{2+} and ammonia is conducted in three stages. The first step of the reaction is the phosphorylation of bicarbonate by ATP [1] that generates carboxyphosphate, a very unstable molecule. In the second step ammonia conducts a nucleophilic attack on the carboxyphosphate intermediate to yield carbamate, which is even more unstable [2]. In the ensuing final step carbamate is phosphorylated by ATP to synthesize carbamoyl phosphate [3]. The overall reactions is simplified as follows: Glutamine (ammonia) + 2ATP + bicarbonate → ADP + CP + Pi + glutamate. A schematic presentation of carbamoyl phosphate synthesis is shown in Fig. 1.

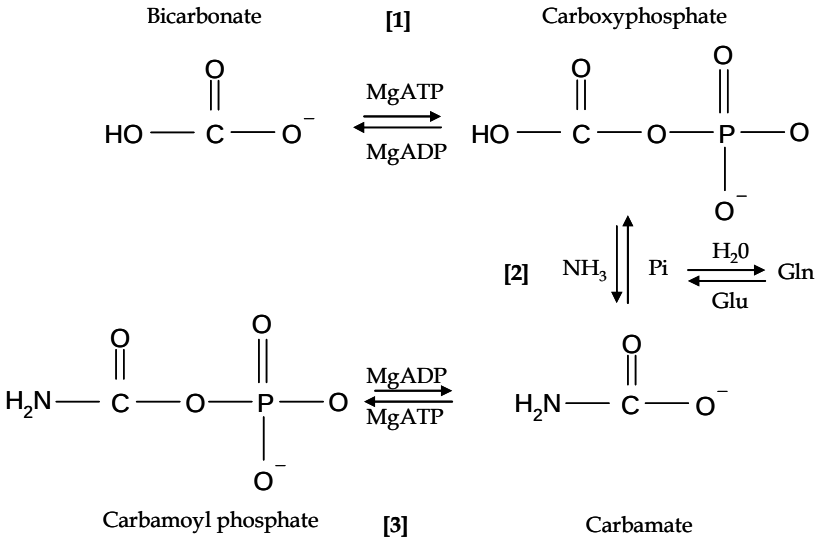

FIGURE 1 Global reaction (formation of carbamoyl phosphate) catalyzed by carbamoyl phosphate synthetases.

All the CPS require Mg^{2+} and K^{+} ions for their activity. The two ATP molecules used in the phosphorylation steps bind to different sites of the enzyme: ATP_A that phosphorylates bicarbonate [1] and ATP_B, which is utilized to phosphorylate carbamate [3] (Rubio & Grisolia 1977, Rubio et al. 1979, Britton et al. 1979, Post et al. 1990, Alonso et al. 1992). In addition to the global reaction described above, CPS can catalyze two partial reactions that reflect the two phosphorylation steps (Jones 1976, Rubio 1993). In the absence of ammonia (or glutamine) the enzyme presents bicarbonate-dependent ATPase activity as a result of the phosphorylation of bicarbonate [1]. In the presence of ADP and CP the enzyme catalyzes synthesis of ATP, which is the reverse of the third step.

2.1.2 Structural types of carbamoyl phosphate synthetases and domain organization

All the CPS share a basic structure of domains and they are very similar on their sequences (Simmer et al. 1990). Different domains are implicated in different stages of the catalysis, and limited proteolysis studies have shown that all the CPS are organized in the same domain structure (Powers-Lee & Corina 1986, Guadalajara et al. 1987, Evans & Balon 1988, Rubio et al. 1991, Mareya & Raushel 1995). Table 1 presents the different structural types of carbamoyl phosphate synthetases.

Three types of CPS enzymes have been reported based on the nitrogen-donating substrate (ammonia or glutamine) and the requirement or not for the allosteric activator NAG. CPSI, which utilizes excusively ammonia, is found in ureotelic vertebrates while CPSIII, which uses preferentially glutamine, is present in invertebrates (Trammel & Campbell 1970, 1971) and fish species (Anderson 1976, 1980, Mommsen & Walsh 1989). CPSII, which uses

preferentially glutamine, can be classified in four groups according to structural characteristics, the organism in which it is present and its allosteric regulation. The first group appears in most prokaryotes and produces CP for both arginine and pyrimidines biosynthetic routes. The second group can be found in fungi and the genus *Bacillus* and synthesizes only arginine. Finally, fungi and superior eukaryotes have a specific CPS devoted to pyrimidine biosynthesis, which form the third and fourth groups of CPSII, respectively.

TABLE 1 The structural types of the carbamoyl phosphate synthetases. In the second column (+) means activator and (-) means inhibitor.

CLASS ROUTE	ALLOSTERIC EFFECTOR	GLUTAMINASE AND SYNTHETASE DOMAINS	ORGANISM
CPSI Urea& Arginine	NAG (+)	Fused	Ureotelic vertebrates
CPSII Arginine& Pyrimidines	Orn & IMP (+) UMP (-)	Separated	Most prokaryotes
Arginine	None	Separated	Fungi and bacillus
Pyrimidines	UTP (-)	Fused/bifunctional	Fungi
Pyrimidines	PRPP (+), UTP (+)	Fused/multifunctional	Superior eukaryotes
CPSIII Urea& Arginine	NAG (+)	Fused	Invertebrates & Fishes

Domain organization of CPS is presented in Fig. 2. *E. coli* CPS is constituted of two subunits: the large subunit of 120 kDa bearing the CPS activity, and the small subunit of 40 kDa employed in the hydrolysis of glutamine (Trotta et al. 1971). Thus, the small subunit carries the binding site for glutamine and its glutaminase activity generates ammonia, which is channeled towards the large subunit. The CPS of *E. coli* can also use external ammonia as nitrogen source though with less affinity compared to glutamine (Anderson & Meister 1965, Kalman et al. 1966) due to the structural changes in the small subunit produced by glutamine binding. Upon glutamine binding the enzyme adapt a catalytically active conformation in which access to the ammonia site is restricted (Guy et al. 1997 a, b).

In mammalian CPSI and in CPSIII the small and large subunits are fused due to an evolutionary change. The two genes coding for the subunits of bacterial enzyme have undergone a fusion event in *CPS1,* and further on CPSI has lost the glutaminase activity by a subsequent mutation in the

amidotransferase domain (Nunoya et al. 1985). The 120 kDa CPS domain is composed of two homologous halves of 60 kDa each one responsible of one of the steps of phosphorylation. The homologous halves have been formed by a duplication and tandem-fusion of one ancestral gene (Nunoya & Lusty 1983).

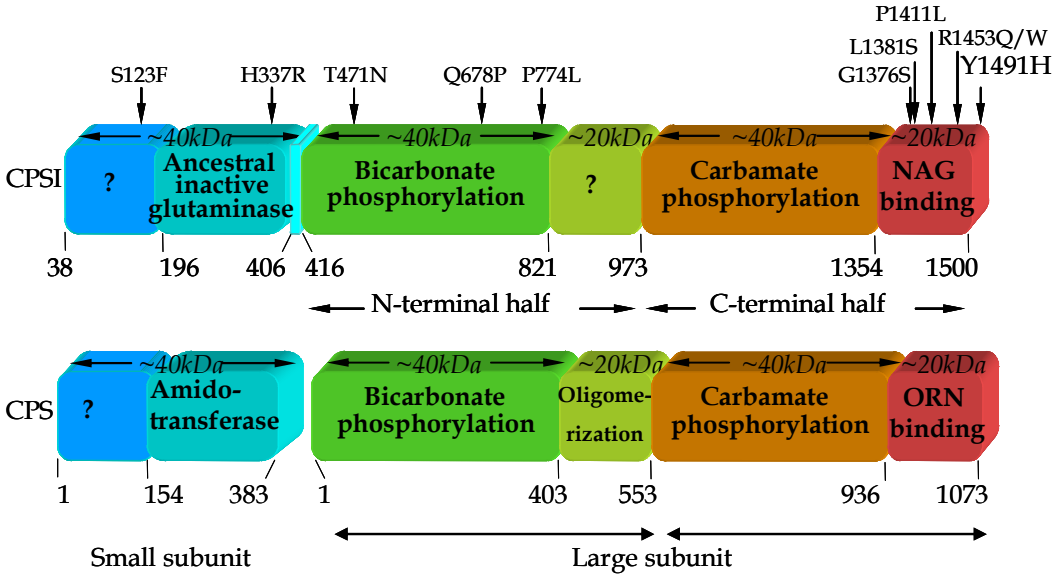

FIGURE 2 Simplified presentation of the domains of CPSI and *E. coli* CPS. Clinical mutations (Publication II) are mapped at their respective sites. All the mutations studied in Publication I fall at the regulatory domain.

2.1.3 Function of the domains of carbamoyl phosphate synthetases

The small subunit of CPS is known to bind and hydrolyze glutamine. When the enzyme is treated with 1 M potassium thiocyanate, it is reversibly dissociated into its subunits (small and large) that retain catalytic activity (Meister 1989). Early studies of site-directed mutagenesis of *E. coli* CPS revealed the catalytic role of cysteine 269 lying on the glutaminase domain (Rubino et al. 1986). Later other mutagenetic studies established that the catalytic triad is Cys269, His353 and Glu355 (Gaillard. et al 1991, Mareya & Raushel 1994, Thoden et al. 1998). If the aminoterminal third of the glutaminase subunit is deleted in CPS of *E. coli* the interactions with the carbamoyl phosphate domain are abolished, suggesting that this subdomain functions in stabilizing the complex (Guillou et al. 1989).

The glutaminase domain of CPS is homologic to *trpG* type of amidotransferases (Zalkin & Smith 1998), which have the catalytic triad Cys-His-Glu characteristic to this protein family (Rubino et al. 1986, Chaparian & Evans 1991, Miran et al. 1991). Amidotransferases, such as anthranilate synthase, GMP synthase and CTP synthase are known to channel substrates from one active site to another (Huang et al. 2001). These enzymes hydrolyze glutamine in the N-terminal domain and then transfer the ammonia product to another site through an intramolecular tunnel. Now the crystal structure of many amidotransferase-family proteins has been solved. Structural information

shave shown how flexible loops of the synthase and glutaminase domains move to shield the two catalytic sites and how the ammonia channel forms, opens and closes (Mouilleron & Golinelli-Pimpaneau 2007).

Mammalian CPSI does not have the catalytic triad at the 40 kDa N-terminal domain and thus is unable to hydrolyze glutamine. The reactive cysteine 269 has changed to serine. Interestingly, although the CPSI of frog (*Rana cateisbeiana*) harbor the triad it does not exhibit glutaminase activity (Helbing & Atkinson 1994, Saeed-Koethe & Powers-Lee 2002). A gain of glutaminase function in CPSI of frog can be achieved mutating a single amino acid in the N-terminal domain (Lys258) (Saeed-Koethe & Powers-Lee 2003). In accordance with the statement of the authors, in glutamine-utilizing *E. coli* CPS the equivalent residue is leucine, and when mutated to lysine, the enzyme is prevented from using glutamine as a substrate (Saaed-Koethe & Powers-Lee 2002). The function of this N-terminal domain in CPSI is not known, but it may have a role in intermolecular interactions and in the correct folding of the protein (Marshall & Fahien 1988). In addition, if the N-terminal domain is completely deleted from human CPSI, the enzyme is not able to fully assume the catalytically competent conformation and produces CP 700-fold less (Ahuja & Powers-Lee 2008). This is different from the effect that elimination of the N-terminal domain produces on glutamine-utilizing CPSs since the formation of CP remains normal using ammonia as the nitrogen source (Powers & Meister 1978, Lim & Powers-Lee 1996).

The synthetase domain bears the two sites of phosphorylation, which was initially proposed basing on the internal sequence homology (Nunoya & Lusty 1983). The location of the ATP subsites was first demonstrated by direct photoaffinity labelling of CPSI with ATP (Potter & Powers-Lee 1993, Alonso & Rubio 1995) and later the sites were confirmed by site-directed mutagenesis studies (Post et al. 1990, Miles et al. 1993, Javid-Majd et al. 1996, Stapleton et al. 1996). These studies corroborated that the first half of the CPS domain (carboxyphosphate domain) phosphorylates bicarbonate and the second half (carbamoyl phosphate domain) carbamate. Finally, the exact binding sites of the two ATP-molecules were solved when CPS of *E. coli* was crystallized in the presence of ADP (Thoden et al. 1997), and afterwards in the presence of AMPPNP, a non-hydrolyzable analogue of ATP (Thoden et al. 1999b). Though the synthetic components are homologous, the carbamoyl phosphate domain could not perform the function of the carboxyphosphate domain, and *vice versa* (Thoden et al. 1997).

The most C-terminal 20 kDa part of the synthetase domain is called regulatory domain. This domain binds the effector molecules, which control the activity and modify the affinity of the enzyme for ATP and other substrates (Rubio et al. 1983, Meister 1989, Liu et al. 1994). The activator N-acetyl-L-glutamate (NAG) is required for the activity of mitochondrial CPSI and CPSIII (Grisolia & Cohen 1948, Hall et al. 1958, Julsrud 1998). CPSII of CAD is phosphorylated by a specific kinase that reverses the inhibitory effect of UTP (Carrey et al. 1985). Finally, the regulatory domain of CPS of *Escherichia coli* is

implicated in the binding of ornithine, IMP and UMP (Rubio et al. 1991, Cervera et al. 1993, Bueso et al. 1994, Cervera et a. 1996, Fresquet et al. 2000).

2.1.4 3-D structure of carbamoyl phosphate synthetase

The crystal structure of CPS of *Escherichia coli* was first determined at 2.8 Å resolution from an ADP-ornithine-CPS complex (Thoden et al. 1997). Later on, other crystals were solved complexed with either AMPPNP, IMP, glutamine or UMP, and several mutant variants were also solved (PDB 1jdb, 1a9x, 1bxr, 1ce8, 1cs0, 1c30, 1m6v, 1t36) (Thoden et al. 1997, Thoden et al. 1998, Thoden et al. 1999a, Thoden et al. 1999b, Thoden et al. 1999c).

The 40 kDa small subunit of CPS (glutaminase domain) is bilobal and composed of four α-helices and two layers of β-sheet in the N-terminus. The C-terminal part is composed of ten-stranded β-sheet flanked on either side by two and three α-helices, respectively (Fig. 3). The active site consisting of Cys269-His353-Glu355 is located at the C-terminal end. The N- and C-terminal halves of the small subunit are connected by a hinge loop that is important in maintaining the proper interface interactions (Huang & Raushel 2000a).

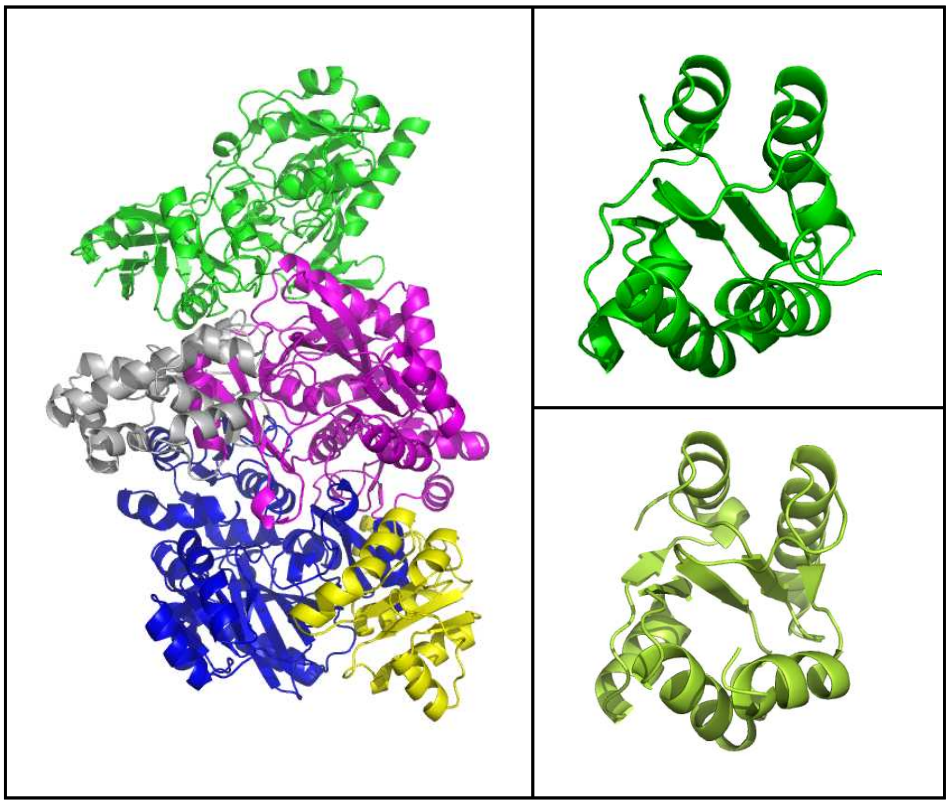

FIGURE 3 Structure of CPS. The left panel presents the 3-D structure of the *E. coli* CPS heterodimer: N-terminal small subunit is colored in green, carboxyphosphate domain in magenta, oligomerization domain in gray, carbamoylphosphate domain in blue and the 20 kDa C-terminal regulatory domain in yellow. On the right side of the figure are presented the regulatory domains of *E. coli* CPS (up) and human CPSI (down). Mapping of the different mutations performed in this thesis are shown in Publications I-III.

The 120 kDa large subunit has overall dimensions of 88x78x77 Å, and is folded into two similar halves corresponding to Met1-Ala553 (carboxyphosphate domain) and Asn554-Lys1073 (carbamoylphosphate domain) (Fig. 3). As it was previously proposed, these two homologous halves fold in a complementary isologue association (Cervera et al. 1993) (Fig. 3, the first half is colored in magenta and gray and the second half in blue and yellow). In addition, each component is divided in domains A, B, C and D. The first three domains are similar to those of biotin carboxylase that also utilizes ATP and bicarbonate as substrates (Climent & Rubio 1986, Ogita & Knowless 1988, Waldrop et al. 1994).

The first three domains of the carboxy- and carbamoylphosphate synthetic components of *E. coli* CPS are very similar, but the D-domain is completely different (Thoden et al. 1997). The A-domain consists of a five stranded of β-sheet flanked by α-helices that are followed by a helix-turn-helix motif leading to the B-domain. The B-domain is a four-stranded antiparallel β-sheet covered by two α-helices. The structure of the C-domain is the most complicated and consists of an antiparallel β-sheet of five strands and four helical regions. The carbamoylphosphate active site is more open respect to the carboxyphosphate active site, which is logical since the very unstable carboxyphosphate generated during the synthesis must not leave the interior of the protein. The D-domain of the carboxyphosphate synthetic component has two lobular units, each built from three short α-helices connected by a longer α-helix. The D-domain of carbamoylphosphate synthetic component, in turn, consists of a five stranded, parallel β-sheet and of five α-helices, which form, a modified Rossmann fold, and thus, is very similar to the A domains. In the *E. coli* carboxyphosphate domain there are 19 amino acids that interact with the small subunit. Despite of being very similar the two synthetic components share out of these 19 residues only four (Thoden et al. 1999a). In addition, most of the tunnel-forming amino acids of the two synthetic components differ from each other (Thoden et al. 1997).

The first evidence for the existence of the intramolecular tunnel came from the crystallized CPS of *E. coli* (Thoden et al. 1997). The reactive cysteine at the N-terminal domain was 45 Å from the ADP bound in the carboxyphosphate active site, which in turn was 35 Å from the ADP at the carbamoyl phosphate synthetic component. From the distances it was evident that the reaction intermediates must travel somehow in the protein interior without touching the solvent. Finally, the 100 Å long tunnel was detected in the resolution of the crystal (Thoden et al. 1999, Mullins & Raushel 1999), and the critical amino acids belonging to the ammonia tunnel have been determined by site-directed mutagenesis studies (Huang & Raushel 2000b, Kim & Raushel 2004), and by crystallization of the CPS mutant G359F, in which the delivery of ammonia was impeded (Thoden et al. 2002). The transfer of ammonia through the tunnel has also been demonstrated by combined theoretical and molecular dynamics simulations (Fan et al. 1998, 1999). Almost all the enzymes that belong to the amidotransferase family use intramolecular tunnels to channel ammonia from

the site of its generation to the site of its utilization (Hyde et al. 1988, Krahn et al. 1997, Mullins & Raushel 1999, Anderson 1999, Raushel et al. 1999, Vanoni & The passage of carbamate through the carbamate tunnel where it is phosphorylated by the second molecule of ATP has been assessed by site-directed structural blockages of the putative tunnel forming residues and by molecular dynamics (Kim et al. 2002a, Lund et al. 2010). The tunnel is capped at each end by ATP-binding residues Arg306 and Arg848 (Thoden et al. 1999, Kim & Raushel 2004).

When the structure of CPS was determined at 2.1 Å resolution (PDB 1a9x) also the allosteric D-domain of the enzyme was described in more detail (Thoden et al. 1999a). As mentioned, the core is a modified Rossmann fold: a five-stranded parallel β-sheet flanked on each side by two and three α-helices, respectively. Each of the α-helices ends in a type I turn, and in addition, there are two additional type I turns that correspond to Lys993-Glu996 and Asp1057-Glu1060.

In the crystal structures of CPS, in the presence of ornithine and IMP, the enzyme is tetramer in which contacts exist between the regulatory domains of each pair of enzyme molecules, involving residues near the binding site for the effector nucleotides (Thoden et al. 1999a, b). Additional intermolecular contacts are provided by hydrophobic residues of the oligomerization domain (Thoden et al. 1999a).

The entire structure of CPSI has not been determined though according to the amino acid sequence similarity between the mammalian and bacterial CPS it can be assumed that their structure is very similar. The structural similarity was confirmed when the crystal structure of a fragment of the regulatory domain of human CPSI was deposited in the Protein Data Bank (PDB) in 2008 (PDB file 2yvq, deposited by Xie, Ihsanawati, Kishishita, Murayama, TAkemoto, Shirozu, Yokoyama; RIKEN Structural Genomics/proteomics Iniative (RSGI).

2.1.5 Regulatory domain and binding of the allosteric effectors

The first data about the localization of the binding site of the effector of CPSI comes from limited proteolytic studies (Powers-Lee & Corina 1986, Guadalajara et al. 1987). NAG accelerates the digestion rate of CPSI by proteolytic enzymes. Afterwards direct measurement of NAG was carried out by Rodriguez-Aparicio et al (1989).

CPSI has an absolute requirement of NAG to adapt an active conformation. NAG (Fig. 4) is produced by NAG synthase (NAGS) from glutamate and acetyl-CoA (Caldovic & Tuchman 2003). The only known function of NAGS in mammalians is to provide NAG for CPSI activation. It seems that intramitochondrial concentration of NAG, in the short-term, is important for the control of ureagenesis via the NAG dependent activation of CPSI.

CPS of *E. coli* is activated by ornithine and IMP, and inhibited by UMP, which also bind to the 20 kDa regulatory domain of the enzyme. IMP and UMP

bind to overlapping sites (Boettcher & Meister 1982). The binding site of the monoculeotide effectors was first deduced from photoaffinity labeling and limited proteolysis experiments (Rubio et al. 1991), and afterwards by scanning calorimetric studies of truncated C-terminal mutants of CPS (Cervera et al. 1993). More exact binding site for the effectors was determined by photoaffinity labeling and site-directed mutagenesis (Bueso et al. 1999, Mora et al. 1999, Fresquet et al. 2000, Pierrat & Raushel 2002). In addition, these studies confirmed that the binding site for the activator IMP overlaps with that for the inhibitor UMP.

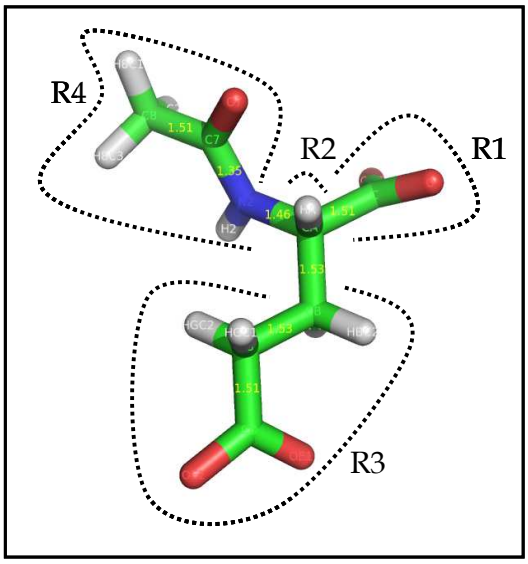

FIGURE 4 3-D structure of NAG. R1 corresponds to α-COO^-, R2 to a hydrogen atom, R3 to δ-COO^-, and R4 to the acetamide group.

Ornithine binds to the large subunit of bacterial CPS at the interface located between the allosteric and carbamoylphosphate domains (Thoden et al. 1999) (Fig. 5). Ornithine forms a hydrogen bond with T1042, which in turn interacts with Y1040. These residues start a network of interactions that lead to E761 thereby establishing a direct connection between the allosteric effector-binding region and the active site of the carbamoylphosphate domain. By site-directed mutagenesis it has been shown that the residues E783, T1042 and T1043 are primarily responsible for the binding of ornithine to CPS, while E783 and E892, located within the carbamoylphosphate domain are necessary for the transmission of the allosteric signal (Pierrat et al. 2002, Rochera et al. 2002).

The binding of the mononucleotides, IMP and UMP into CPS of *E. coli* occurs at different location as ornithine. In the crystal of ADP-Orn-CPS-complex, an inorganic phosphate is observed in the regulatory domain (Thoden et al. 1999a). The phosphoryl oxygens interact with the side chains of lysines 954 and 993 and of threonines 974 and 977. This phosphate could occupy the site of the phosphoryl groups of the mononucleotide effectors. Afterwards the enzyme was crystallized in the presence of IMP and in the complex the residues

that interact with the phosphate molecule also interact with IMP (Thoden et al. 1999b). CPS is known to discriminate between UMP and IMP, but curiously, the only direct contact between the hypoxanthine base of IMP and the protein is through V994 (Fig. 5). The IMP ribose form direct hydrogen bonds with the side chain groups of N1015 and L1017, and with the backbone of T1016. S1026 is thought to function in differentiating the mononucleotides (Pierrat & Raushel 2002) (Fig. 5).

More recently a crystal complex containing UMP and a mutant form of *E. coli* CPS was solved (Thoden et al. 2004). Except with V994, all the same interactions of the effectors with the proteins were observed for IMP and UMP. In addition, later an ensemble of residues involved in the binding of all the effector molecules, which were observed in the crystallized CPS, has been confirmed also by different site-directed mutagenesis studies of the corresponding residues (Delanney et al. 1999, Mora et al. 1999, Fresquet et al. 2002, Pierrat & Raushel 2002, Pierrat et al. 2002, Rochera et al. 2002).

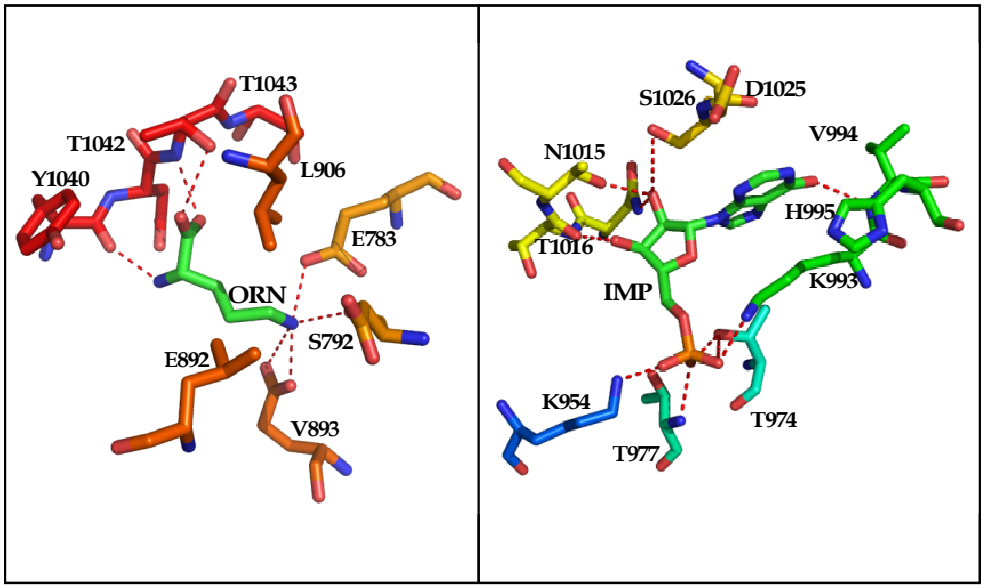

FIGURE 5 Binding site for the allosteric effectors of *E. coli CPS*. On the left side of the figure are presented the residues that are involved in the binding of the enzyme activator ornithine (ORN), and on the right side the residues that are involved in the binding of the mononucleotide activator IMP.

For CPSII (of CAD) the 20 kD C-terminal domain has also been identified as the regulatory domain, which was first demonstrated by construction of *E. coli*-hamster hybrid CPS. The hybrid was able to synthesize carbamoyl phosphate and bind the effectors of CPSII, PRPP and UTP, but was no longer regulated by the prokaryotic allosteric effectors (Liu et al. 1994). A more recent study has identified by site-directed mutagenesis a set of residues that are critical to the allosteric control of CAD. According to sequence alignments these residues are equivalent to *E. coli* T974, T977 and K993 (Simmons et al. 2004). K993 is a residue that has been shown to be important in *E. coli* for the regulation, and is

replaced by a hydrophilic glutamine in CPSII of at least two different kinetoplasts, *Trypanosoma cruzi* and *Leishmania Mexicana*. This replacement is in accordance with the fact that CPSII of kinetoplasts is inhibited by UDP (Nara et al. 1998).

The carbamoyl phosphate synthetase of *Saccharomyces cerevisae* is a 240 kDa large bifunctional protein that possesses CPS and ATC activities, which are feedback inhibited by the end product of the metabolic route, UTP. However, in this enzyme the allosteric site is presumably not located at the equivalent site as in *E. coli* CPS, as stated by enzymatic analysis of naturally existing mutant yeast strains (Jaquet et al. 1995, Serre et al. 2004).

The crystal structure of a fragment containing most of the regulatory domain of human CPSI (PDB 2yvq) is shared by the members of MGS-protein family (Murzin 1999) and composes the whole protein of *E. coli* methylglyoxal synthetase that has been crystallized (Saadat & Harrison 1999). The known structures in this family show a common phosphate binding site (Murzin 1999). The important threonines in *E. coli* MGS (T45 and T48) that interact with the phosphate correspond to T974 and T977 in the CPS of *E. coli*, and to the homologous threonines 1391 and 1394 in the CPSI of known sequence.

2.1.6 CPSI and regulation of metabolism

Mitochondria are one of the most important organelles of living cells since several biochemical pathways take place there. The mitochondrial inner membrane contains the carriers necessary for electron transfer of oxidative phosphorylation and ATP synthase. In the matrix can be found pyruvate dehydrogenase complex and enzymes of citric acid cycle, of fatty acid β-oxidation and of amino acid oxidation (Lehninger et al. 2005).

Since many pathways are interconnected they must be tightly regulated. First of all, oxidative phosphorylation is regulated by cellular energy needs. The relative concentrations of ATP and ADP control not only the rates of electron transfer and oxidative phosphorylation but also the rates of citric acids cycle, pyruvate oxidation and glycolysis (Lehninger et al. 2005). The activity of urea cycle, which functions in eliminating ammonia, is regulated at two levels. First, CPSI is allosterically activated by NAG, and second, during prolonged starvation and, thus, high protein catabolism, all the urea cycle enzymes are synthesized at higher rates.

Lately it has been discovered that all metabolic routes have common players in regulation. The sirtuin family of protein deacetylating enzymes act as metabolic sensors and contribute to the complex process of energy metabolism and aging in organisms. These sirtuin proteins with homology to yeast SIR2 are found in organisms ranging from bacteria to humans (Frye 2000, Guarente 2007). Unlike other classes of histone deacetylases sirtuins require NAD^+ as a substrate and they catalyze the removal of acetyl moiety from specific lysine residues within protein targets (Imai et al. 2000).

The least investigated of the sirtuin deacetylases is SIRT5, which biochemical activity and cellular functions have not been clearly determined.

SIRT5 is widely expressed with highest levels in brain, heart, liver and kidney (Nakagawa et al. 2009). Very recently it has been shown that SIRT5 is mitochondrial matrix deacetylase that deacetylates CPSI, which in fact is the only substrate for SIRT5 known by far (Nakagawa et al. 2009). Hepatic SIRT5 activity responds to the metabolic state of the organism, leading to increased deacetylation and thus activation of CPSI under calorie restriction conditions. This mechanism augments energy metabolism by using amino acids as alternative energy source (Hagopian et al. 2003). Amino acid catabolism leads to accumulation of toxic by-product, ammonia. SIRT5-dependent activation of CPSI enables efficient detoxification of ammonia through its incorporation to urea.

2.2 Urea cycle and associated disorders

The urea cycle, which takes place in the periportal hepatocytes (Gaasbeek Janzen et al. 1984), is the major route to excrete waste nitrogen in humans and other ureotelic organisms (Ratner 1973). Substrate availability is the main determinant of fast changes in the flux of the urea cycle, which, without delay, reacts to increases in the substrate concentration. Changes in the amount of the enzymes of the urea cycle or in their activities originate from changes in the dietary protein intake or catabolism of endogenous protein, mediated by insulin, glucagon and glucocorticoides (Lehninger et al. 2005). Deficiency of any of the five enzymes in the urea cycle results in the accumulation of ammonia and leads to encephalopathy. Most of the these disorders (N-acetylglutamate synthetase (NAGS) deficiency, carbamoyl phosphate synthetase deficiency, arginosuccinate synthase (ASS) deficiency, argininosuccinic acid lyase (ASL) deficiency, and arginase 1 (ARG1) deficiency) are inherited in an autosomal recessive fashion, whereas ornithine transcarbamoylase (OTC) deficiency is X-linked (Scaglia et al. 2004). The five enzymes composing the urea cycle and the connections links to other metabolic routes are presented in Fig. 6. All the disorders are mainly caused by specific mutations in the genes that encode the enzymes. The mutations cause the enzyme to be dysfunctional because of a mutation in the coding region or the final product can be too short due to an unwanted stop codon in the cDNA. Lately, at least for CPSI it has been shown that also a process called non-sense mediated RNA decay can be responsible for the deficiency of the enzyme in the patient (Eeds et al. 2006) since the RNA decay leads to the absence of the functional enzyme.

The clinical symptoms of the urea cycle disorders and the related disorders can be caused either by hyperammonemia or by other specific condition caused by an individual metabolic defect (Table 2). The actual clinical manifestations depend on the severity of the metabolic defect, the condition of the patient and include factors such as age, nutritional stage, other diseases, etc. (Endo et al. 2004). In general, the prognosis for urea cycle disorders presenting in the neonatal period is poor (Msall et al. 1984, Uchino et al. 1998).

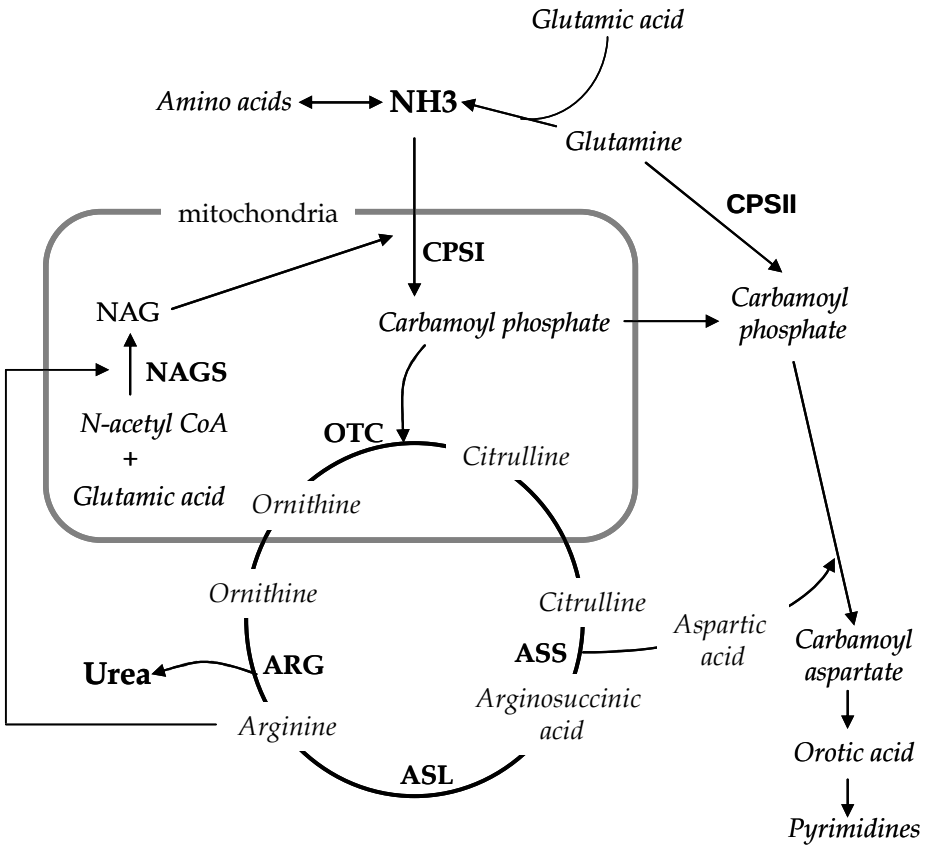

FIGURE 6 Schematic presentation of the urea cycle, the enzymes that participate in it and the intermediates and the final products of the cycle. NAG, N-acetyl-L-glutamate; NAGS, N-acetyl-L-glutamate synthetase; OTC, ornithine transcarbamoylase; CPSI, carbamoyl phosphate synthetase I; CPSII, carbamoyl phosphate synthetase II; ASS, arginosuccinate synthase; ASL, arginosuccinate lyase; ARG, arginase.

It is difficult to control hyperammonemia with standard treatments in newborn patients with severe urea cycle defects. Increase of the levels of urea cycle intermediates, such as arginine and citrulline, can increase the rate of urea production. Some new treatments have lately been proposed to improve the metabolic control, such as prevention of protein catabolism by intravenous glucose and alternative pathways for nitrogen excretion (Leonard et al. 2008). In some cases ammonia-scavenging drugs can be used based on the use of alternative pathways for disposal of waste (Scaglia et al. 2004). Some urea cycle disorders, such as NAGS deficiency and propionic aciduria, can be treated by administering Carbaglu®, a structural analog of NAG, which activates CPSI and thus antagonizes hyperammonemia (Morizono et al. 2004, Gebhardt et al. 2005). Lately, attempts to correct OTC deficiency in mice by gene therapy trials have been successful (Moscioni et al. 2006).

TABLE 2 Urea cycle and related disorders. The table is adapted from research article of Endo et al. (2004).

ABNORMALITIES OF METABOLISM			
Metabolic disorder	Excess metabolites	Reduced metabolites	Clinical features
CPSI deficiency	Ammonium, glutamate	Citrulline, arginine	------ ------
OTC deficiency	Ammonium, glutamate	Citrulline, arginine	------ ------
Citrullinemia	Ammonium	Arginine	------
Arginosuccinic aciduria	Ammonium, argino-succinic acid, citrulline	Arginine	Hepatomegaly
Arginemia	-----	-----	Spastic paraplegia
Adult onset citrullinemia type II	Ammonium, citrulline	Arginine	Liver damage
Hypeammonemia-hyperornithenemia-homocitrullinemia	Ammonium, ornithine homocitrulline	------	-----
Lysinuric protein intolerance	Ammonium	Lysine, arginine	Hepatosplenomegaly, osteoporosis

2.2.1 Carbamoyl phosphate synthetase I deficiency

Carbamoyl phosphate synthetase I deficiency (CPSID, OMIM #237300) is an autosomal recessive inborn error of metabolism of the urea cycle, which causes hyperammonemia (Mc Reynolds et al. 1981). The incidence of this enzymopathy has been estimated to be 1/62 000 in USA (Brusilow & Maestri 1996), 1/800 000 in Japan (Nagata et al. 1991) and 1/539 000 in Finland (Keskinen et al. 2008). However, the exact incidence of CPSID is unknown, and probably underestimated, as many infants born with the disorder die without a definitive diagnosis. Two forms of CPSID are recognized: a lethal neonatal type and less severe, delayed-onset type. The early-onset form was first described by Freeman et al. (1970) in a patient with congenital hyperammonemia. The neonatal presentation of CPSID is relatively uniform being the major cause of morbidity hyperammonemia, which leads to respiratory alkalosis, brain damage, coma and death shortly after the birth (Brusilow & Horwich 2001).

The neurotoxicity is a result of accumulation of ammonia, although the manner by which ammonia exerts its effects upon the central nervous system is not completely understood (Gropman et al. 2007). The pathogenic mechanisms of hyperamonemia include astrocyte swelling (Norenberg et al. 2005), affection of axonal growth (Braissant et al. 2002), and alterations of multiple neurotransmitter systems (Butterworth 2000). The most acute effects include increased blood-brain barrier permeability, depletion of intermediates of cell energy metabolism, and disaggregation of microtubules (Butterworth et al. 2002).

Late-onset CPSID can occur during and after the first year of life (Wong et al. 1994), and the onset of symptoms is often associated with increases in protein intake, infection, stress or exposure to medications such as valproic acid (Batshaw 1994, Brusilow 1985, Verbiest et al. 1992).

As is the case for many metabolic diseases, the presentation of CPSID reflects the severity of the underlying molecular defects. In genomic DNA, the mutations can be found either in coding (exons) or non-coding regions (introns). The mutations mapping at coding regions include missense and nonsense mutations and insertions or deletions. The magnitude of insertions or deletions can vary from a single nucleotide to gross mutations, which may comprise several exons or introns (Aoshima et al. 2001, Häberle et al. 2003). Sequencing the cDNA encoding CPSI (Haraguchi et al. 1991) and the knowledge of the intron/exon structure (Häberle et al. 2003, Funghini et al. 2003, Summar et al. 2003) opened the way to mutation identification in patients, and now a number of mutations have been reported (Haraguchi et al. 1991, Hoshide et al. 1993, Summar 1998, Finkch et al. 1998, Aoshima et al. 2001a, Aoshima et al. 2001b, Rapp et al. 2001, Häberle et al. 2003, Funghini et al. 2003, Wakutani et al. 2004, Eeds et al. 2006, Kurokawa et al. 2007, Mitchell et al. 2008, Gomez-Lopez et al. 2008, Ono et al. 2009, Khayat 2009). Although the molecular bases for the CPSID have been determined, a particular genotype does not necessarily predict the clinical severity. The CPSI gene is large (>120kb encompassing 37 introns and 38 exons, with 4500 coding nucleotides) (Häberle et al. 2003, Funghini et al. 2003, Summar et al. 2003), and thus the presence of a missense mutation does not automatically prove the causative role. Therefore it is important to test the specific effects of each mutation on the function and structure of CPSI. Our laboratory has used *E. coli* CPS as model to determine the impact of some clinical mutations on CPSI (Yefimenko et al. 2005), but giving the differences between the bacterial and eukaryotic enzymes the mutations mapping at the regulatory and amidotransferase domains could not had been studied.

The enzymatic diagnosis of hyperammonemia can lead to misinterpretation, as reported in a case of a patient who was first diagnosed with CPSID on the basis of low CPSI activity in the liver, but afterwards was found to carry a gain-of-function mutation in glutamate dehydrogenase I gene, which caused a hyperinsulinism/hyperammonemia syndrome (Ihara et al. 2005). On the other hand the enzymatic diagnosis of hyperammonemia can be

confusing since several urea cycle disorders, such as NAGS deficiency, can cause very similar symptoms (Elpeleg et al. 1990).

The gene encoding CPSI was assigned to human chromosome 2 (2q35) by Hoshide and co-workers (1995) using fluorescence *in situ* hybridization. Later, another laboratory found in one patient an interstitial deletion of chromosome 2q32-34 that was associated with multiple congenital anomalies and CPSID (Loscalzo et al. 2004). These results demonstrated not only that the point mutations alone do not always cause the CPSID, but also mapped the *CPS1* gene at position 2q34. This result is consistent with the information provided by ENSEMBL (http://ensembl.org/).

2.2.2 Polymorphism of CPSI and related diseases

In the case of missense mutations, where the altered nucleotide leads to a single amino acid change, its pathogenic role can not be assigned automatically since several non-pathogenic genetic variants (polymorphisms) have been reported to be present in the population (Summar et al. 2003, Mitchell et al. 2009). Furthermore, sometimes different genetic variants can be found in each allele, leading to compound heterozygous patients, which makes it difficult to attribute the pathological role to a single mutation or to the accumulative effect of different mutations.

Some of the putative, published missense mutants have been found to be kinetically indistinguishable from the wild type enzyme (unpublished results from our laboratory), suggesting the possibility of these mutation being mere polymorphisms instead of disease-causative genetic variants, and highlighting the importance of a pathogenicity test. As a proof of the above, there is, for instance, one polymorphism in CPSI, T1405N, which possible implication on the pathology remains controversial. Clinical research has shown that T1405N influences nitric oxide (NO) metabolite concentrations and NO-mediated vasodilatation (Summar et al. 2004b).

Nitric oxide (NO) has been identified as an endothelia-derived relaxing factor and has an important role in pulmonary vascular resistance (Palmer et al. 1987, Furchgott & Vanhoutte 1989). The vascular endothelium converts L-arginine via nitric oxide synthase to L-citrulline and NO (Palmer et al. 1988), which in turn causes vasodilation and modulates oxidative stress among other important functions (Gewaltig & Kojda 2002). Since L-arginine is a urea cycle intermediate it relates also NO to urea cycle deficiencies, and therefore it was hypothesized that certain polymorhisms in CPSI may affect the enzyme function in correlation with environmental stressors in a manner that the availability of the substrates of NO may become clinically relevant (Summar et al. 2003, 2004a).

The T1405 variant of CPSI is known to be associated with 30-40% lower enzymatic activity (Summar et al. 2004a) though in a recent publication of Ahuja and Power-Lee (2008) the asparagine-variant of the residue 1405 in recombinant purified human CPSI is shown to be less active. However, since the physiological conditions in the hepatic mitochondria are not as optimal as

enzymatic assay conditions used *in vitro* studies, these recent results (Ahuja & Powers-Lee 2008) can not be directly interpret with a clinical sense. Conversely, in another study it has been shown that this functional polymorphism in CPSI limits the availability of the precursors for NO synthesis and consequently results in persistent pulmonary hypertension of the newborn (Pearson et al. 2001). However, none of the infants with pulmonary hypertension in the study was homozygous for the T1405N polymorphism. Lately the polymorphism T1405N in CPSI has been considered also as a risk factor for necrotizing enterocolitis (Moonen et al. 2007), which is a leading cause of morbidity and mortality in neonatal intensive care units.

During the characterization of the genomic structure, mRNA and protein, also other polymorphisms in CPSI have been depicted by several authors, although none of them have been associated with other pathologies (Finckh et al. 1998, Haraguchi et al. 1991, Mitchell et al. 2009; Summar et al. 2003).

3 OBJECTIVE OF THE STUDY

The objective of the present study was to express recombinant mammalian CPSI to study functionally the CPSI deficiency, and to characterize the binding site for the enzyme activator, NAG. The more detailed aims of this study were:

1. Optimize the expression and production of rat CPSI in 293T cells and/or in Sf9 insect cells

2. Produce mutant forms of CPSI bearing specific mutations that have been detected in patients with CPSI deficiency and study the effects of the mutations on the enzyme to better understand CPSID

3. Evaluate the expression system used as a suitable method to confirm the pathogenicity of the clinical mutations in the CPSID patients

4. Identify the binding site for NAG by site-directed mutagenesis of the putative residues, enzymatic activity studies and docking experiment

5. Determine CPSI residues implicated in the transmission of the allosteric signal by site-directed mutagenesis of the putative residues and enzymatic activity studies to understand the mechanism of allosteric signal transmission.

4 MATERIALS AND METHODS

4.1 General methods

4.1.1 Manipulation and purification of plasmid DNA

Recombinant DNA techniques were carried out fundamentally as described in general methods (Sambrook et al. 1989). In general, when plasmid DNA was cut with restriction endonucleases (New England Biolabs, Ipswich, MA, USA) by plasmid incubating in a suitable buffer solution with the endonuclease for 2 hours at 37°C. Afterwards the endonuclease was inactivated at 68°C for 5 minutes. To dephosphorylate the vector DNA, it was incubated with 1U of alkaline phosphatase (Boehringer Mannheim, Ingelheim, Germany) in a suitable buffer solution for 1 hour at 37°C, and afterwards the enzyme was inactivated at 75° for 10 minutes. To ligate DNA fragments, the insert DNA was incubated with the vector DNA in a suitable buffer solution with T4 DNA ligase (Promega, Madison, WI, USA) overnight at 16°C. To purify plasmid DNA from overnight bacterial cultures PlasmidPrep Mini Spin Kit of GE Healhcare (Buckinghamshire, UK) was used.

4.1.2 DNA electrophoresis

To visualize DNA, agarose gel electrophoresis was used. The agarose (Pronadisa-Conda, Barcelona, Spain) was used generally in concentrations of 0.7-1% in TAE-solution (40 mM Tris-acetate, 1 mM EDTA) containing 0.5 µg/ml ethidiumbromide. The electrophoresis was carried out in Mupid-2 chambers (Cosmo Bio Ltd., Japan), and the gels were visualized with BioRad imaging system (Hercules, CA, USA).

4.1.3 Protein electrophoresis and quantification

Protein electrophoresis was carried out as described by Laemmli (1970) in Miniprotean II electrophoresis chambers of BioRad (Hercules, CA, USA) using a 8% staining gel and 5% stacking gel.

The protein was quantified as generally described by Bradford (1976) using a commercial BioRad Protein Assay reagent (Hercules, CA, USA) and BSA as protein standard, and measuring the absorbance spectrophotometrically at 595 nm with Helios γ spectrophotometer (Thermo Scientific, Waltham, MA, USA).

4.1.4 Production of competent DH5α cells

The competent *E. coli* DH5α cells were prepared modifying the method of Cohen et al. (1972). First a single bacterial colony was inoculated into 5 ml of Luria Broth (LB) medium (Pronadisa-Conda, Barcelona, Spain) and grown overnight at 30°C. The next day this culture was inoculated into 500 ml of 2 x LB medium supplemented with 2% glucose and grown up to an optical density of 0.45-0.55 measured at λ of 600 nm. When the optimal cell density was reached the culture was centrifuged at 4°C and 2000 x g for 10 minutes. The cellular pellet was resuspended in 250 ml of a solution containing 100 mM $CaCl_2$, 70 mM $MnCl_2$ and 40 mM sodiumacetate pH 6.4, and the suspension was incubated at 0°C for 45 minutes. Afterwards it was centrifuged during 5 minutes at 4°C and using 1500 x g, and the pellet was resuspended in 25 ml of the solution described above supplemented with 5ml of 80% glycerol. The competent cells were stored at -80°C.

4.1.5 Transformation of DH5α competent cells

Competent bacterial cells (100µl) were first incubated with the plasmid DNA for 30 minutes on ice and afterwards a heat shock was produced at 42°C 100 seconds. Then 700 µl of SOC medium was added to the cells and they were grown for 1 hour with continuous agitation. After the growth period the cells were plated on Luria Agar plates and the plates were incubated overnight at 37°C.

4.1.6 Cell cultures

The Sf9 cells (line IPLB-Sf21-AE, Invitrogen Life Technologies, Gaithersburg, MD, USA) were maintained in suspension cultures using Sf-900 serum free media from Invitrogen supplemented with 0.1% Pluronic F-68 (Sigma-Aldrich, St. Louis, MO, USA). Every 3 to 4 days the culture was diluted to a viable cell density of 3-4 x 10^5 cells per ml. Sf9 suspension cultures were agitated at 105 rpm at a temperature of 27.5°C in sterile Erlenmeyer flasks (Sigma-Aldrich, St. Louis, MO, USA).

The 293T-cells (a gift from Dr. Juan Saus, Centro de Investigación Principe Felipe, Valencia, Spain) were cultured in 75 cm^2 culture flasks (Corning, NY, USA) using DMEM supplemented with L-glutamine, FBS and penicillin-streptomycin solution (all from Sigma-Aldrich, St. Louis, MO, USA) as culture media. The cell cultures were diluted 1/10 into a fresh culture medium generally twice a week by detaching the cells from the bottom of the culture flask with sterile Trypsin-EDTA solution (Sigma-Aldrich, St. Louis, MO, USA).

4.2 Construction and purification of expression vectors

4.2.1 Production of the functional baculovirus vector

To construct the expression vector for the production of CPSI in insect cells the complete cDNA encoding rat CPSI (4500 bp) contained in the plasmid pHN3491 (ATCC/National Institutes of Health Repository) (Nyunoya et al. 1985), which was obtained from Dr. Carol Lusty (Public Health Research Institute, New York) was ligated into pFastBac-HTA expression vector containing a 6 x His-tag (Invitrogen Life Technologies, Gaithersburg, MD, USA) as *BamH*I/*BamH*I/*EcoR*I-fragment by Dr. Igor Yefimenko (at present CNIO, Madrid, Spain): first a 4000 bp (bases 500-4500 of the cDNA) *BamH*I/*EcoR*I fragment was ligated to the cloning vector generating the construct pFB1, and then a 500 bp fragment (without the mitochondrial targeting signal) from the 5' most terminus of the rat CPSI cDNA was amplified by PCR introducing to the 5' and 3' ends of the amplified fragment recognition sites for *BamH*I and ligated to the *BamH*I-site of the construct pFB1. The correctness of the construction was confirmed by complete DNA sequencing (Servicio de sequenciación, Centro de Investigación Príncipe Félipe, Valencia, Spain).

E. coli Max Efficiency DH10Bac cells (Invitrogen Life Technologies, Gaithersburg, MD, USA) were transformed with 5 ng of recombinant donor plasmid according to the manufacturer's instructions, and plated onto Luria Agar plates containing 50 µg/ml kanamycin, 7 µg/ml gentamycin, 10 µg/ml tetracyclin, 40 µg/ml IPTG, and 100 µg/ml Bluo-gal (Sigma-Aldrich, St. Louis, MO, USA). According to the Bac-to-Bac Baculovirus Expression System manual, the recombinant bacmid DNAs were isolated from the transformed bacterial cells and the recombination (insertion of the cDNA to the genome of baculovirus) was confirmed by PCR with M13/pUC forward and reverse primers (5'CCCAGTCACGACGTTGTAAAACG3' and 5'AGCGGATAACAATTTCACACAGG3', respectively). 10 µl of the recombinant DNA of one positive clone mixed with 6 µl of Cellfectin reagent (Invitrogen Life Technologies, Gaithersburg, MD, USA) was used to transfect 9 x 10^5 Sf9 cells, from exponentially growing cell suspension cultures, plated on a well of a 6-well plate (Corning, NY, USA). The plates were incubated at 27.5°C for 5 hours and then the transfection mixture was replaced by 2 ml of complete

Sf900 medium. Recombinant baculoviruses were harvested at 3 days post-transfection detaching the cells by pipetting with the proper culture medium and centrifuging (100 x g) them for 5 min. The functional baculoviruses were stored at 4°C.

The positive viral stocks (confirmed by Western blotting) were further amplified by infecting a suspension culture of 1.5 x 10^6 Sf9 cells per ml with low multiplicity of infection (m.o.i., 0.05-0.1). The cells were incubated with the virus in serum-free Sf900 medium at 27°C with orbital shaking (105 rpm). The viruses were harvested at 48 h post-infection by centrifuging the cultures for 5 minutes at 100 x g. Viral titers were determined either by end-point dilution method or by plaque assay (O'Reilly et al. 1992), and the stocks were stored at 4°C.

4.2.2 Cesium chloride-purification of pCIneoCPS45 expression vector

The expression vector pCIneoCPS45 (Park et al. 2000) was a kind gift from Dr. Hog-Jin Kim (Seoul, South Korea). In the vector the 4500 bp fragment containing the rat CPSI open reading frame is inserted in the *Eco*RI site of pCIneo-vector (Promega, Madison, WI, USA). The cDNA includes the mitochondrial targeting signal of CPSI.

Prior to transfection of 293T cells the expression vector was purified by cesium chloride (CsCl) extraction. The vector was first purified from 500 ml bacterial culture using Qiagen Plasmid Maxi Kit (Qiagen, Venlo, The Netherlands) and then centrifuged with CsCl for 21 hours at 63000 rpm (rotor 70.Ti) in Beckman ultracentrifuge. Afterwards the DNA was washed with CsCl-saturated isopropanol four times, precipitated with 100% ethanol and finally washed with 70% ethanol. The DNA pellet was resuspended in 300 µl of TE buffer. Then the DNA was again precipitated with 7.5 M Ammonium acetate and 100% ethanol, and washed with 70% ethanol. The DNA pellet was dried with Speedvac and resuspended in 300µl of TE buffer. The concentration of the vector DNA was measured spectrophotometrically at 260 nm with Helios γ spectrophotometer (Thermo Scientific, Waltham, MA, USA).

4.3 Production and purification of CPSI with baculovirus expression system

To optimize the expression of CPSI, 2 x 10^6 cells in Falcon T25 tissue culture flasks were infected with recombinant baculovirus virus at m.o.i. (multiplicity of infection) of 0.1, 1, and 2 in complete growth medium and the cells were collected at different intervals post-infection (24-80 hours), centrifuged (100xg) for 5 minutes, and analyzed by Western blotting.

To purify CPSI in larger scale, 30-50 ml suspension cultures of Sf9 cells (1.5 x 10^6 cells/ml) in serum-free Sf-900 medium were infected with the recombinant virus at m.o.i 2 and incubated at 27^{0}C in the absence of serum

using a shaker platform (105 rpm) for 65 hours. Afterwards the cells were centrifuged (100 x g) for 5 minutes at 4°C, washed twice with cold PBS, and the protein was extracted as follows: The cells were kept on ice for 30 min in a lysis buffer containing the solution A (50 mM glycylglycine pH 7, 20 mM KCl, and 20% glycerol) supplemented with 0.1% Triton X-100, 5 mM imidazole, and the Sigma's protease inhibitors E-64 (5 μM) and the specific cocktail for His-tagged proteins (0.1%). The suspension was sequentially frozen in liquid nitrogen and defrost on ice twice, followed by 10 min centrifugation (16000 x g) at 4°C. The supernatant was used for further experiments. To determine the insoluble fraction of the total protein extract, the pellet was resuspended in the lysis buffer in a volume equal to the volume of the supernatant.

The recombinant 6 x His-tagged CPSI was affinity-purified with cobalt-based BD TALON™ resin (BD BioSciences, San Jose, CA, USA). The supernatant of the extracts of the infected Sf9 cells prepared as described above were incubated for 30 min at 4ºC with the resin previously equilibrated in solution A. The resin was then washed twice with 10 bed volumes of washing buffer (solution A supplemented with 5 mM imidazole) for 10 min and packed into a Polyprep chromatography column (BioRad, Hercules, CA, USA). The His-tagged proteins were eluted with two bed volumes of elution buffer (solution A, supplemented with 150 mM imidazole). CPSI containing fractions were pooled, DTT was added to a final concentration of 1mM, and the preparation was immediately used or concentrated with Amicon centrifugal filter devices (Millipore, Billerica, MA, USA) with a cut off of 100 kDa and stored at -80ºC.

To optimize the purity and yield of the protein the enzyme purification was afterwards modified and improved using FPLC ÄKTA system (GE Healthcare). For the purpose the pellet from a 50-ml 65-hour culture at 27ºC of Sf9 cells infected using m.o.i 2, was suspended in 3 ml of a solution containing 20 mM Na phosphate, pH 7, 20 mM KCl, 1 mM dithiothreitol, 10% (v/v) glycerol, 0.1% Triton X-100, 0.4 mM phenylmethylsulphonyl fluoride, Sigma's protease inhibitors E-64 (5 μM) and the specific cocktail for His-tagged proteins (0.1%). The suspension was kept on ice for 30 min and then it was twice frozen and thawed in liquid nitrogen and ice. Following centrifugation (15 min, 16000xg, 4 °C), the supernatant was applied to a HisTrap column in FPLC, which was equilibrated and run with buffer A (20 mM Na phosphate pH 7, 0.5 M NaCl, 1 mM dithiothreitol, 20 mM imidazole, and 10% glycerol) at 4ºC. After washing with 10 bed volumes of buffer A, a 10-ml linear gradient of 20-500 mM imidazole in buffer A was applied. Fractions containing CPS I (monitored by SDS-PAGE) were pooled and concentrated to >1 mg protein ml^{-1} by centrifugal ultrafiltration (100 kDa cutoff Amicon Ultra, from Millipore). The concentrated enzyme was supplemented with 10% extra glycerol, and it was either used immediately or kept frozen at -80ºC.

4.4 Expression of CPSI in 293T cells

To express rat CPSI in 293T cells, the cells were transfected with cesium chloride-purified and linearized pCIneoCPS45 expression vector as follows: 24 hours prior to transfection 8 x 10^5 293T cells were plated on 100 mm culture dishes (Corning, NY, USA) using Opti-MEM® I Reduced Serum Medium (Invitrogen Life Technologies, Gaithersburg, MD, USA) without antibiotics. At the day of the transfection, 8 µg of pCIneoCPS45-vector was mixed with 20 µl of Lipofectamine2000™ transfection reagent (Invitrogen Life Technologies, Gaithersburg, MD, USA) and incubated for 30 minutes at RT. Finally the transfection mixture was diluted up to 6.4 ml with Opti-MEM and added to the cell culture plates. The 293T cells were incubated with the transfection medium for 48 hours at 37°C. The protein was extracted as described above in the section 4.3 to analyze the expression rate in 293T cells.

To try to amplify the expression rate of CPSI the transfected cells were selected by using Geneticin (G-418, Sigma Aldrich, St. Louis, CA, USA) since the expression vector carries a neomycin resistance gene. After the 48 hours incubation with the transfection medium the transfected 293T cells were diluted in 1:4 ratio in the selection medium (complete DMEM, supplemented with 500µg/ml of geneticin). When the culture plates reached confluence, the cells were again diluted 1:4. The protein was extracted from the cells after 4, 10 and 17 days of selection as described above in the section 4.3.

4.5 Characterization of protein expression

To characterize the expression rate of CPSI both in Sf9 insect cells and in 293T cells by Western blotting the protein was extracted from the cells as described in the section 4.3 and the quantity of total protein in the extract was determined as described in the section 4.1.3. Known quantities of native rat liver CPSI (kindly provided by Dr. Belén Barcelona, Centro de Investigación Príncipe Félipe, Valencia, Spain) together with 10 µg of soluble protein extracts were applied to SDS-Page. From the gel the proteins were transferred to nitrocellulose transfer membranes (Whatman, Dassel, Germany) using Sigma's semi-dry blotting system. The membrane was then blocked with 2% non-fat milk powder dissolved in TBS for 1 hour at RT, and afterwards it was incubated with a monoclonal antibody previously raised in our lab against native rat liver CPSI (18A1; 1/10000 dilution) for 1 hour at RT, washed three times with TBS (supplemented with 0.01% Tween) and finally incubated for 1 hour with the secondary antibody, anti-mouse-AP from Promega (Madison, WI, USA) (1/10000 dilution). The proteins were detected with NBT and BCIP as described in Sambrook et al. (1989).

To further characterize the expression of CPSI in 293T cells, immunofluorescence analysis was performed. The cells were transfected as

described above in the section 4.4 in the culture plates containing microscope slides. After 48 hours of transfection, the slides were treated as follows: First the slides containing the transfected 293Tcells were washed with PBS, and then fixed with 1:1 mixture of ethanol-acetone at 4°C for 10 minutes. After the fixation the slides were dried and then again rehydrated with PBS, blocked with sheep serum for 20 minutes at room temperature, and then incubated with the mAb 18A1 (1/10000 dilution) for 1 hour at RT. After the incubation the slides were washed five times with PBS, and incubated with the secondary antibody (anti-mouse-FITC 1/10000 dilution) for 1 hour at RT. Finally the slides were washed five times with PBS and analyzed by a fluorescence microscope.

4.6 Production of mutant forms of CPSI

Site-directed mutagenesis was performed according to QuickChange method of Stratagene (LaJolla, CA, USA). In this method the pFastBac-HTA expression vector (Invitrogen Life Technologies, Gaithersburg, MD, USA) containing the cDNA coding for CPSI was amplified by PCR using primers that introduce the desired mutation into the cDNA. Afterwards the PCR product was digested with DpnI restriction endonuclease (New England Biolabs, Ipswich, MA, USA) to get rid of the template DNA, and transformed to DH5α cells. The mutation-containing expression vectors were purified as explained in the section 4.1.1, the clones were scored for the mutation and confirmed by sequencing not to carry any undesired mutations in the cDNA. Finally the mutant forms of CPSI were produced and purified exactly as described in the sections 4.2.1 and 4.3.

4.7 Enzyme activity assays

In the standard assay, carbamoyl phosphate (CP) synthesis was measured by coupling the CPS reaction to that of ornithine transcarbamoylase (OTC) and quantitating the resulting citrulline (Nuzum & Snodgrass 1976). CPS activity was assayed at 37°C in a solution containing 50 mM glycyl glycine pH 7.4, 0.1 M KCl, 0.1 M NH_4Cl, 5 mM ATP, 7 mM $MgSO_4$, 20 mM $KHCO_3$, 5 mM L-ornithine, 1 mM DTT, 10 U/ml ornithine transcarbamoylase (OTC), 10 mM N-acetylglutamate (NAG), and between 5-200 µg/mL of enzyme (wild-type and mutants forms of CPSI), determining after 10 min the amount of CP and/or ADP produced (Fresquet et al. 2000). When indicated, intramitochondrial conditions refer to use of 0.1 mM NAG and 1 mM NH_4Cl instead 10 mM AG and 100 mM NH_4Cl of the standard assay.

Production of ADP was also assayed by monitoring continuously the decay of NADH in a coupled pyruvate kinase-lactate dehydrogenase system as previously described (Bergmeyer 1986). Wild-type and mutant forms of CPSI (3-200 µg), were incubated at 37°C in 1 ml of a solution containing 50 mM

glycylglycine pH 7.4, 0.1 M KCl, 0.1 M NH_4Cl, 5 mM ATP-Mg, 2 mM $MgSO_4$, 20 mM $KHCO_3$, 1 mM DTT, 2.5 mM phosphoenol pyruvate, 0.25 mM NADH, 0.04 mg/ml pyruvate kinase, 0.025 mg/ml lactate dehydrogenase, with and without 10 mM NAG (Guthöhrlein & Knappe 1968). Bicarbonate-dependent ATP hydrolysis (the ATPase partial reaction) was assayed with the same reaction mixture but eliminating the nitrogen source. The partial reaction of ATP synthesis was assayed in a mixture containing 50 mM glycyl-glycine pH 7.4, 0.1 M KCl, 15 mM $MgSO_4$, 15 mM glucose, 1 mM ADP, 5 mM carbamoyl phosphate, 10 mM NAG 1 mM NADP, 0.1 mg/ml hexokinase, and 0.025 mg/ml glucose-6-phosphate dehydrogenase, monitoring continuously ATP production by the increase in the absorbance at 340 nm.

The enzymatic inactivation by temperature was determined by measuring the CPSI activity at 37ºC after incubation of the recombinant proteins (1µg/µl) for 15 minutes at different temperatures (42ºC, 44ºC, 46ºC, 48ºC, 50ºC and 55ºC). The synthesis of CP was assayed by conversion to citrulline, and carried out as described above after placing on ice for 5 minutes.

Dependence of the CPS activity on the concentration (0-100 mM) of NAG was determined by assaying the formation of carbamoyl phosphate as citrulline. The program GraphPad Prism (GraphPad Software, San Diego, California) was used for curve fitting.

4.8 Circular dichroism

CD spectra in the far-UV region (195–250 nm) were obtained with a Jasco 810 spectropolarimeter (Jasco, Easton, MD, USA). Protein samples were measured at 4°C in 0.2 ml of buffer solution (20 mM Tris–HCl pH 7,4, 20mM KCl, 20% glycerol containing 0.5 mM DTT), and using in a 0.1 cm path-length cell. An average of ten scans was performed on the resulting spectra. The temperature was maintained constant with a circulating water bath.

4.9 CPSI mutation analysis (II)

CPS1 cDNA was amplified by PCR using exonic primers (Finckh et al. 1998), and *CPS1* genomic DNA was amplified using intronic primers deduced from genomic GenBank entries (NC_000002). The PCR products were sequenced using standard dye terminator chemistry (Applied Biosystems, Foster City, USA). All the detected mutations were confirmed by duplicate analysis or - if possible – by restriction fragment analysis. Segregation analysis of the mutations detected (see Table 3, results) was done in parental DNA.

4.10 Programs used in protein modeling and visualization

The homology modeling of mammalian (*Rattus norvegicus*) CPSI was made using the structures of bacterial CPS and the regulatory domain of human CPSI as templates and the MODELER program (Sali & Blundell 1993) principally by Dr. Belén Barcelona (Centro de Investigación Príncipe Félipe, Valencia, Spain). Several models based on slightly different sequence alignments were generated, and finally the models were evaluated with MODELER Dope Score function. The best energy model was selected and its stereochemical quality was verified with Procheck (Laskowski et al. 1996).

To find a possible binding site for the allosteric activator N-acetyl-L-glutamate (NAG), the structure of the regulatory domain of human CPSI was screened for cavities employing Voidoo (Kleywegt & Jones 1994). The cavity was visualized with PyMOL (DeLano 2002).

Structural superimpositions were performed with the LSQKAB option of the CCP4 suite (CCP4 1994). Solvent accessibility (probe radius, 1.4 Å) of residues within the eCPS-IMP complex (PDB 1CE8 (Thoden et al. 1999) and hCPS (PDB 2yvq) structures was calculated with the AREAIMol program of CCP4. Surface potential was calculated with GRASP (Honig & Nicholls 1995). Multiple sequence alignments were prepared with CLUSTALW (Thompson et al. 1994), using default parameters. Figures depicting protein structures were prepared with PyMOL.

For automatic plotting of CPSI-NAG interactions a version 4.4.2 of LIGPLOT was used (Wallace et al. 1995). The program automatically generates schematic diagrams of protein-ligand interactions. The interactions shown are mediated by hydrogen bonds and by hydrophobic contacts.

4.11 Fine-mapping of NAG binding site by photoaffinity labelling and mass spectrophotometry

For mass spectrometric (MS) analysis, the enzyme was subjected as described in Rodriguez-Aparicio et al. (1981) to UV-irradiation in the presence of either ClNAG (experimental irradiation) or NAG (control irradiation) followed by limited proteolysis with V8 protease, which was done by Dr. Javier Cervera. After SDS-Page, the Coomassie-stained 18.9-kDa band corresponding to the C-terminal domain of the enzyme from the experimental and control samples was excised from each gel and was subjected to peptide fingerprinting using trypsin (Promega, Madison, WI, USA) (Shevchenko et al. 1996) and MALDI-TOF MS analysis in a 4700 Proteomics Analyzer (Applied Biosystems, Foster City, USA) used in linear mode, with concomitant MS/MS analysis of relevant peaks to acquire sequence information. The MS and MS/MS information was analyzed with MASCOT (Perkins et al. 1999). The mass spectrometric analysis was

carried out in the Proteomics Core Facility of the Centro de Investigación Príncipe Felipe (CIPF Valencia)-Proteored (Genoma España).

4.12 Docking of the NAG molecule

NAG was docked into the cavity identified with VOIDOO (see above) using GOLD Package (version 4.0.1) (Verdonk et al. 2003). Dr. José Gallego performed the docking experiments. Docking calculations were unrestrained and used the GoldScore fitness function. GOLD calculations indicated the need for movement of the W1410 residue for full NAG entry. The side chains of W1410, F1445 and Q1413 were allowed to rotate freely. The final hCPS-NAG model was generated by further refining the best GOLD solution by restrained energy minimization using the ff03 force field (Verdonk et al. 2003) of AMBER (Case et al. 2005), and a generalized Born model for solvent simulation. This last minimization used as restraints the protein-NAG hydrogen bonds that were detected in the convergent GOLD binding poses.

4.13 General material

Enterococcus faecalis ornithine transcarbamylase was prepared as reported by Marshall and Cohen (1972) and was a kind gift from Dr. Vicente Rubio (IBV, CSIC, Valencia, Spain), but was also prepared in our laboratory as described in the literature cited above. When used for enzyme activity assays it was freed from ammonium sulphate and placed into the assay buffer by centrifugal gel filtration (Penefsky 1977). Ammonium-free pyruvate kinase, lactate dehydrogenase (both from rabbit muscle), trypsin (from bovine pancreas), and hexokinase and glucose-6-phosphate dehydrogenase (both from yeast), were from Sigma-Aldrich (St. Louis, CA, USA) or Roche Biochemicals (Basel, Switzerland). The primers used in PCR were purchased from Invitrogen Lifetechnologies (Gaithersburg, MD, USA). The general laboratory reagents to prepare solutions were all supplied by Sigma-Aldrich (St. Louis, CA, USA). The native CPSI purified from rat liver in our laboratory by Dr. Belén Barcelona.

5 REVIEW OF RESULTS

5.1 Expression of recombinant CPSI in 293T cells (unpublished results)

With the final aim in mind of choosing the best expression system for recombinant CPSI, the 293T cells were transfected with pCIneoCPS45 expression vector (Park et al. 2000) to obtain recombinant CPSI. The efficiency of the transfection was studied by immunofluorescence. In Fig. 7 it can be seen that individual cells expressed at good rate the recombinant CPSI, but the transfection efficiency was relatively poor since in a confluent culture dish approximately 50% of the cells were apparently transfected with pCIneo CPS45.

To improve the expression rate the transfected 293T cells were selected with geneticin. When the protein expression was analyzed after 4, 10 and 17 days, little improvement in the expression rate can be observed in 17 days (Fig. 8). However, it seems that the selection was not efficient enough or the cells probably lost the transfected expression. The expression levels of CPSI in 293T cells, judged by Western blotting, were too low to obtain sufficient quantities of protein for the enzyme activity measurements.

5.2 Expression of CPSI in Sf9 insect cells with baculovirus expression system (I-III)

5.2.1 Expression and purification of the recombinant wild-type CPSI

The expression of mature CPSI (without the mitochondrial targeting signal) in Sf9 insect cells was already detected at 48 hours post-infection and a maximum was obtained at 65-72 hours (Fig. 9) since with longer infection times degradation of the recombinant CPSI was detected. Variation of m.o.i had important effect on the expression rate though very high m.o.i (10) increased

the insolubility of the protein perhaps due to the presence of inclusion bodies and also degradation of the protein, which can be explained by the liberation of the proteases from the dying cells that were observed when high m.o.i was employed.

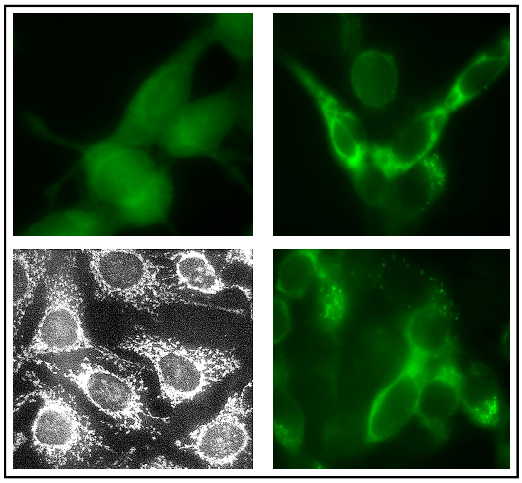

FIGURE 7 Immunofluorescence of the 293T cells transfected with the expression vector coding for rat CPSI. On the upper left panel are presented control cells treated only with the secondary FITC-labeled antibody, and on the lower left panel as a positive control of the immunofluorescence method human lung epithelial, L132 cells processed with the same method as 293T cells (down). On the right panel (up and down) are shown 293T cells treated with the monoclonal antibody against CPSI.

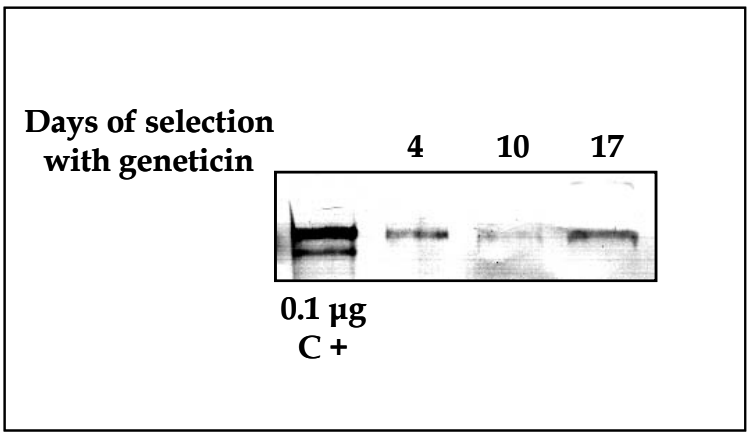

FIGURE 8 Immunoblot of 293T cells transfected with a plasmid encoding rat CPSI and a geneticin resistance marker. The transfected cells were selected with geneticin and the protein was extracted after 4, 10 and 17 days. 20 µg of soluble protein was applied to SDS-Page, and afterwards the Western blot was performed with a monoclonal antibody raised against rat liver CPSI. The left lane corresponds to 0.1 µg of native CPSI purified from rat liver.

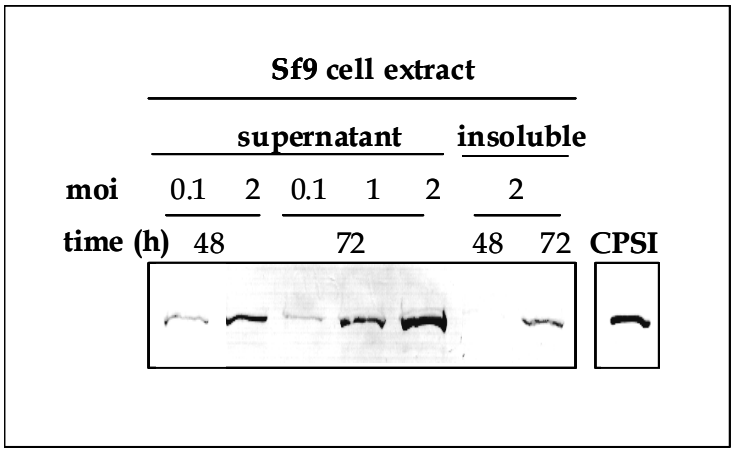

FIGURE 9 Western blot of soluble and insoluble protein extracts from CPSI encoding recombinant baculovirus infected Sf9 cells containing similar amount of total protein. Different times of post-infection and m.o.i were used to optimize the expression of recombinant CPSI. Right lane corresponds to 0.1 µg of purified rat liver CPSI used as a standard.

The expression conditions were easily scaled up to 50 ml of Sf9 suspension culture, in which, under optimal conditions determined by the expression optimization experiments (m.o.i 2 and 65 hours incubation post-infection), 85% of the expressed CPSI appeared in the soluble fraction of the protein extract (Fig. 9).

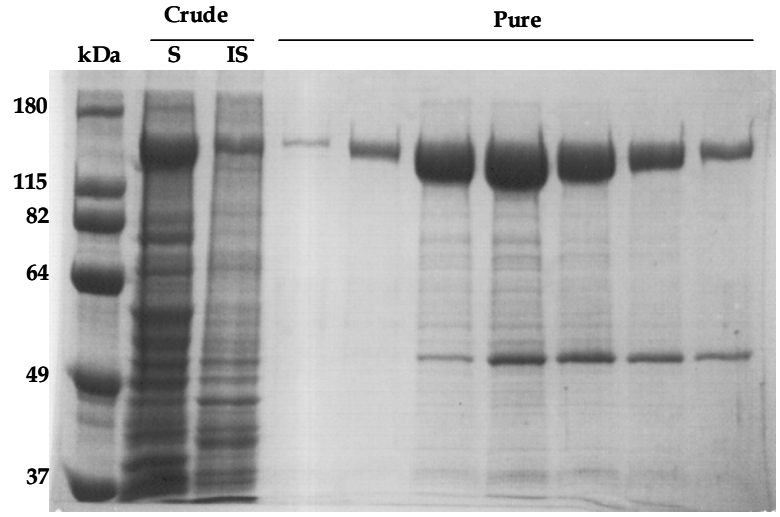

FIGURE 9 SDS-Page of soluble (S) and insoluble (IS) protein extracts from CPSI encoding recombinant baculovirus infected Sf9 cells, and fractions eluted from affinity chromatography-purified recombinant wild-type CPSI.

Finally, CPSI was purified from the Sf9 insect cell extracts near to homogeneity by immobilized Co^{2+} affinity chromatography with typical yields of 0.5-1 mg of CPSI from 50 ml Sf9 suspension cultures (Fig. 9). Improved purity (>95%) was

reached when a chromatographic step was carried out using FPLC (results not shown).

5.2.2 Characterization of the recombinant CPSI

Neither the relative mobility of recombinant CPSI (160 kDa) nor the immunological properties against a monoclonal antibody raised against native CPSI were different from those of the native CPSI of rat liver, as observed in SDS-Page and Western blotting, respectively (Fig. 8 and 10).

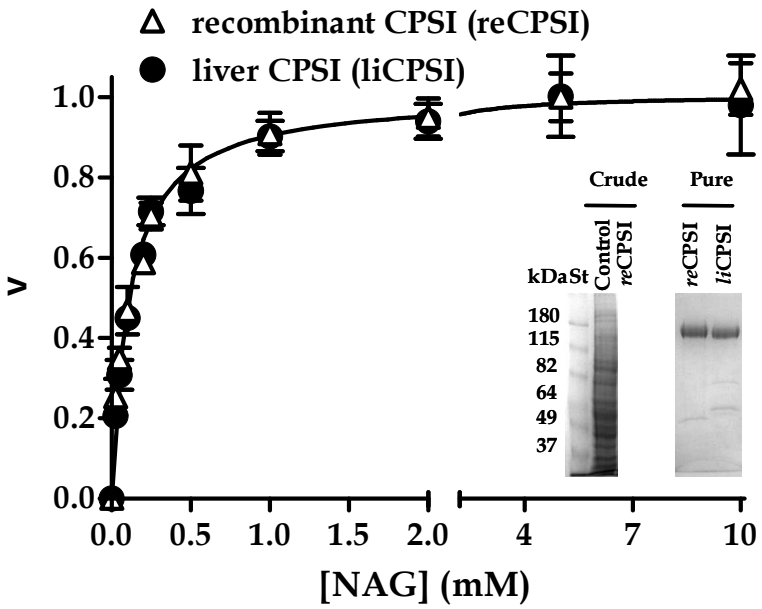

FIGURE 10 Recombinant (reCPSI) and liver-purified (liCPSI) rat CPSI exhibit identical NAG activation kinetics. Velocity is expressed as a fraction of the maximal velocity extrapolated at infinite NAG concentration. The inserts illustrate SDS-Page analysis (Coomassie staining) of CPSI expression. Left panel, crude centrifuged extracts of the insect cells infected with the baculovirus lacking or carrying the CPSI coding sequence (lanes labelled Control and reCPSI, respectively; St denotes mass standards). Right panel, purified recombinant enzyme (reCPSI), and comparison of it with the enzyme purified from rat liver (liCPSI).

The CPSI activity was determined and compared from purified enzymes. The specific activity of recombinant CPSI was 1.3±0.08 μmol CP min^{-1} mg^{-1} under standard assay conditions. The enzyme exhibited normal substrate kinetics (K_m values for ATP, HCO_3^- and NH_4^+, 1.06±0.11 mM, 6.43±0.60 mM and 1.07±0.1 mM, respectively) and NAG activation kinetics (K_a^{NAG} 0.11 ± 0.01 mM). The kinetic constants or activity values of the recombinant CPSI did not differ from those of native rat liver enzyme measured simultaneously or from previously reported.

5.3 N-acetyl-L-glutamate binding site mutants (I)

5.3.1 Production of the mutant enzyme forms

Five residues (T1391, T1394, W1410, N1437 and N1440) within the regulatory domain of CPSI were selected for mutagenesis based on the known structure of *E. coli* CPS (PDB 1jdb), and also based on the hypothesis that the residues involved in the binding of IMP (and UMP) in *E. coli* CPS would be also crucial in binding N-acetyl-L-glutamate (NAG) in CPSI. The residues involved in ornithine-binding were excluded from the analysis because of low level of sequence conservation. In addition, earlier experiments in our laboratory have determined the sequence of a pentapentide that is important in the binding of NAG (J. Cervera, unpublished results). The process to determine the peptide went as follows: the NAG was labeled with $[Cl]^{14}$ and allowed to bind to native CPS; the complex was digested by V8 protease and trypsin; the resulting fragments were separated by HPLC and their masses were determined. The highest radioactivity appeared in a fraction that corresponded to a pentapentide consisting of 1388-1392 (Leu-Phe-Ala-Thr-Glu).

All of the mutant CPSI were purified near to homogeneity from Sf9 insect cell suspension cultures. The proteins were over-expressed similarly to the wild-type CPSI and were reasonably stable since none of the mutants showed differences in their CD-spectra suggesting that the mutations did not affect the structure and folding of the enzyme.

5.3.2 Influence of the mutations on the activation by NAG

The CPSI activity was measured as production of CP and ADP. Under the standard assay conditions both carbamoyl phosphate and ADP synthesis in the mutants was lower respect to the wild-type enzyme. As expected for residues from the regulatory domain and predicted to be involved in NAG binding, mutations did not affect the stoichiometry of the CPS reaction (ADP/CP ratio of 2). Several mutations clearly affected the binding of NAG and the activation of CPSI altering the hyperbolic dependence of CPSI activity on the concentration of NAG characteristic to the wild-type CPSI, as predictable for residues involved in NAG binding. The K_a^{NAG} values increased markedly (370-850 times) in mutants T1391V and T1394A and moderately (70-110 times) in mutants W1410K, N1437D, and N1440D (Fig. 3C, Publication I). In addition, all the mutants were activated less efficiently than the wild-type CPSI. Mutations T1391V and T1394A reduced the V_{max} approximately by 90%, W1410K and N1440D by 75%, and N1437D by 40%.

5.3.3 Fine-mapping of NAG binding site by photoaffinity labeling and mass spectrometry

In MS fingerprinting a tryptic peptide was detected in similar amount after control irradiation in the presence of NAG and/or in the experimental irradiation with chloro-acetylglutamate (ClNAG), which is in accordance with the fact that only a very small fraction of CPSI is labeled with ClNAG (Rodriguez-Aparicio et al. 1989). However, in the tryptic digest of the sample that was photoaffinity labeled with ClNAG, but not in the digest, in which the ClNAG was replaced by NAG, a small peak of ~4155 Da was observed. This mass (4155.94 Da) corresponds within the experimental error to the expected mass of the tryptic fragment encompassing the residues 1388-1424 and modified by cross-linking to NAG (4155.09 Da). Nevertheless, the small amount of this peptide prevented further experiments though its mass and its presence in the experimental photoaffinity-labeled sample is in accordance with the conclusion that ClNAG labeling takes place in residues 1388-1424 of CPSI.

5.3.4 Search of cavities in the regulatory domain of hCPSI

The crystal structure corresponding to a fragment of the regulatory domain of human CPSI (PDB 2yvq) enabled us to screen for cavities in the structure. A single cavity able to accommodate a NAG molecule was detected between the β sheet and the helical layer containing the α-helices 3 and 4 (Fig 1A, Publication I). The residues forming the cavity were identified as L1363, I1364, G1365, I1366, T1391, T1394, W1410, I1423, N1437, L1438, N1440, N1449, I1452 (Fig. 11). They are aligned with the residues that form the allosteric UMP/IMP binding site of *E. coli* CPS regulatory domain (L946, L947, S948, V949, T974, T977, K993, I1001, N1015, T1016, S1018, S1026, and I1029). The three-armed cavity was visualized with the PyMOL Molecular Graphics System (DeLano Scientific), and exhibited geometry compatible with the size and form of NAG.

5.3.5 Docking of the NAG molecule

NAG was initially docked manually into the cavity identified with Voidoo (Fig. 11) and later using GOLD Package (version 4.0.1) by Dr. José Gallego (Centro de Investigación Príncipe Félipe, Valencia, Spain) (Fig. 1D, Publication I). NAG docked with preference into this cavity and not elsewhere in the human CPSI regulatory domain. Docking required free rotatation of the side chain of W1410 and of the overlaying F1445 and Q1413 side chains. This rotation, where the indole ring of W1410 ring had flipped 180°, yielded a highly stable binding pose. Subsequent calculations using this protein conformation led to very good NAG docking scores, with almost total convergence (95%) of the NAG binding poses.

5.3.6 CPSI activation by the NAG analog N-acetyl-β-phenylglutamate

From previous structure-activity studies of native CPSI (Britton et al. 1990) it was known that phenyl substitution of the hydrogen atom of the NAG β-carbon scarcely modifies activation of CPSI although it provokes a 4-fold increase in the activation constant for NAG. This is in agreement with the NAG binding mode proposed here, in which the NAG C^{β} atom is partially exposed and contacts the pocket roof residue, W1410 (Fig. 11). According to our model of NAG binding site, the mutant W1410K is predicted to have an enlarged cavity where to accommodate NAG because of the substitution of the tryptophan indolic ring. In this mutant, N-acetyl-β-phenylglutamate exhibits activation constant eight times lower than that for NAG, what can be explained by the interaction of the phenyl moiety of the analog and the residue at position 1410 in the mutant CPSI.

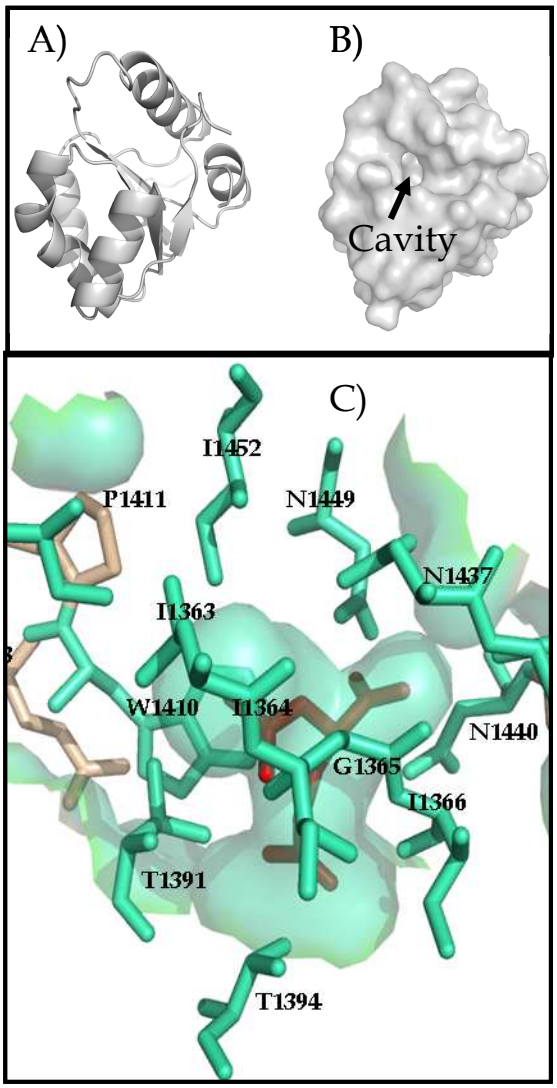

FIGURE 11 Detection of the cavity in the human CPSI regulatory domain. Panel A represents the structure, panel B illustrates clearly the cavity, and panel C shows the residues that line the cavity.

5.4 Clinical mutations in CPSI deficiency (II)

Several clinical mutations detected in the patients of CPSI deficiency were selected to study their effects on the enzyme activity and function, and also to determine their pathological impact on CPSI. The mutations are presented in Table 3.

TABLE 3 The clinical mutations selected for this study. LO, late onset; NE, neonatal; NE, non-expressed, homozygosis in cDNA ; [a] The codon 1411 in the *CPS1* gene coding for proline is CCG in human and CCA in rat (experimental mutation was CCA>CTA at 4232; * Due to redundancy of 3 bp at the deletion breakpoints it is not possible to determine the exact position of the deletion. The deletion encompasses 486 bp, including 428-430 bp of the 3'-region of the intron 7 and 56-58 bp pf the exon 8. The skipping of the exon 8 was shown in PCR products of cDNA generated with exonic primers flanking exon 8.

		Allele A		**Allele B**		
Patient	Onset	Protein	Nucleotide	Protein	Nucleotide	Reference
1	NN	p.Q678P p.G1376S	c.2033>A c.4126G>A	116624 (±1)_116139(±)del (del 486bp)incl. 56-58 bp of ex. 8, ex. 8 skipped in-frame*		Publication II
2	NN	p.P774L	c.2321C>T	p.R1453Q	c.4358G>A	Publication II
3	NN	p.T471N	c.1412C>A	p.R1453W	c.4357C>T	Publication II
4	NN	p.L1381S	c.4142T>C	NE		Summar et al. 1998
5	LO	p.S123F	c.368C>T	NE		Summar et al. 1998
6	LO	p.P1411L	c. 4232C>T[a]	p.Q478X	c.1432C>T	Summar et al. 1998 Eeds et al. 2006
7	LO	p.H337R	c.1010A>G	p.238-362del	c.714-1088 del	Aoshima et al. 2001
8	LO	p.Y1491H	c.4471T>C	NE		Summar et al. 1998

5.4.1 Patients and CPSI mutation analysis

Analysis of patients 1, 2 and 3 was done in the Department of Human Genetics of University Hospital Eppendorf, in Hamburg, Germany. From patients 1 and 2 both cDNA and genomic DNA, and from patient 3 only genomic DNA was available for molecular genetic diagnostics ordered for clinical purposes. CPSI activity in liver and duodenum of patients 1 – 3 was severely reduced or absent. Patients 1 and 2 died within a few months after birth due to the severe

complications of CPSID. Patient 3 survived after an early liver transplantation. However, due to early hyperammonemia, she developed microcephaly, spastic tetraplegia, and is mentally retarded. Other patients have been described in the respective research papers cited in Table 3.

5.4.2 Production of the mutant enzyme forms

The mutant forms of CPSI bearing the clinical mutations presented in Table 3 were efficiently over-expressed in Sf9 cells. The distribution of the protein in soluble and insoluble fractions was similar to the wild-type CPSI, except for the mutant Q678P, which was poorly expressed and most of the protein was found in the insoluble fraction of the Sf9 cell extract.

In general, the mutants were correctly folded, which was documented by their CD spectra. However, the partial degradation of L1381S (not shown) did not permit its analysis by circular dichroism. The mutants S123F, Q678P, P1411L, R1453Q and Y1491H showed slight differences in their spectra respect to the wild-type CPSI, which gives a hint that the mutations may cause very small local structural changes still detectable by circular dichroism.

5.4.3 Effects of the clinical mutations on CPSI activity

Under the standard assay conditions, the synthesis of carbamoyl phosphate was undetectable (≤ 0.005 nmol/min/μg) in four (P774L, L1381S, R1453Q and R1453W) of the eleven mutants analyzed (Table 4). On the contrary, mutation G1376S had no effect on CPSI activity. Other mutations reduced the activity by approximately 45% (P1411L, S123F), 60% (H337R), 75% (Y1491H), 85% (Q678P), and 95% (T471N). For those mutants exhibiting detectable activity, the stoichiometry of the reaction was essentially equal to two molecules of ADP produced per molecule of carbamoyl phosphate, which is the normal rate for wild-type CPSI. When concentrations of NAG (0.1 mM), ATP (5 mM) and ammonia (1 mM) corresponding to the values near to those expected to be physiological within mitochondria were used, effects of the mutations paralleled those observed under standard assay conditions except for the T471N and Y1491H enzymes, for which the activity decreased.

All the mutants were reasonably stable, which was determined by measuring the production of carbamoyl phosphate after incubation of the wild-type and mutant enzyme forms at 42ºC, 44ºC, 46ºC, 48ºC, 50ºC and 55ºC. The lack of activity (measured as production of CP) of the mutants T471N, P774L, L1381S, R1453Q and R1453W excluded them from thermal stability studies, but for the rest of the mutants no changes or very light decreases (mainly in H337R and Q678P proteins) relative to the wild-type CPSI were observed in the thermal stability.

5.4.4 Influence of the mutations on the activity of the partial reactions

Three of the five mutations mapping at the 20-kDa C-terminal regulatory domain (G1376S, P1411L, and Y1491H) and one at the bicarbonate phosphorylation domain (T471N) did not disturb the partial reactions of bicarbonate-dependent ATP hydrolysis and ATP synthesis carried out at saturating concentrations of substrates and NAG. This suggests that the lower CPS activity caused by T471N, P1411L and Y1491H detected in the global activity measurements should not involve directly the two phosphorylation centers. On the contrary, for the other four regulatory domain mutants (P774L, L1381, R1453W and R1453Q) the activities of the partial reactions were undetectable (Table 4).

TABLE 4 Overall and partial CPSI activities of the clinical mutants and wild-type CPSI and on enzyme activation by NAG. Data from at least three different experiments correspond to the average ± standard deviation except for the column corresponding to the activation by AG that reflects the value of the activation constant (K_a^{AG}) ± standard error of the fit calculated by the Graph Path Prism Software. [a] Production of ADP and CP in the CPSI reaction was determined simultaneously in final time assays as it is described in methods; [b] Activity of partials reactions were monitored continuously as indicated in methods; [c] Dependence of CPSI activity on the concentration of N-acetylglutamate was assayed as indicated in methods for the determination of carbamoyl phosphate. Activation data of the global reaction were fitted to hyperbolic kinetics (see methods). [d,e,f] Mutations belonging to patients harboring the double mutations T471N-R1453W, Q678P-G1376S, P774L-R1453Q, respectively.

	CPSI reaction[a]			**Partial reactions[b]**	
	Rate at 10 mM NAG (µmol.min^{-1}.mg^{-1})		Activation by NAG[c]	Rate at 10 mM NAG (µmol.min^{-1}.mg^{-1})	
Enzyme	CP	ADP/CP	K_a^{NAG} (mM)	ATPase	ATP synthesis
Wild-type	1.31 ± 0.03	2.07	0.13 ± 0.01	0.19 ± 0.03	0.17 ± 0.03
S123F	0.51 ± 0.09	1.99	0.20 ± 0.02	0.12 ± 0.02	0.14 ± 0.02
H337R	0.38 ± 0.04	2.24	0.16 ± 0.04	0.06 ± 0.01	0.13 ± 0.03
T471N[d]	0.10 ± 0.02	1.80	4.90 ± 0.26	0.17 ± 0.03	0.13 ± 0.01
Q678P[e]	0.22 ± 0.02	1.92	0.21 ± 0.04	0.07 ± 0.04	0.05 ± 0.02
P774L[f]	ND	--	ND	ND	ND
G1376S[e]	1.32 ± 0.06	2.20	0.21 ± 0.04	0.16 ± 0.07	0.19 ± 0.05
L1381S	ND	--	ND	ND	ND
P1411L	0.83 ± 0.03	1.90	0.15 ± 0.02	0.18 ± 0.02	0.14 ± 0.05
R1453Q[f]	ND	--	ND	ND	ND
R1453W[d]	ND	--	ND	ND	ND
Y1491H	0.31 ± 0.01	2.40	6.9 ± 0.50	0.19 ± 0.02	0.19 ± 0.05

The mutants of the 40-kDa N-terminal domain showed similar decrease in the partial activities as in the overall reaction. The ATPase activity was decreased

by 40% in S123F and by 70% in H337R. Neither of the mutations produced significant effects on the ATP synthesis partial reaction (Table 4). Finally, mutation Q678P affecting the catalytic domain decreased approximately in the same extent (65-70%) both partial reactions.

5.4.5 Influence of the mutations on the activation of CPSI by NAG

Most of the clinical mutants (S123F, H337R, Q678P, G1376S, and P1411L) were activated by NAG indistinguishable from the wild-type CPSI and did not alter the hyperbolic dependence of CPSI activity on the concentration of NAG characteristic to the wild-type enzyme form. Contrarily, the main effect of the mutations T471N and Y1491H was focused on the NAG activation of the CPSI activity causing about 45- and 65-fold increase in the value of the activation constant (K_a^{NAG}), respectively. The four mutant enzymes P774L, L1381S, R1453Q and R1453W were unable to synthesize CP even at high concentration (100mM) of NAG.

5.5 Transmission of the allosteric signal (III)

5.5.1 Expression and purification of mutant enzyme forms

All of the mutant CPSI were purified in single step by Co^{2+} affinity chromatography and were easily over-expressed. No differences in the solubility were observed between them and they were reasonably stable as detected by SDS-Page of soluble and insoluble fractions of the protein extracts (results not shown).

5.5.2 Effects of the mutations in global and partial activities

The global CPSI activity was measured as production of CP and ADP, and also the activity for the partial reactions of bicarbonate-dependent ATP hydrolysis and ATP synthesis were determined. Using standard assay conditions both carbamoyl phosphate and ADP synthesis in the mutants was lower or negligible respect to the wild-type CPSI though the stoichiometry (ADP/CP ratio) of the overall reaction was correct being approximately 2. The mutation T471N reduced the CPSI global activity approximately 95%, and L1438T and Y1491H 75%. The mutants T1391V and T1394A synthesized CP 40-times less efficiently than the wild-type enzyme and N1449S reduced the CPSI global activity approximately 75%. P1439V and R1453Q enzymes did not show any detectable CPSI activity in the global reaction. For P1439V the stoichiometry of the reaction was measured in presence of 10% DMSO since P1439V was not activated by NAG. The stoichiometry resulted being normal.

For T1391V, P1439V and R1453Q also both partial reactions were greatly perturbed and below the detection limit. T1394 showed a great deal less activity

in the partial reactions, but the rest of the mutants, T471N, L1438T and Y1491H catalyzed the ATP hydrolysis and synthesis comparable to wild-type CPSI.

5.5.3 Effects of the mutations on activation by NAG and DMSO

Several mutations clearly affected the activation of CPSI altering the hyperbolic dependence of CPSI activity on the concentration of NAG. The K_a^{NAG} value increased markedly (370-850 times) in mutants T1391V and T1394A, and 10-80 times in mutants T471N, L1438T, N14491S and Y1491H. For P1439V and R1453Q it was not possible to determine the activation constant since these mutants were not activated even with 150 mM NAG suggesting complete lack of binding of the activator or disturbance of the transmission of the allosteric signal.

To further demonstrate that the lack of activation was because the mutations interfered with the activation, and not because of any structural or other catalytical effect, the enzyme activity was measured in the presence of 10 % DMSO. CPSI can be activated by cryoprotectants, though the activity is more or less 20% of that produced in the presence of NAG (Britton et al. 1981). The activation of P1439V was accelerated with DMSO reaching the values obtained for the wild-type CPSI. The rest of the mutants showed somewhat lower activities in the presence of DMSO as compared to the wild-type CPSI. It seems that the mutations stabilize non-active conformations, which can not be fully activated neither by unspecific effectors, such as DMSO or glycerol, nor by specific effectors (NAG).

5.5.4 Protein modeling

Rat liver CPSI shares 40% sequence identity with *E. coli* CPS (43.5% identity with the catalytic domain, 37.3% with the N-terminal domain, and 24.3% with the regulatory domain). We undertook a homology modeling of mammalian (*Rattus norvegicus*) CPSI using the structure of bacterial CPS (PDB 1jdb) and the fragment of the regulatory domain of human CPSI (PDB 2yvq) as templates and the MODELER program (Sali & Blundell 1993). Several models were generated working with slightly different alignments, and the models were evaluated with MODELER Dope Score function. The best energy model was selected for further analysis and its stereochemical quality was verified with Procheck (Laskowski et al. 1996). Superposition of the α-carbons of the 3-D-model and the *E. coli* CPS is very similar (~90% similarity), and thus, gives credibility to the model.

6 DISCUSSION

6.1 Production of recombinant CPSI (I)

When this study was initiated the recombinant mammalian CPSI had not yet been expressed in soluble and active form. Moreover, there was no suitable expression system to obtain the enzyme in active form and in sufficient amount to purify it. Purification of CPSI is important in order to confidently assay the partial reactions catalyzed by the enzyme, which reflect the first and the third steps of the CPS reaction. In 2003 Saaed-Koethe and Powers-Lee reported the heterologous expression of the ammonia-specific CPSI from frog *Rana catesbeiana*. Although the frog CPSI shares almost 80% identity with the mammalian enzyme, important interspecific differences seem to occur between both since purified frog enzyme but not the rat or pig enzyme can be crystallized. Moreover, if considered for to study the effects of clinical mutations detected in the patients with CPSI deficiency (CPSID) on the enzyme activity, this enzyme could not be used because of the relatively poor sequence identity with human CPSI. Recently, the expression of recombinant human CPSI in yeast (*Schizosaccharomyces pombe*) has also been described (Ahuja & Powers-Lee 2008), although with lower yield than with the baculovirus expression system used in the present study.

Our laboratory has a long history in studying CPS of *E. coli* and the native CPSI from rat liver. Therefore we undertook the challenge to produce recombinant mammalian CPSI for its use to characterize the pathogenic role of clinical mutations detected in the patients with CPSID, and on the other hand, to characterize the unknown binding site for the allosteric activator, NAG.

To produce recombinant CPSI, two different expression systems were proved: transfection of 293T cells with a geneticin-resistance expression vector coding for CPSI and recombinant baculovirus-infection of Sf9 insect cells. First, the expression of CPSI was studied in 293T cells by Western blotting and immunofluorescence. Transfection efficiency was estimated to be ~50% and, even though the transfected cells were selected with geneticin the expression

rate of CPSI did not improve. Poor transfection efficiency can be due to failures in expression vectors, cell type, transfection reagents, DNA sequences or undesirable signals in the DNA (Morrow 2008). However, the expression vector was cesium chloride-purified and linearized, which should improve the transfection efficiency since linearization enables stable transfection of the cells (Kiss-Toth et al. 2000) and CsCl-purification of the plasmid should eliminate, from the plasmid preparation, impurities that can be deleterious to the transfection efficiency (Kingston et al. 2003). Therefore the probable explanation for the failed selection with geneticin could be the loss of the plasmid from the transfected cells during the cell division though this possibility is not very well documented in the literature. Another explanation might be that the 293T cells are not able to process the needed quantities of protein correctly since the CPSI is very complex multidomain protein. Given that the correct intracellular localization of CPSI is also crucial for its correct folding, the precursor CPSI retaining the mitochondrial targeting signal might not had been correctly folded. Nevertheless, the yield of CPSI from 293T cells was not sufficient for the characterization of the enzyme activity since milligram quantities are needed to measure all the parameters of enzyme activities.

By means of the baculovirus expression system and using Sf9 insect cells (*Spodoptera frugiperda*) we finally succeeded in overexpressing a soluble and active form of recombinant CPSI from *Rattus norvegicus*. The yield was approximately 0.5-1 mg from 50 ml Sf9 insect cell suspension culture. The recombinant rat CPSI in our study was expressed as mature form without mitochondrial targeting signal, and its physiological and catalytic properties did not differ from those of the enzyme obtained from rat liver. This indicates that the structure of the recombinant CPSI faithfully imitates that of the native enzyme and that the His-tag incorporated to the N-terminal end of the recombinant CPSI does not affect the enzyme activity or the correct folding of the protein. Lepidopteran insect cells are able to produce high yields of mammalian proteins endowed with authentic post-translational modifications, such as oligomerization and phosphorylation, and unlike the reducing environment of *E. coli* cytoplasm the insect cells permit disulfide bond formation (Summers 2006, Hitcman et al. 2009). In addition, insect cells acylate the recombinant proteins correctly (Horstmeyer et al. 1996). CPSI is known to be post-traslationally modified by active site fatty acylation (Corvi et al. 2001). Besides to play role in signal transduction, protein acylation has been postulated to play a potential role in the regulation of aminoacid catabolism (Kirchner et al. 2009, Pérez-Chacón et al. 2010). Since our expression system uses Sf9 cells, a subclone of Sf21 (IBLB-Sf21AE) isolated from pupal ovarian tissue of the fall army worm, Spodoptera frugiperda (Vaughn et al. 1977), the recombinant CPSI should present all modifications correctly, and thus, the baculovirus expression system is a reliable and efficient method to produce recombinant mammalian CPSI.

6.2 Characterization of the binding site for N-acetyl-L-glutamate (I)

For long it has been known that CPSI is allosterically activated by N-acetyl-L-glutamate (NAG) (Grisolia & Cohen 1948, Hall et al. 1958), and that the activation is mediated by binding of the activator to the 20 kDa C-terminal regulatory domain (Rodriguez-Aparicio et al. 1989). However, the precise site and mode of binding of the enzyme activator has remained unknown. To characterize the binding site, several residues were mutated in this study and the effects of the mutations on enzyme activation by NAG were analyzed. The mutations were selected basing on a hypothesis that the residues that in CPS of *E. coli* bind the effector molecules would also be crucial for activator binding in CPSI. On the other hand, the enzyme activators NAG and IMP, and the inhibitor UMP, do not share same molecular structure or nature, and the residues in the allosteric site of bacterial CPS and CPSI are not fully conserved. However, the amino acids that in CPS anchor IMP and UMP to the enzyme (N1015, T1016, T1017 and S1026) forming hydrogen bonds with the ribose of the mononucleotides (Thoden et al. 1999a, 1999b, Pierrat & Raushel 2002), in the light of the results of this study have their equivalent residues in mammalian CPSI (N1437, L1438, P1439 and N1449, respectively) that also function interacting or lay nearby the enzyme activator, NAG. In addition, the residues equivalent to those that interact with the phosphate moiety of IMP and UMP (T1391, T1394 and W1410 in CPSI, and T974, T977 and K993 in *E. coli*, respectively), when mutated in CPSI, have even greater effect on the NAG-dependent activation of CPSI. In a contrary, residues implicated in ornithine-binding were discarded from the mutational study since the residues at equivalent position in CPSI are not conserved.

Finally, the crystal structure of a fragment of regulatory domain of human CPSI (PDB 2yvq) enabled the screening for cavities with VOIDOO (Kleywegt & Jones 1994). A single cavity was detected and its constitutive residues were identified. Seven of these residues (T1391, T1394, W1410, N1437, L1438, N1440 and N1449) were mutated in this dissertation work and predictions of interactions of the cavity with NAG were carried out and probed by mutagenesis. They affect in different extent both the NAG-dependent activation of CPSI and the apparent affinity for NAG. Contrarily, mutations of residues neighboring the pocket but predicted not to be involved in making the cavity have very little or no effect on the NAG binding and enzyme activation.

6.2.1 The cavity of the human CPSI regulatory domain

Since the structure of the C-terminal domain of hCPS (PDB file 2yvq) was obtained using the acellularly-produced, isolated domain there could be doubts on whether the structure is the genuine one or an artefact. However, despite of the poor sequence identity between the allosteric domain of human and *E. coli*

CPS (20% identity), these two structures are very similar both being an αβα open sandwiches in which the central parallel sheet of five elements (strand order, 32145) is covered on one side by helices 2, 1 and 5 and on the other side by helices 3 and 4. The structure of human CPSI is missing the last α-helix of the regulatory domain, which actually does not form a part of the regulatory domain but folds upon the two synthetic domains.

A single cavity was found in this structure, which could fit tightly a molecule of NAG. Amino acid sequences of the regulatory domain in rat and human CPSI are identical except for three semi-conservative substitutions and therefore it was assumed that both regulatory domains are structurally equivalent. The identified cavity is situated at the C-terminal region of the first β-sheet of the regulatory domain. The residues forming the NAG-binding cavity (L1363, I1364, G1365, I1366, T1391, T1394, W1410, I1423, N1437, L1438, N1440, N1449, I1452) (Fig. 12) are aligned with the residues that outline the allosteric UMP/IMP binding site of *E. coli* regulatory domain (L946, L947, S948,V949,T974, T977, K993, I1001, N1015, T1016, S1018, S1026, I1029), but in the bacterial regulator, the binding site is an open furrow on the surface of the protein, whereas in the human CPSI regulatory domain this furrow is not found. The site of the groove where the pyrimidine and purine rings of IMP and UMP lie, is in part occluded in the regulatory domain of CPSI by the side chains of the residues K1444, F1445, W1410 and D1448. Residues N1449 and N1442 partially fill the space occupied by the ribose (Fig. 12). On the surface of the CPSI regulatory domain a narrow entrance to the cavity can be observed (Fig. 12). This entrance is lined by residues, of which T1391 and T1394 are equivalent to those that in CPS of *E. coli* hydrogen bond to the phosphate moiety of the nucleotide effectors (T974 and T977).

6.2.2 Docking of NAG in CPSI

Initial docking experiments showed that the side chain of W1410 would impede the maximal fitting of NAG inside the cavity detected by VOIDOO (Kleywegt & Jones 1994). Thus, when flexibility of the side chains of W1410 and the overlying F1445 and Q1413 residues was permitted, a highly stable binding pose, where W1410 aromatic ring had flipped 180^{o} was created. This alternative conformation of W1410 side chain is commonly observed in proteins (Verdonk et al. 2003). The following calculations by means of this alternative protein conformation led to much better NAG docking scores. In the converged, energy-minimized binding solution, NAG adopts a largely extended conformation (Fig. 1 A & D, Publication I). Its α-COO^- and acetamido groups are oriented towards one wall and the floor of the pocket, respectively, while the glutamate side chain is oriented towards the pocket entry. This NAG binding mode results in appropriate interactions with the residues lining the cavity: the α-COO^- is surrounded by the N1440 and N1449 side chain amide groups on one side and by the NH-group of the flipped side chain ring of W1410 on the other side; the α-NH group forms a hydrogen bond with the side

chain of T1391; the carbonyl group points towards the N1437 side chain amide forming a hydrogen bond with this residue; the acetamido group is placed in a hydrophobic patch of residues L1363, and the γ-methyl of T1391, W1410, I1423 and I1452. The OH-groups of T1391 and T1394 are close to the solvent-facing NAG γ-COO^-, donating hydrogen bonds to it, and, finally, the C^{β} atom of the glutamate side-chain also points outwards, making contacts with the indolic ring of W1410.

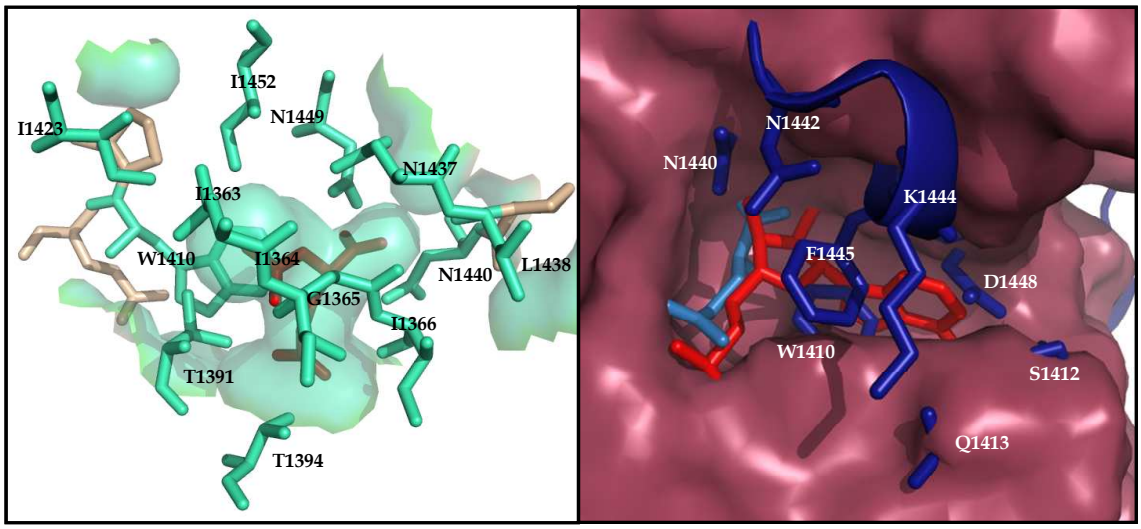

Figure 12 The NAG-binding cavity. On the left side are presented the residues that form the cavity in human CPSI regulatory domain, and NAG molecule adjusted into the cavity. On the right side are superimposed IMP and NAG in the IMP/UMP binding grove.

6.2.3 Identification of the NAG-binding residues by site-directed mutagenesis of CPSI

Out of the residues mutated in this study, the two threonines, 1391 and 1394, when replaced by valine and alanine, respectively, had greatest effect on the activation of CPSI by NAG. T1391 and T1394 are clearly implicated in the binding of the effector since the K_a for NAG of these mutants was 370 and 850-fold higher (for T1394A and T1391V, respectively) respect to the wild-type CPSI.

According to our docking results, T1391 and T1394 interact with the carboxyl end of NAG. One of the oxygens of T1391 can form a hydrogen bond with the acetylgroup and with the Oε of the carbonyl group of NAG. When T1391 is mutated to valine, the hydrogen bonds are lost. A decrease between 2 and 3 orders of magnitude in the apparent affinity for NAG would be expected according to the hydrogen bond removal predictions for both mutant enzymes (Fersht 1977), what is coincident with the experimental data. The $O\gamma^1$ of T1394 is able to form a hydrogen bond with the Oε of NAG. Excision of the side chain by

mutation to alanine would abolish the interaction of this residue with NAG, which in turn explains the reduced activation and very high K_a^{NAG}.

In *E. coli* CPS the side chain functional groups of T974 and T977 (equivalent to T1391 and T1394, respectively) form direct hydrogen bonds with the phosphoryl oxygens of the activator IMP (Thoden et al. 1999c). In addition, the backbone amide group of T977 also lies within a hydrogen bonding distance to two of the phosphoryl oxygens of the mononucleotides IMP and UMP. Since the threonine residues are conserved, their roles seem to be conserved in the evolution.

The C-terminal domain of all CPSs corresponds to methylglyoxal synthetase (MGS) of *E. coli* that has been crystallized (Saadat & Harrison 1999) and shares considerable structure similarity with CPSs. The known structures in MGS protein family show a common phosphate binding site (Murzin 1999) including the two important conserved threonines: Thr45 and Thr48 of *E. coli* MGS correspond to Thr974 and Thr977 of *E. coli* CPS, and to the threonines 1391 and 1394 of all CPSI of known sequence. This conservation is in accordance with their importance for the function of the protein and the essentiality for the binding of the effectors.

The mutation W1410K significantly lowers the activation of CPSI by NAG. W1410 forms part of the wall of the binding pocket for NAG, and when mutated to lysine, the cavity will deform and therefore the interactions of the remainder of residues with the activator would be affected. In addition, loss of important hydrophobic interactions also explains the effect of the mutation on the activation of CPSI. The hydrophobic interactions are predicted to take place between the indole ring of W1410 and the aliphatic part (carbons β and γ) of NAG. The distance between W1410 and NAG is minimal, and it seems logic that the side chain of W1410 must move to accommodate the activator in the binding pocket, which is also corroborated by our docking experiments. In fact, there is a loop, which does not solve in the crystal structure of human CPSI regulatory domain likely because of its motility. This loop that is connected to the α-helix containing W1410 must be flexible and seems to be important for the enzyme to adapt an active conformation.

Mutation of the residue equivalent to W1410 in CPS of *E. coli* (K993) to alanine disturbs the allosteric effects of IMP because of an increased dissociation constant as a consequence of the elimination of an interaction between the phosphoryl oxygen of the mononucleotide and the ε-amino group of the lysine (Fresquet et al. 2000). However, it is interesting to notify that mutation of the same residue to tryptophan does not affect the overall enzyme activity or the binding of IMP (Fresquet et al. 2000). The indolic ring of the tryptophan might replace K993 in its interaction with the phosphate, and the indolic ring would help to place the nucleotide correctly in the binding pocket. Interestingly, the mutant W1410K of the present study is better activated with an analogue of NAG, N-acetyl-β-phenylglutamic acid (PheNAG), in which the hydrogen atom linked to the β-carbon of NAG is replaced by a phenyl group. As our results show, enlargement of the binding pocket causes the 80-fold decrease in the affinity of W1410K to NAG and the improvement in the

activation constant with PheNAG since the analogue is bigger in size and can therefore be better accommodated in the binding pocket. In addition, this finding supports the interaction of the NAG C^{β} atom with W1410.

The increase of ~70-110-fold in the K_a^{NAG} caused by the N1437D and N1440D mutations agrees with the role of these asparagines as hydrogen bond donors to the NAG α-COO^- and acetamido carbonyl group. When Pierrat and Raushel (2002) mutated the homologous residue of *E. coli* CPS (N1015), the allosteric effects of IMP and UMP were completely lost. This residue in CPS forms a hydrogen bond with the 2'OH group of IMP's ribose moiety (Thoden et al. 1999a) and the role of this residue seems to be conserved in CPS and CPSI. Mutagenetic analysis of the equivalent residue of N1440 in *E. coli* has not been described in the literature.

6.2.4 Clinical importance of the identification of the NAG-binding site

Ureagenesis (ammonia detoxification) and CPSI activity are controlled by NAG, which is synthesized by NAG synthase (NAGS). NAGS deficiency also causes hyperammonemia because of a secondary CPSI deficiency, but this disease is treated successfully by administering N-carbamoyl-L-glutamate (carglumic acid, Carbaglu®), an NAG analogue that activates CPSI (Hinnie et al. 1997). Despite of the long-time knowledge of CPSI and NAG and the use of carglumic acid in the treatment of NAGS deficiency for nearly 30 years, the CPSI site for NAG, and thus the receptor for carglumic acid, has not been characterized.

Our findings about the NAG site/carglumic acid receptor open a way for identification of CPSID mutations that hinder NAG binding without compromising the enzyme catalytic machinery. This raises hopes for NAG analog-based treatments, including the design of NAG analogs that are tailored on the basis of specific NAG site mutations in CPSI. An example of such analog design, leading to improved mutant activation (by Phe-NAG), is documented in this dissertation work.

6.3 Clinical mutations of CPSI deficiency (II)

The clinical mutations selected for this study affect residues that are invariant in all the CPSI of known sequence. If also bacterial and other less evolved CPS from other organisms are considered, H337, T471, P774 and R1453 are invariant, and S123, Q678 and L1381 are highly conserved suggesting that they are structurally or functionally important residues. More variation can be observed for the three residues that lay on the 20 kDa regulatory domain, which is the domain with lowest sequence identity among different CPS: G1376 is very heterogeneous, the residues at the position equivalent to P1411 are charged residues in almost all CPS except for CPSI, and Y1491 is semi conserved as hydrophobic residue.

Though sequencing of the patients' genomic DNA is a relatively rapid method to detect mutations, it is not always reliable for a diagnosis since polymorphisms can be confounded with disease causing mutations (Summar et al. 2003) or non-sense mediated RNA decay can disturb the detection of disease-causing mutations (Eeds et al. 2006). In addition, as mentioned above, the CPSI gene is large (>120kb encompassing 37 introns and 38 exons, with 4500 coding nucleotides) (Häberle et al. 2003, Funghini et al. 2003, Summar et al. 2003), and thus the presence of a missense mutation does not automatically prove the disease-causative role. In some cases the enzymatic diagnosis of hyperammonemia can lead to misinterpretation on the type of metabolic alteration since several urea cycle disorders, such as N–acetyl-L-glutamate synthase (NAGS) deficiency, cause very similar symptoms (Elpeleg et al. 1990). Therefore it is important to test the specific effects of each mutation on the function and stability of CPSI. The standard testing procedure with most enzymes is to use site-directed mutagenesis and an *in vitro* expression system, as we have done in this study.

6.3.1 Suitability of the recombinant model to characterize CPSID

CPSI of *R. norvegicus* shares more than 95% sequence identity with human CPSI and therefore no significant differences in the function of the two enzymes should be expected. The baculovirus expression system resulted to be efficient in producing sufficient amount of recombinant CPSI, which is necessary to allow the analysis of the global activity, the partial reactions that reflect the two steps of phosphorylation catalyzed by the enzyme, and also the dependence of the enzyme activity of NAG. All this is important in order to understand the basis of the pathogenicity of the clinical mutations.

The baculovirus expression system for protein production is relatively rapid though it can not be compared to the very fast protein production in bacterial cultures. Nevertheless, our laboratory has tried unsuccessfully express CPSI in *E. coli*, which resulted in only insoluble protein probably due to the incorrect folding of this very complex mammalian protein.

The recombinant CPSI produced in baculovirus-insect cell system exhibits kinetic parameters for the substrates and dependence on the NAG concentration on the activity indistinguishable from those of the enzyme prepared from rat liver.

6.3.2 Pathogenic role of the clinical mutations

The results (activity and stability) obtained from the analysis of the recombinant CPSI mutant enzymes are consistent with the onset and evolution of the disease suffered by the patients harboring the natural mutations.

Onset and severity of the symptoms in CPSI deficiency are clinically correlated to the amount of ammonia in blood. The decreased or lacking CPSI activity observed in enzyme assays from biopsies or necropsies might be due to a malfunction of the enzyme or to a partial or complete absence of CPSI in the

liver either as a consequence of a failure in the expression or stability of its mRNA or due to protein instability. Neonatal onset of symptoms is generally accompanied by lacking or very low CPSI activity although in the majority of the reported cases only enzyme activity assays but not immunological CPSI detection has been performed impeding to conclude if the failure affected the level of enzyme present in liver or its functionality.

In our study, patients 4, 5, 6, and 8 (Table 3) have been reported to be homozygous in cDNA for the missense mutations L1381S, S123F, P1411L, and Y1491H, respectively (Summar et al. 1998). However, later it has been shown that the "missing allele" appears to be due to a nonsense-mediated decay (NMD) effect as it has been reported for patient 6 in which a premature termination codon (Q478X) has been found (Eeds et al. 2006). Therefore, the CPSI activity exhibited by these patients can only be displayed by the enzyme forms coded by the allele harboring the respective missense mutations.

Patients 1 and 7 are compound heterozygous, which carry in one allele a gross deletion resulting in non-functional truncated CPSI. Patient 1 bears two independent mutations, Q678P and G1376S, in one allele, and the deletion in the other, which causes a skipping of exon 8. Since G1376S is known as a CPSI polymorphism caused by G/A transversion in exon 35 of *CPS1* (Summar et al. 2003), the mutation Q678P would be responsible of the defective enzyme activity in the patient 1. Patient 7 carrying the mutation H337R in one allele, was shown to have in the second allele a deletion of 375 base pairs in frame (three-exon skipping), which was suspected to cause a loss of the CPSI activity (Aoshima et al. 2001). Thus, the enzyme with the mutation H337R would account to the measurable and deficient CPSI activity in patient 7.

Patients 2 and 3 carry different missense mutations in each allele: P774L and R1453Q (patient 2) and T471N and R1453W (patient 3). Mutations in both alleles would account to the final CPSI activity in these patients.

6.3.2.1 Late onset cases of CPSID

The CPSI activity exhibited by the liver of the patients 5, 6, 7 and 8 is exclusively originated from the enzymes displaying the mutations S123F, P1411L, H337R, Y1491H, respectively.

Purified S123F, P1411L, H337R and Y1491H enzymes display a reduced CPS activity (~50%, 55%, 40%, and 35%, respectively). Assuming a similar contribution of each allele to the CPSI activity, the expected activity in the liver would be 25%, 27.5%, 20%, and 17.5% (for Y1491H in physiological conditions due to the expected intramitochondrial NAG concentration this activity was 3%) in these patients, respectively, of that of a healthy control. Therefore the actual ability of these enzymes to detoxify ammonia is at the upper limit reported for late onset cases (see below) and would be enough under normal life conditions for the patient to survive. However, if the patient confronts a difficult situation in his/her life, such as stress, pregnancy or infection, these events can place an increased demand on the liver to metabolize ammonia, and

when the threshold is reached, plasma ammonia levels increase and result in life-threatening hyperammonemia (Wong et al. 2004).

The modest decrease in CPSI activity caused by P1411L mutation is in good agreement with the late onset type of CPSID (Summar 1998). The ~50% decrease in CPSI activity triggered by the mutation, would predict an enzyme activity in the liver cells of patient 6 (compound heterozygous for this mutation and a nonsense change) of about 25% of normal, possibly in the limit for substantial deficiency (Eather et al. 2006).

The 70-fold increase in the activation constant (K_a^{NAG}) caused by the Y1491H mutation limits very much the rate of synthesis of carbamoyl phosphate at the physiological range of intramitochondrial concentrations of NAG (0.1 mM), which clearly explains the pathogenicity of the mutation.

Mutations S123F and H337R affect very slightly the thermal stability of CPSI, which could partly contribute to the decrease in the amount of the available CPSI in the liver. Thus, the expected enzymatic activity found in the patients 5 and 7 seems to be in accordance with the activity values reported for the late onset patients. Although not all the reported late onset cases include data from enzymatic activity, the CPSI activity levels required for a normal ammonia detoxification can be generally stated according to the activity levels found in late onset patients who could live without problems until the onset of the disorder. CPSI activity measurements performed on late onset CPSID clinical reports vary from approximately 20% of the lower normal limit (Eather et al. 2006) to 30% of the lower value of the standard interval (Gómez-López et al. 2008). Lower activity values (9% of the lower normal limit) have been found in two siblings who had mental retardation and slow psychomotor development and avoided high-protein foods while their parents presented a 46% and 78% of CPSI activity (lower normal limit) and had no symptoms (McReynolds et al. 1981).

6.3.3 Early onset cases of CPSID

Reported CPSI activity in neonatal disorders varies from being under detection levels (Finckh et al. 1998) to minuscule activity (6% in a Japanese boy who died at day 28 of life; Aoshima et al. 2001b). In patients 2 and 3 that carry different missense mutations in each allele, P774L and R1453Q (patient 2) and T471N and R1453W (patient 3), expected liver activity would be an average of the contribution of the two mutant CPSI forms. In the case of patients 1 and 4 it would be only due to the contribution of only one CPSI form, Q678P/G1376S and L1381S, respectively.

The mutation Q678P has been described in a patient harboring the double mutation Q678P/G1376S and who died at an age of two months. G1376S is actually known as a CPSI polymorphism (Summar et al. 2003). The mutant Q678P was poorly expressed and the majority of enzyme appeared in the insoluble fraction of the baculovirus-infected insect cell extracts. The lack of consequences of the G1376S mutation and the impairment of the overall and partial reactions, as well as the stability of the Q678P mutant of CPSI confirm

that the mutation Q678P is causative of the clinical symptoms found in the patient, while mutation G1376S is without an apparent effect.

Mutations P774L and R1453Q have a dramatic effect inactivating almost completely all reactions of the enzyme what justifies their pathogenic character and agrees with the early onset type of CPSID in the patient carrying the mutations (patient 2).

The mutation T471N is expected to reduce the CPSI activity by ~85% at standard assay conditions. This mutant is almost inactive at physiological conditions because of the high K_a^{NAG} it presents, which together with inactive character produced by the mutation R1453W is in accordance with the neonatal onset of the metabolic disorder found in patient 3.

The inactive character of L1381S mutant of CPSI completely explains the early onset of the symptoms in the patient 4 carrying this mutation (Summar 1998).

6.3.4 Effects of the clinical mutations on CPSI

Since the clinical mutations detected in the patients are likely to cause important changes in the enzyme, we undertook a more complete characterization of the mutations with the aim to provide new insights into the function or structure of CPSI. In order to analyze the effects of the mutations on enzyme activity and to try to understand the impact of the clinical mutations on enzyme functionality, several activity and stability assays were performed. In addition to measuring the production of ADP and carbamoyl phosphate in the global reaction we assayed the ATPase and ATP synthesis partial reactions that reflect the different phosphorylation steps of the global reaction. Besides, we examined the dependence of CPSI activity on the concentration of the essential activator NAG.

6.3.4.1 Mutations affecting the N-terminal domain

The mutation S123F reduced the overall CPSI activity by 47% and the mutation H337R 60% respect to the wild-type CPSI. The most intriguing effect of the two mutations is that both of them selectively disturbed the ATPase partial reaction leaving the ATP synthesis unaffected, which suggests that there exists some type of intercommunication between the N-terminal and carboxyphosphate domain. The role of the 40 kDa N-terminal domain of CPSI is unknown but CPSII, CPSIII and bacterial CPS carry a glutamine amidotransferase activity in this domain (Hong et al. 1994, Rubio & Cervera 1995). It is tempting to propose that the small subunit-like region of CPSI constitutively triggers on the large subunit-like region the highly efficient use of ammonia that is characteristic for CPSI (Lusty 1983). According to this hypothesis the amino acids that are important in CPS of *E.coli* for glutamine binding and hydrolysis (Miran et al. 1991) would be important in ammonia management in CPSI. However, we have found out that the K_m for ammonia and bicarbonate are unaffected by the mutations (unpublished results) and therefore the hypothesis is not sustainable.

Larger mutagenetic study would be needed to judge the role of the N-terminal domain of CPSI though the present results suggest that the main role of this N-terminal region is to activate constitutively CPSI.

6.3.4.2 Mutations affecting bicarbonate phosphorylation domain

Since both partial reactions are retained but CPSI activity is practically abolished in the T471N mutant, the synthesis of carbamate or its channeling between the phosphorylation centers may be impaired. The corresponding residue in the *E. coli* CPS, Thr56, is near the carbamate tunnel, an intramolecular tunnel that links the two phosphorylating active sites of the enzyme allowing the channeling of the unstable carbamate intermediate. Blockage of the ammonia tunnel (Fan et al. 2009) or perforation of its wall (Kim & Raushell 2004) prevents the migration of intermediates or causes its leakage, respectively. The effects of the T471N mutation on the overall and partial reactions and the predicted location of the residue Thr471 match well with a tunnel impairment hypothesis.

The mutation Q678P was detected in the patient with CPSI deficiency as double mutation with G1376S. G1376S does not change the overall neither the partial activities, and as demonstrated experimentally, the mutation Q678P causes the clinical symptoms found in the patient.

The equivalent residue of Q678 in CPS of *E. coli* (Q262) is located in an α-helix belonging to the ammonia tunnel (Thoden et al. 1997, Thoden et al. 1999, Kim & Raushel 2004) and perturbation of this α-helix can affect the enzyme structure rendering it unstable. The reduced solubility and stability of Q678P is in accordance with the helix-breaking possibility of the mutation and therefore it is understandable that the mutation causes an 80% decrease in the enzyme activity. The homologous mutation in *E. coli* CPS (Q262P) also decreased the stability of the enzyme (Yefimenko et al. 2005).

It has been reported that interdomain interactions stabilize importantly the *E. coli* CPS (Cervera et al. 1993) and, in the bacterial enzyme, Gln262 along with several preceding residues mediate water-bridged interdomain interactions (Thoden et al. 1999). Therefore the helix-breaking properties of the Q262P (*E. coli*) and Q678P (rat) mutations can explain the decreased stability and activity of the mutants Q262 (Yefimenko et al. 2005) and Q678P of the present study because they disturb the α-helix, cause local disordering, and abolish the stabilizing interdomain interactions.

The residue equivalent to P774 in *E. coli* CPS, which is P360, has been previously mutated (Yefimenko et al. 2005). Mutation P360L rendered the enzyme supersensitive to ornithine and increased significantly the K_m for the nucleotide substrates of the two partial reactions. In the present study the lack of activity of P774L mutant impeded further kinetic analysis, but as is the case for the equivalent mutation in CPS described above, the mutation strongly disturbs the two phosphorylation steps. The location of P360 in *E. coli* CPS at the boundary between both phosphorylation domains and near the important

K-loop (Rochera et al. 2002) suggests that the residue is involved in allosteric signal transmission.

6.3.4.3 Mutations affecting the C-terminal regulatory domain

The clinical mutations affecting the regulatory domain were expected to affect the binding of the allosteric activator, NAG, but the experimental results showed that the hypothesis was incorrect.

The mutation L1381S completely inactivated the enzyme, and the activity was not augmented with higher concentrations of NAG, which reflects that the mutation does not affect the binding of the allosteric activator. The change of the large hydrophobic side chain of L1381 for that of the polar serine seems to cause an important local disorder with fatal consequences in the activation and stability of the enzyme. L1381 is highly conserved among known CPS, and when observed in the crystal structure of human CPSI regulatory domain (PDB 2yvq), it is located at the end of an external α-helix, in an important hydrophobic patch together with V1377, L1388 and F1386. Interactions between these residues must be crucial to maintain the correctly folded state of the regulatory domain since change in only one of the non-polar residues provokes rapid degradation of the protein.

The mutation P1411L decreased relatively slightly the overall CPSI activity but did not affect the partial reactions. P1411 is surrounded by hydrophobic residues, and thus mutation of P1411 to leucine would not disturb this hydrophobic site. Therefore the moderate effect of the mutation could be due to steric hindrance caused by the bulky side chain of leucine. The site where P1411 is located in the human CPSI regulatory domain is limited in size and hence the mutation would disturb the proximate residues V1333 and I1408, which was probed by using PyMOL utilities.

The residue R1453 is totally conserved among all the documented CPS sequences, which reflects its structural and/or functional importance. Mutation of R1453 to glutamine or tryptophan inactivates completely all reactions catalyzed by the enzyme independently of the concentration of NAG used in the assay. It seems that R1453Q provokes the enzyme to obtain an inactive conformation or disturbs the allosteric signal transmission.

The mutation Y1491H enables the enzyme to carry out the partial CPSI reactions but decreases the overall activity by 65%. The activation of the mutant by NAG is greatly perturbed (70-fold increase in K_a^{NAG}). Although Y1491 varies among the members of the CPS family, in the majority of species the hydrophobic character of the residue is conserved. Therefore it is likely that the substitution of the hydrophobic tyrosine by the charged histidine causes a local perturbation in the regulatory domain of the Y1491H mutant that impairs the activation of the enzyme by NAG.

6.4 Towards understanding of allosteric signal transmission (III)

Since carbamoylphosphate synthetases are key enzymes in regulating important metabolic pathways, it is evident that they must be strongly regulated. CPSI is allosterically regulated by NAG (Grisolia & Cohen 1953), which is synthesized by NAG synthase (NAGS) (Caldovic & Tuchman 2003). NAGS in turn is activated by arginine produced in the urea cycle. *E. coli* CPS is feedback inhibited by the end product, UMP, of the biosynthetic route in which it plays a key role (Meister 1989), and activated by ornithine and IMP, which, however, is a weak activator (Cervera et al. 1993, Bueso et al. 1994). The effectors of all the CPS modulate the activity and affinity of the enzyme to the substrates, essentially to ATP.

Though the structure, allosteric sites and catalytical mechanism are now well characterized in CPS, there is little information about the transmission of the allosteric signal to the catalytic sites. The catalytic sites are located far away from each other (Thoden et al. 1997, 1999) and major conformational changes upon effector binding are described to take place for the signal to be transmitted (Potter & Powers-Lee 1992, Hart & Powers-Lee 2009).

In *E. coli* CPS despite of the conformational changes that have been shown to be important in allosteric regulation (Johnson et al. 2007), the potassium-binding loop and changes in the carbamate tunnel are important in ornithine-derived enzyme activation (Delanney et al. 1999, Rochera et al. 2002)

According to the present results in NAG binding site of CPSI there are two important threonines, 1391 and 1394 that in addition to bind the enzyme activator (Fig. 13) also play a role in signal transmission since when these threonines are mutated, CPSI is unable to be fully activated even at high concentrations of NAG. It has also been shown that there must occur a conformational change upon NAG binding since NAG can not be docked computationally to the NAG binding cavity in CPSI if the side chain of W1410 is not shifted (Pekkala et al. 2009). W1410 is at one end of a flexible loop that does not solve in the crystal structure of human CPSI regulatory domain perhaps because its mobility (Fig. 13). Therefore, in addition to the signal that originates from T1391 and T1394, this conformational shift provoked by W1410 upon NAG binding could be passed to nearby residues, such as F1445 and N1449 (Fig. 13 and Publication III). Mutation N1449S disturbs the activation of CPSI by NAG and the mutant enzyme does not reach the V_{max} of wild-type CPSI. This asparagine locates in an α-helix that leads to R1453 (Fig. 13). The present work documents that the mutant CPSI form, R1453Q, is completely inactive in the presence of NAG or DMSO, which suggests that the mutation completely blocks the allosteric signal transmission. Though CPSI can be normally activated by cryoprotectants, it seems that the mutation R1453Q stabilizes a non-active conformation of the protein, which can not be fully activated neither by unspecific effector, DMSO, nor by a specific effector, NAG. R1453 could

function as bottleneck to pass information from the effector binding site to the catalytic domains of CPSI.

On the other hand, the conformational change can affect the stacked Y1491 located at the beginning of the last α-helix of the C-terminus, which folds upon the synthetic domains and moreover stays just between them, and therefore this helix does not actually belong to the allosteric domain of CPSI (Fig. 13). Though Y1491 is not located at the NAG binding pocket, the mutation Y1491H importantly affects the activation constant of CPSI but does not significantly lower the overall or partial CPSI activities, which indicates its contribution to allosteric signal transmission. This result is in accordance with the results obtained with *E. coli* CPS since deletion of the C-terminal helix of eCPS has been shown to completely abolish the enzyme activation (Marshall & Fahien 1988).

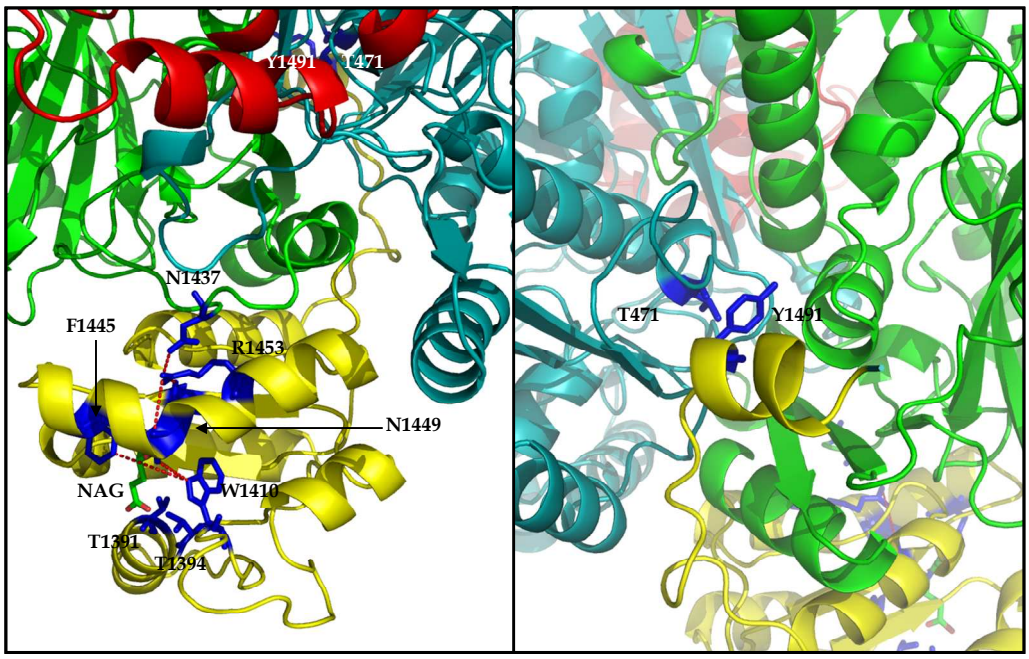

Figure 13 Location and interactions of residues implicated in the allosteric signal transmission.

According to rat CPSI protein modeling, residue T471 is encountered in close association with Y1491 in an important hydrophobic patch of residues near the ending of the carbamate tunnel. Though Thr side-chain has a hydroxyl group, which is polar, the 3-carbon chain of Thr (Cα, Cβ and Cγ) is not polar and is found with high frequency in hydrophobic clusters of proteins, with the OH group branching out away from the cluster. The phenotype of CPSI mutant T471N is similar to that of Y1491H and therefore it seems that residues in the vicinity of the intramolecular tunnel play an important role in the allosteric control as was already proposed by Thoden et al. (1997). In agreement with the role of T471 and Y1491 are the results of Hart and Powers-Lee (2009) that show through a mutational analysis of Cys1327 and Cys1337 of CPSI the importance

of conformational changes at the boundary of the carbamate phosphorylation and regulatory domains for CPSI activation. However, the disulfide bond formation must involve gross conformational changes since the cysteins are placed at approximately 23 Å from eachother.

In conclusion, the present study highlights a set of amino acid residues involved in the allosteric signal transmission in CPSI and suggests a route for the transmission, which would originate from T1391 and T1394 and from conformational changes triggered by the shift of W1410. The signal would then be passed to R1453 that could function as a bottleneck in passing information to the catalytic domains. The last α-helix of the C-terminal domain also plays an important role and from this helix different networks of interactions or conformational changes must control the two phosphorylation centers. However, since the phenotype of the two mutants at the boundary of the two synthetic domains studied here, T471N (closer to the bicarbonate phosphorylation site) and Y1491H (closer to the carbamate phosphorylation site) do not differ from each other specifically related to partial reactions, larger mutational analysis is needed to differentiate in the allosteric control of the two catalytical sites.

6.5 Future prospects

The structure of the human CPSI regulatory domain (PDB 2yvq) does not correspond to the whole regulatory domain since 22 amino acids from the most C-terminal end are missing. However, the successful crystallization of this domain encouraged us to begin the construction of various expression vectors to produce the CPSI regulatory domain in Sf9 insect cells. A further the goal is to optimize crystallization of the regulatory domain in the presence of NAG, or to solve the structure in the presence of the activator by nuclear magnetic resonance. Finally, if we succeed to solve the 3-D structure, the purpose is to crystallize piece by piece all the domains of CPSI. The most important goal would be to understand the function and meaning of the N-terminal domain of CPSI since it differs functionally from that of the N-terminal domain of prokaryotic CPS.

Recently it has been shown that mitochondrial lysine deacetylase, SIRT5, activates CPSI. It may be possible that failed interaction between these two proteins could provoke CPSID. Indeed, it is not documented how and at which site SIRT5 deacetylates CPSI and through which amino acids they interact. Therefore we want to study the substrate specificity of SIRT5 and exact deacetylation site/s using as a tool the recombinant CPSI produced in our laboratory. Taken into account the important role of sirtuins it is valuable to obtain information of how they interact with the target substrates since this knowledge permits development of specific sirtuin inhibitors/activators useful for treatment of metabolic and aging-related diseases.

Ornithine transcarbamylase (OTC) was the pioneer candidate of all the urea cycle enzymes for gene therapy trials. In 1999 it was shown in mice that recombinant adenoviruses carrying OTC cDNA finally yielded an efficient mitochondrial import of OTC and correction of OTC deficiency (Zimmer et al. 1999). However, when the same procedure was used for a human patient the consequences of this gene therapy trial were fatal since the patient died. The collapse was due to the uncontrolled vector transduction, which hit not only the direct organ, but also all the other organs of the patient (Marshall 1999). The setback led to intense investigation of adenovirus vectors, which nowadays have been modified to be much safer. However, in some of the latest gene therapy trials in mice, where *OTC* gene was used, the treated mice lived longer than the control mice (Moscioni et al. 2006), but during the trials the mice showed increased risk of tumor formation (Bell et al. 2006). It appears that the adenoviral gene transfer vectors may contribute to tumor arousal.

Since in numerous current gene therapy projects baculoviruses have been used very efficiently and safely for gene delivery (Hu 2008) it would be interesting to considerate, as an ultimate goal of this project, to construct a baculoviral vector for gene delivery to patients suffering from carbamoyl phosphate synthetase I deficiency. Nevertheless, the expression vector described in the present thesis could not be used since the promoter would not be efficient in mammalian cells. Therefore in the future the vector should be modified for the future experiments in mammalian cells. The baculoviruses have many good characteristics for safe gene therapy since they do not replicate in mammalian cells, which in turn excludes secondary effects that for example adenoviruses can cause (inflammatory effects and tumor formation due to uncontrollable cell proliferation) (Russell 2000). As many mitochondrial proteins that are synthesized in the cytoplasm, CPSI should be introduced to liver cells as precursor protein which then would be imported to the liver mitochondria and processed. Since CPSI is almost exclusively expressed in liver therefore no targeting of the gene delivery vector should be needed. In conclusion, the techniques used for this thesis can open a way for a more profound application of recombinant baculoviruses: a gene therapy trial to cure CPSID, which nowadays does not have any efficient treatment.

7 CONCLUSIONS

1. Recombinant CPSI (of *Rattus norvegicus*) can be efficiently produced in insect cells by baculovirus expression system, and the recombinant enzyme faithfully imitates all the properties of the native CPSI purified from rat liver, which permits its use to structural and functional studies.

2. The recombinant rat CPSI served as model to identify the binding site for the allosteric activator, NAG, and to study the effects of the clinical mutations detected in patients with CPSI deficiency. The recombinant expression system developed in this study is a reliable and relatively fast tool to test the pathogenicity and disease-causing role of clinical mutations.

3. The effects of the clinical mutations of early onset CPSID that were studied using recombinant CPSI are in accordance with the clinical symptoms and prognosis presented by the respective patients suffering from CPSI deficiency. However, in the late onset cases the activity of the recombinant enzymes cannot always straightforward explain the detrimental outcome of the mutation found in the respective patient.

4. The hypothesis for the binding site for NAG in CPSI was proved by site-directed mutagenesis of residues T1391, T1394, W1410, N1437 and N1440. In addition, the binding site and the interactions of NAG with these residues were proved by automated docking. The experimental results of the hypothetical NAG-binding residues that were mutated in the present work are in accordance with the cavity that was found in the crystal structure of a fragment of the regulatory domain of human CPSI (PDB 2yvq).

5. Several of the mutations studied in this thesis seem to be involved in the transmission of the allosteric signal from the binding site of the CPSI activator, NAG, to the catalytic centers in the phosphorylation domains. These residues are T471, T1391, T1394, P1439, R1453 and Y1491.

6. The 3-dimensional model of CPSI help to interpret the results of the present study and give hints of the possible route of the allosteric signal, opening therefore possibilities to new mutagenetic studies, which might determine the residues implicated in the transmission.

Acknowledgements

I owe my deepest gratitude to my supervisor, Dr. Javier Cervera (at Centro de Investigación Príncipe Félipe, Valencia, Spain) for giving me the opportunity to perform my dissertation work in his lab. In addition to provide me first-class facilities, Javier has let me grow into an independent researcher. I thank also my other supervisor, Professor Jaana Bamford (Department of Biological and Environmental Sciences, at the University of Jyväskylä, Finland) for always helping me with the grants and providing good advice. My first lab experiences at the University of Jyväskylä I owe to my earlier professor, Markku Kulomaa, and my earlier colleagues Dr. Mervi Ahlroth and Dr. Varpu Marjomäki, who really inspired me to be a scientist. Thank you very much, "Kuku", Mervi and Varpu.

I thank my reviewers, Professor Kari Keinänen and Professor Tomi Airenne for their careful reading of this thesis and their valuable comments and advice in improving the final version.

I am grateful to all my collaborators in the publications. Especially I thank our "protein and structure expert", Belén Barcelona, and my best colleague, Ana Martinez, with who I shared not only the lab tasks but also the bad and good moments in the everyday life and in the science. A special acknowledgement goes also to Dr. Igor Yefimenko for helping me at the beginning of my thesis. I am also very grateful to Dr. Vicente Rubio who has been very important in writing the manuscripts and in all scientific discussions.

The nice atmosphere that prevails in our research group has been very valuable in everyday life. Sharing good and bad experiences with Paquita Ripoll, Ana Martinez, Cristina Alcantara, Belén Barcelona, Paco Carmona, Roberto Gozalbo, Jesus Rodriguez, Lorena Pérez, and Vicente Fresquet has provided me a great help in surviving in the turmoil of the science.

One of the most important persons for me in ongoing during this long PhD student time have been with no doubt my mother, Heli, and my sister, Sari. Thank you for always being so loving, encouraging and supportive. I could not imagine a life without my family.

And I could never leave without mentioning the tight network of my friends in Spain – thanks to you: Cristina Segurola, Pablo Ponce, Isabel López, Dioni López and Migue Herreras. I have shared so many troubled days and so nice moments and relaxing conversations with you guys!! And in the latest months of writing my thesis I got to know my loving boyfriend, Saúl, who has been very supportive and has always understood my changing attitudes…

This study was financially supported by Fundación Valenciana de Investigaciones Biomédicas, Spanish Ministry of Science and Education and Nyyssösen Säätiö.

YHTEENVETO (RÉSUMÉ IN FINNISH)

Karbamyylifosfaatti syntetaasi I:n puutteen patologian toiminallinen karakterisaatio ja entsyymin aktivaattorin sitoutumiskohdan identifikaatio

Jo 40 vuoden ajan on tiedetty, että karbamyylifosfaatti syntetaasi I:n puute (engl. carbamoylphosphate synthetase I deficiency, CPSID) aiheuttaa vastasyntyneillä lapsilla hyperammonemiaa, mikä johtaa koomaan ja aikaiseen kuolemaan. Hyperammonemian patologisiin mekanismeihin lukeutuvat solun energiametabolian häiriöt, astrosyyttien paisuminen, aksonien kasvun häiriytyminen ja muutokset useissa neurotransmitterisysteemeissä. CPSID luokitellaan harvinaisiin sairauksiin, sillä sen esiintymistiheyden on arvioitu olevan 1/62000 USA:ssa, 1/539000 Suomessa ja 1/800000 Japanissa. Todennäköisesti nämä luvut ovat kuitenkin aliarvioituja, koska useat vastasyntyneet, joilla on mutaatioita karbamyylifosfaatti syntetaasi I:a koodaavassa geenissä, kuolevat ennen lopullista diagnoosia.

Karbamyylifosfaatti syntetaasi I (CPSI) on multidomeeninen ureasyklin entsyymi, jonka tarkoitus on ihmiskehossa detoksifioida proteiinien kataboliassa syntyviä ammoniumioneja. N-asetyyli-L-glutamaatti (NAG) kontrolloi allosteerisesti CPSI:a, joka katalysoi maksassa yhden merkittävimmistä biokemiallisista reaktioista: karbamyylifosfaatin (CP) muodostamisen ammoniumionista, bikarbonaatista ja kahdesta ATP-molekyylistä. CP toimii porttina joko pyrimidiinien biosynteesissä tai arginiinin ja/tai urean muodostuksessa.

Kliiniset mutaatiot *CPS1* geenissä aiheuttavat CPSID:n. Ottaen huomioon geenin suuren koon (>120kb, 37 intronia ja 38 eksonia, joista 4500 nukleotidia koodaavaa aluetta) ei mutaatioiden detektio ainoastaan genomisen DNA:n tasolla (nopein sairauden diagnostiikkamenetelmä sairaalalaboratorioissa) välttämättä osoita, että ne ovat CPSID:n syy. Siksi on tärkeää testata jokainen mutaatio diagnoosin osoittamista varten toiminnallisesti. Tässä väitöskirjassa on karakterisoitu CPSID-potilailta löydettyjen 11 geneettisen pistemutaation patogeenisyyttä. Mutaatioista neljä ovat uusia ("novel"), jotka löydettiin yhteistyössä saksalaisen sairaalalaboratorion kanssa. Projektissa tuotettiin ensin nisäkkään rekombinanttia CPSI:a bakulovirus-hyönteissolu-systeemin avulla, ja puhdistettiin entsyymi his-tagia hyväksikäyttäen. Halutut mutaatiot CPSI:iin tuotettiin paikkaspesifisen mutageneesin avulla, ja tutkittiin mutaatioiden vaikutusta entsyymin toimintaan ja stabiilisuuteen. Mutaatioista kolme inaktivoivat entsyymin täydellisesti ja loput osittain, ja lisäksi yksi aiheutti entsyymin epästabiilisuuden.

Tutkimuksen tulokset rekombinanteista mutanttientsyymeistä, jotka ovat täysin yksimielisiä kliinisten tulosten kanssa, osoittavat, että rekombinantti CPSI ja paikkaspesifinen mutageneesi ovat täysin päteviä mutaatioden patogeenisyyden testauksessa. Lisäksi tulokset mahdollistavat mutaatioiden

aiheuttamien rakenteellisten ja toiminnallisten vaikutusten identifionnin ja tuottavat uusia näkökohtia CPSI:n toiminnasta.

Ottaen huomioon CPSI:n tärkeä biokemiallinen rooli, on selvää, että sen allosterisen säätelyn täytyy olla kurinalaista. Tähän asti CPSI:n aktivaattorin, NAG:n, tarkkaa sitoutumiskohtaa entsyymin säätelydomeenissa tai allosterisessa signaalin siirrossa toimivia aminohappoja ei kuitenkaan ole tunnettu. Me identifioimme dockingin avulla NAG:n sitoutumiskohdan ihmisen CPSI:n C-terminaalisen domeenin kristallirakenteessa, joka tallennettiin Protein Databankiin Riken Structural Genomics/Proteomics Consortiumin toimesta. Dockingin tuloksena NAG asettuu domeenissa kohtaan, joka tarjoaa sopivia aminohappotähteitä NAG:n sitoutumiseen. Näiden aminohappojen paikkaspesifinen mutageneesi ja bakulovirus-hyönteissolu-systeemin avulla tuotettujen mutanttientsyymien aktivaation analyysi *in vitro* osoittavat dockingin tulokset päteviksi. Tulokset antavat myös preliminäärisiä tietoja aminohappotähteistä, jotka aktivaattorin sitoutumisen lisäksi toimivat allosteerisen signaalin siirrossa CPSI:n katalyyttisiin domeeneihin. Olemme tehneet lisäkokeita näistä mutanttientsyymeistä ja lisäksi analysoineet tarkemmin kolme kliinistä CPSI mutanttientsyymiä, joissa signaalin siirto on selvästi häiriytynyt.

Tutkimusprojektin viimeinen päämäärä, joka ei kuitenkaan ole osa tätä väitöskirjaa, on kehittää bakulovirukseen perustuva geeniterapiavektori. Lukemattomissa geeniterapia projekteissa bakulovirusta on tehokkaasti ja turvallisesti käytetty geenin siirrossa. Tarkoituksena on tuottaa duaali bakulovirusvektori, joka koodaa CPSI:n prekursoriproteiinia, ja toisaalta maksa-spesifisen geenin siirron aikaansaamiseksi manipuloida viruksen vaippaa baculovirus display-teknologian avulla.

REFERENCES

Ahuja, V., Powers-Lee, S. G. 2008. Human carbamoyl-phosphate synthetase: Insight into *N*-acetylglutamate interaction and the functional effects of a common single nucleotide polymorphism. J. Inherit. Metab. Dis. 31: 481-491.

Alonso, E., Cervera, J., García-España, A., Bendala, E., Rubio, V. 1992. Oxidative inactivation of carbamoyl phosphate synthetase (ammonia). Mechanism and sites of oxidation, degradation of the oxidized enzyme, and inactivation by glycerol, EDTA, and tilo protecting agents. J. Biol. Chem. 267: 4524-4532.

Alonso, E., Rubio, V. 1995. Affinity cleavage of carbamoyl-phosphate synthetase I localizes regions of the enzyme interacting with the molecule of ATP that phosphorylates carbamate. Eur. J. Biochem. 229: 377-384.

Anderson, P. M. 1976. A glutamine- and N-acetyl-l-glutamate-dependent carbamyl phosphate synthetase activity in teleost *Micropterus salmoides*. Comp. Biochem. Physiol. 54B: 261-263.

Anderson, P. M. 1980. Glutamine- and N-acetylglutamate-dependent carbamoyl phosphate synthetase in elasmobranchs. Science 208: 291-293.

Anderson, K. S. 1999. Fundamental mechanisms of substrate channelling. Methods. Enzymol. 308: 111-145.

Anderson, P. M., Meister, A. 1965. Evidence for an activated form of carbondioxide in the reaction catalysed by *Escherichia coli* carbamoyl phosphate synthetase. Biochemistry 4: 2803-2809.

Anderson P. M., Meister A. 1966. Control of *Escherichia coli* carbamoyl phosphate synthetase by purine and pyrimidine nucleotides. Biochemistry 5: 3164-3169.

Aoshima, T., Kajita, M., Sekido, Y., Kikuchi, S., Yasuda, I., Saheki, T., Watanabe, K., Shimokata, K., Niwa, T. 2001. Novel mutations (H337R and 238-362del) in the *CPS1* gene cause carbamoyl phosphate synthetase deficiency. Hum. Hered. 52: 99-101.

Aoshima,T., Kajita, M., Sekido, Y., Mimura, S., Itakura, a., Yasuda, I., Saheki, T., Watanabe, K., Shimokata, K., Niwa, T. 2001. Carbamoyl phosphate synthetase I deficiency: molecular genetic findings and prenatal diagnosis. Prenat. Diagn. 21: 634-637.

Batshaw, M. L. 1994. Inborn errors of urea synthesis. Ann. Neurol. 35: 133-141.

Bell, P., Moscioni, A. D., McCarter, R. J., Wu, D., Gao, G., Hoang, A., Sanmiguel, J. C., Sun X., Wivel, N. A., Raper, S. E., Furth, E. E., Batshaw, M. L., Wilson, J. M. 2006. Analysis of tumors arising in male B6C3F1 mice with and without AAV vector delivery to liver. Mol. Ther. 14: 34-44.

Bergmeyer, H. U. 1986. Methods in Enzymatic Analysis, 3rd edn. Weinheim: Verlag Chemie.

Bradford, M. M. 1976. A rapid and sensitive method for the quantitation of microgram quantities of protein utilizing the principle of protein-dye binding. Anal. Biochem. 72: 248-254.

Braissant, O., Henry, H., Villard, A. M, et al. 2002. Ammonium-induced impairment of axonal growth is prevented through glial creatine. J. Neurosci. 22: 9810-9820.

Britton, H. G., Rubio, V., Grisolia, S. 1979. Mechanism of carbamoyl phosphate synthetase. Properties of the two binding sites for ATP. Eur. J. Biochem. 102: 521-530.

Britton, H., Rubio, V., Grisolia, S. 1981. Synthesis of carbamoyl phosphate by carbamoyl phosphate synthetase I in the absence of acetylglutamate. Activation of the enzyme by cryoprotectants. Biochem. Biophys. Res. Com. 99: 1131-1137.

Britton, H. G., Garcia-España, A., Goya, P., Rozas, I., Rubio, V. 1990. A structure-reactivity study of the binding of acetylglutamate to carbamoyl phosphate synthetase I. Eur. J. Biochem. 188: 47-53.

Brusilow, SW., Maestri, NE. 1996. Urea cycle disorders: diagnosis, pathophysiology, and therapy. Adv. Pediatr. 43: 127-70.

Brusilow, S. W. & Horwich, A. L. 2001. Urea cycle enzymes. In The metabolic and molecular bases of inherited disease (Scriver, C. R., Beaudet, A. L., Sly, N. S., Valle, P., eds), vol 2, p. 1909, McGraw-Hill, New York.

Brusilow, S. W. 1985. Disorders of the urea cycle. Hosp. Prac. 20: 65-72.

Bueso, J., Lusty, C. J., Rubio, V. 1994. Location of the binding site for the allosteric activator IMP in the COOH-terminal domain of *Escherichia coli* carbamyl phosphate synthetase. Biochem. Biophys. Res. Commun. 203: 1083-1089.

Bueso, J., Cervera, J., Fresquet, V., Marina, A., Lusty C. J., Rubio, V. 1999. Photoaffinity labeling with the activator IMP and site-directed mutagenesis of histidine 995 of carbamoyl phosphate synthetase from *Escherichia coli* demonstrate that the binding site for IMP overlaps with that for the inhibitor UMP. Biochemistry 38: 3910-3917.

Butterworth, R. F. 2000. Glutamate transporter and receptor function in disorders of ammonia metabolism. Ment. Retard. Dev. Disabil. Res. Rev. 7: 276-279.

Butterworth, R. F. 2002. Pathophysiology oh hepatic encephalopathy: a new look at ammonia. Metab. Brain. Dis. 17: 221-227.

Caldovic, L., Tuchman, M. 2003. N-acetylglutamate and its changing role through evolution. Biochem. J. 372: 279-290.

Carrey, E. A., Campbell, D. G., Hardie, D. G. 1985. Phosphorylation and activation of hamster carbamyl phosphate synthetase II by camp-dependent protein kinase. A novel mechanism for regulation of pyrimidine nucleotide biosynthesis. EMBO J. 4: 3735-3742.

Case, D. A., Cheatham, T. E. III, Darden, T., Gohlke, H., Luo, R., Merz, K. M. Jr., Onufriv, A., Simmerling, C., Wang, B., Woods, R. 2005. The Amber biomolecular simulation programs. J. Computat. Chem. 26: 1668-1688.

CCP4 (Collaborative Computational Project, Number 4) 1994. The CCP4 Suite: programs for protein crystallography. Acta. Crystallogr. D 50: 760-763.

Cervera, J., Conejero-Lara, F., Ruiz-Sanz, J., Galisteo, M. L., Mateo, P. L., Lusty, C. J., Rubio, V. 1993. The influence of effectors and subunit interactions of *Escherichia coli* carbamyl phosphate synthetase studied by differential scanning calorimetry. J. Biol. Chem. 268: 12504-12511.

Cervera, J., Bendala, E., Britton, H. G., Bueso, J., Nassif, Z., Lusty, C. J., Rubio, V. 1996. Photoaffinity labelling with UMP of lysine 992 of carbamyl phosphate synthetase from *Escherichia coli* allows identification of the binding site for the pyrimidine inhibitor. Biochemistry 35: 7247-7255.

Chaparian, M., Evans, D. 1991. The catalytic mechanism of the amidotransferase domain of the Syrian hamster multifunctional protein CAD. Evidence for a CAD-glutamyl covalent intermediate in the formation of carbamoyl phosphate. J. Biol. Chem. 266: 3387-3395.

Christoffels, V. M., van den Hoff M. J., Moorman, A. F., Lamers, W. H. 1995. The far-upstream enhancer of the carbamoyl-phosphate synthetase I gene is responsible for the tissue specificity and hormone inducibility of its expression. J. Biol. Chem. 270: 24932-40.

Christoffels, V. M., van den Hoff, M. J., Lamers, M. C., van Roon, M. A., de Boer, P. A., Moorman, A. F., Lamers, W. H. 1996. The upstream regulatory region of the carbamoyl-phosphate synthetase I gene controls its tissue-specific, developmental, and hormonal regulation in vivo. J. Biol. Chem. 271: 31243-50.

Christoffels, V. M., Habets, P. E., Das, A. T., Clout, D. E., van Roon, M. A., Moorman, A. F., Lamers, W. H. 2000. A single regulatory module of the carbamoylphosphate synthetase I gene executes its hepatic program of expression. J. Biol. Chem. 275, 40020-7.

Climent, I., Rubio, V. 1986. ATPase activity of biotin carboxylase provides evidence for initial activation by HCO3 by ATP in the carboxylation of biotin. Arch. Biochem. Biophys. 251: 465-470.

Cohen, S. N., Chang, A. C., Hsu, L. 1972. Nonchromosomal antibiotic resistance in bacteria: genetic transformation of *Escherichia coli* by R-factor DNA. Proc. Natl. Acad. Sci. USA 69: 2110-2114.

Coleman, P. F., Suttle, D. P., Satrk G. R. 1977. Purification from hamster cells of the multifunctional protein that initiates de novo synthesis of pyrimidine nucleotides. J. Biol. Chem. 252: 6379-6385.

Corvi, M. M., Carrie-Lynn, M. S., Berthiaume, L. G. 2001. Regulation of mitochondrial carbamoyl-phosphate synthetase 1 activity by active site fatty acid acylation. J. Biol. Chem. 276: 45704-45712.

Delannay, S., Charlier, D., Tricot, C., Villeret, V., Perard, A., Stalon, V. 1999. Serine 948 and Threonine 1042 are crucial residues for allosteric regulation of *Escherichia coli* carbamoylphosphate synthetase and illustrate coupling effects of activation and inhibition pathways. J. Mol. Biol. 286: 1217-1228.

DeLano, W. L. (2002) The PyMOL Molecular Graphics System. DeLano Scientific, Palo Alto, CA, USA. http://www.pymol.org.

Eather, G., Coman, D., Lander, C., McGill, J. 2006. Carbamyl phosphate synthase deficiency: diagnosed during pregnancy in a 41-year-old. J. Clin. Neurosci. 13: 702-6.

Eeds, A. M., Hall, L. D., Yadav, M., Willis, A., Summar, S., Putnam, A., Barr, F., Summar, M. L. 2006. The frequent observation of evidence for non-sense mediated decay in RNA from patints with carbamyl phosphate synthetase I deficiency. Mol. Genet. Metab. 89: 80-86.

Elpeleg, O. N., Colombo, J. P., Amir N., Bachmann, C., Hurvitz, H. 1990. Late-onset form of partial N-acetylglutamate synthetase deficiency. Eur. J. Pediatr. 149: 634-636.

Endo, F., Matsuura, T., Yanagita, K., Matsuda, I. 2004. Clinical manifestations of inborn errors of the urwea cycle and related metabolic disorders during childhood. J. Nutr. 134 (6 Suppl.): 1605S-1609S.

Evans, D. R., Balon, M. A. 1988. Controlled proteolysis of ammonia-dependent carbamoyl phopshate synthetase I from syrian hamster liver. Biochem. Biophys. Acta 953: 185-196.

Fan, Y., Lund, L., Yang, L., Raushel, F. M., Gao, Y. Q. 2008. Mechanism for the transport of ammonia within carbamoyl phosphate synthetase determined by molecular dynamics simulations. Biochemistry 47: 2935-2944.

Fan, Y., Lund, L., Shao, Q., Gao, Y. Q., Raushel, F. M. 2009. A combined theoretical and experimental study of the ammonia tunnel in carbamoyl phosphate synthetase. J. Am. Chem. Soc. 131: 10211-10219.

Fersht, A. 1977. Enzyme structure and mechanism. W. H. Freeman and Co., San Fransisco, CA.

Finkch, U., Kohlschütter, A., Schafer, H., Sperhake, K., Colombo, J. P., Gal, A. 1998. Prenatal diagnosis of carbamoyl phosphate synthetase I deficiency by identification of a missense mutation in *CPS1*. Hum. Mut. 12: 206-211.

Freeman, J. M., Nicholson, J. F., Schimke, R. T., Rowland, L. P., Carter, S. 1970. Congenital hyperammonemia: association with hyperglycinemia and decreased levels of carbamoyl phosphate synthetase. Arch. Neurol. 23: 430-437.

Fresquet V., Mora P., Rochera L., Ramón-Maiques S., Rubio V., Cervera J. 2000. Site-directed mutagenesis of the regulatory domain of Escherichia coli carbamoyl phosphate synthetase identifies crucial residues for allosteric regulation and for transduction of the regulatory signals. J. Mol. Biol. 299: 979-991.

Funghini, S., Donati, M. A., Pasquini, E., Zammarchi, E., Morrone, A. 2003. Structural organization of human carbamoyl phosphate synthetase I gene (*CPS1*). Hum. Mut. 22: 340-341.

Furchgott, R. F., Vanhoutte, P. M. 1989. Endothelium-derived relaxing and contracting factors. FASEB J. 3: 2007-2018.

Frye RA. 2000. Phylogenetic classification of prokaryotic and eukaryotic Sir2-like proteins. Biochem. Biophys. Res. Commun. 273: 793-798.

Gaasbeek Janzen, J. W., Lamers, W. H., Moorman, A. F., de Graaf, A., Los, J. A., Charles, R. 1984. Immunohistochemical localization of carbamoyl-

phosphate synthetase (ammonia) in adult rat liver; evidence for a heterogeneous distribution. J. Histochem. Cytochem. 32: 557-564.

Gaillard, S., Chang, S., Raushel, F. 1991. Role of the four conserved histidine residues in the amidotransferase domain of carbamoyl pshosphate synthetase. Biochemistry 30: 7901-7907.

Gebhardt, B., Dittrich, S., Parbel, S., Vlaho, S., Matsika, O., Bohles, H. 2005. N-carbamylglutamate protects patients with decompensated propionic aciduria from hyperammonaemia. J. Inherit. Metab. Dis. 28: 241-244.

Gewaltig, M. T., Kojda, G. 2002. Vasoprotection by nitric oxide: mechanisms and therapeutic potential. Cardiovasc. Res. 55: 250-260.

Gómez-López, L., Artuch, R., Vilaseca, M. A., Briones-Godino, P., Finckh, U., Pineda, M. 2008. Late-onset presentation of carbamoyl phosphate synthetase 1 deficiency in a 6-year-old boy. Rev. Neurol. 47: 500-501.

Grisolia, S., Cohen, P. 1948. The intermediate role of carbamoyl-l-glutamic acid in citrulline synthesis. J. Biol. Chem. 174: 389-390.

Grisolia, S., Cohen, P. P. 1953. Catalytic role of glutamate derivatives in citrulline biosynthesis. J. Biol. Chem. 204: 753-757.

Gropman, A. L., Summar, M., Leonard, J. V. 2007. Neurological implications of urea cycle disorders. J. Inherit. Metab. Dis. 30: 865-879.

Guadalajara, A., Grisolia, S., Rubio, V. 1987. Limited proteolysis reveals low-affinity binding of N-acetyl-L-glutamate to rat liver carbamoyl phosphate synthetase (ammonia). Eur. J. Biochem. 165: 163-169.

Guarente L. 2007. Sirtuins in aging and disease. Cold Spring Harb. Symp. Quant. Biol. 7: 483-488.

Guillou, F., Rubino, S. D., Markovitz, R. S., Kinney, D. M., Lusty, C. J. 1989. *Escherichia coli* carbamoyl-phosphate synthetase: Domains of glutaminase and synthetase subunit interaction. Proc. Natl. Acad. Sci. 86: 8304-8308.

Guthöhrlein, G., Knappe J. 1968. Structure and function of carbamoylphosphate synthase. I. Transitions between two catalytically inactive forms and the active form. Eur. J. Biochem. 7: 119-127.

Guy, H., Evans, D. 1997. Trapping an activated conformation of mammalian carbamoyl-phosphate synthetase. J. Biol. Chem. 272: 19906-19912.

Guy, H., Rotgeri, A., Evans, D. 1997. Activation by fusion of the glutaminase and synthetase subunits of *E.coli* carbamoyl-phosphate synthetase. J. Biol. Chem. 272: 19913-19918.

Hagopian K, Ramsey JJ, Weindruch R. 2003. Caloric restriction increases gluconeogenic and transaminase enzyme activities in mouse liver. Exp. Gerontol. 38: 267-278.

Hall, L., Metzenberg, R., Cohen, P. 1958. Isolation and characterization of a naturally occurring cofactor of carbamoyl phosphate biosynthesis. J. Biol. Chem. 230: 1013-1021.

Haraguchi, Y., Uchino, T., Takiguchi, M., Endo, F., Mori, M., Matsuda, I. 1991. Cloning and sequence of a cDNA encoding human carbamoyl phosphate synthetase I: molecular analysis of hyperammonemia. Gene 107: 335-340.

Hart, E. J., Powers-Lee, S. G. 2009. Role of Cys-1327 and Cys-1337 in redox sensitivity and allosteric monitoring in human carbamoyl phosphate synthetase. J. Biol. Chem. 284: 5977-5985.

Helbing, C. C., Atkinson, B. G. 1994. 3,5,3'-triiodothyronine-induced carbamoylphosphate synthetase gene expression is stabilized in the liver of *Rana cateisbeiana* tadpoles during heat shock. J. Biol. Chem. 269: 11743-11750.

Hinnie, J., Colombo, J. P., Wermuth, B., Dryburgh, F. J. 1997. N-Acetylglutamate synthetase deficiency responding to carbamylglutamate. J. Inherit. Metab. Dis. 20: 839-840.

Hitchman, R. B., Possee, R. D., King, L. A. Baculovirus expression systems for recombinant protein production in insect cells. 2009. Recent Patents on Biotechnology 3: 46-54.

Hong, J., Salo, W., Lusty, C., Anderson, P. 1994. Carbamyl phosphate synthetase III, an evolutionary intermediate in the transition between glutamine-dependent and ammonia-dependent carbamyl phosphate synthetases. J. Mol. Biol. 243: 131-140.

Honig, B., Nicholls, A. 1995. Classical electrostatics in biology and chemistry. Science 268: 1144-1149.

Horstmeyer, A., Cramer, H., Sauer, T., Müller-Esterl, W., Schroeder, C. 1996. Palmitoylation of endothelin receptor A. Differential modulation of signal transduction activity by post-translational modification. J. Biol. Chem. 271: 20811-20819.

Hoshide, R., Matsuura, T., Haraguchi, Y., Endo, F., Yoshinaga, M., Matsuda, I. 1993. One base substitution in an exon of the CPSI gene causes a 9-basepair deletion due to aberrant splicing. J. Clin. Invest. 91: 1884-1887.

Hoshide, R., Soejima, H., Ohta, T., Niikawa, N., Haraguchi, Y., Maatsura, T., Endo, F., Matsuda, I. 1995. Assignment of the human carbamoyl phosphate synthetase I gene (CPS1) to 2q35 by fluorescence *in Situ* hybridization. Genomics 28: 124-125.

Huang, X., Raushel, F. M. 2000. Role of the hinge loop linking the N- and C-terminal domains of the amidotransferase subunit of carbamoyl phosphate synthetase. Arch. Biochem. Biophys. 380: 174-180.

Huang, X., Raushel, F. M. 2000. Restricted passage of intermediates through the ammonia tunnel of carbamoyl phosphate synthetase. J. Biol. Chem. 34: 26233-26240.

Huang, X., Holden, H. M., Raushel, F. M. 2001. Channeling of substrates and intermediates in enzyme-catalyzed reactions. Annu. Rev. Biochem. 70: 149-80.

Hu, Y. C. 2008. Baculoviral vectors for gene delivery: a review. Curr. Gene Ther. 8: 54-65.

Huo, R., Zhu, H., Lu, L., Ying, L., Xu, M., Xu, Z., Li, J., Zhou, Z., Sha, J. 2005. Molecular cloning, identification and characteristics of a novel isoform of carbamyl phosphate synthetase I in human testis. J. Biochem. Mol. Biol. 38: 28-33.

Hyde, C., Ahmed, S., Padlan, E., Miles, E., Davies, D. 1988. Three-dimensional structureof the tryptophan synthetase $\alpha_2\beta_2$ multienzyme complex from *Salmonella typhimurium*. J. Biol. Chem. 263: 17857-17871.

Häberle, J., Scmidt, E., Pauli, S., Rapp, B., Christensen, E., Wermuth, B., Koch, H. G. 2003. Gene structure of human carbamoyl phosphate synthetase 1 and novel mutations in patients with neonatal onset. Hum. Mut. 21: 444-449.

Ihara, K., Miyako, K., Ishimura, M., Kuromaru, R., Wang, H.-Y., Yasuda, K., Hara, T. 2005. A case of hyperinsulinism/hyperammonaemia syndrome with reduced carbamoyl-phosphate synthetase-1 activity in liver: A pitfall in enzymatic diagnosis for hyperammonaemia. J. Inherit. Metab. Dis. 28: 681-687.

Imai, S., Armstrong, C. M., Kaeberlein, M., Guarente, L. 2000. Transcriptional silencing and longevity protein Sir2 is an NAD-dependent histone deacetylase. Nature 403 : 795-800.

Jaquet, L., Serre, V., Lollier, M., Penverne, B., Hervé, G., Souciet, J. L., Potier, S. 1995. Allosteric regulation of carbamoylphosphate synthetase-aspartate transcarbamylase multifunctional protein of Saccharomyces cerevisiae: selection, mapping and identification of missense mutations define three regions involved in feedback inhibition by UTP. J. Mol. Biol. 248: 639-52.

Javid-Majd, F., Stapleton, M. A., Harmon, M. F., Hanks, B. A., Mullins, L. S., Raushel, F. M. 1996. Comparison of the functional differences for the homologous residues within the carboxy phosphate and carbamate domains of carbamoyl phosphate synthetase. Biochemistry 35: 14362-14369.

Johnson, J. L., West, J. K., Nelson, A. D. L., Reinhart, G. D. 2007. Resolving the fluorescence response of *E. Coli* carbamoyl phosphate synthetase: mapping intra- and inter-subunit conformational changes. Biochemistry 46: 387-397.

Jones, M. E., Lipmann, F. 1960. Chemical and enzymatic synthesis of carbamyl phosphate. Proc. Natl. Acad. Sci. USA 46: 1194-1205.

Jones, M. E. 1976. Partial reactions of Carbamyl-P synthetase: A review and an inquiry into the role of carbamate. In The Urea Cycle (Grisolía, S., Báguena, R., Mayor, F., eds.), pp. 107-122, John Wiley and Sons, New York.

Jones, M. E. 1980. Pyrimidine nucleotide biosynthesis in animals: genes, enzymes, and regulation of UMP biosynthesis. Annu. Rev. Biochem. 49: 253-279.

Julsrud, E., Walsh, P., Anderson, P. 1998. *N*-acetyl-L-glutamate and the urea cycle in gulf toadfish (*Opsanus beta*) and other fish. Arch. Biochem. Biophys. 350: 55-60.

Kalman, S., Diffield, P., Brzozozwski, T. 1966. Purification and properties of a bacterial carbamoyl phosphate synthetase. J. Biol. Chem. 241: 1871-1877.

Keskinen, P., Siitonen, A., Salo, M. 2008. Hereditary urea cycle diseases in Finland. Acta Paediatr. 97: 1412-1419.

Khayat, M. 2009. Novel human pathological mutations. Gene symbol: CPS1. Disease: carbamoyl phosphate synthetase I deficiency. Hum. Genet. 125: 336.

Kim, J., Howell, S., Huang, X., Raushel, F. 2002. Structural defects within the carbamate tunnel of carbamoyl phosphate synthetase. Biochemistry 41: 12575-12581.

Kim, J., Raushel, F. 2004. Access to the carbamate tunnel of carbamoyl phosphate synthetase. Arch. Biochem. Biophys. 425: 33-41.

Kim, J., Raushel, F. 2004. Perforation of the tunnel wall in carbamoyl phosphate synthetase derails the passage of ammonia between sequential active sites. Biochemistry 43: 5334-5340.

Kirchner, H., Gutierrez, J. A., Solenberg, P. J., Pfluger, P. T., Czyzyk, T. A., Willency, J. A., Schürmann, A., Joost, H. G., Jandacek, R. J., Hale, J. E., Heiman, M. L., Tschöp, M. H. 2009. GOAT links dietary lipids with the endocrine control of energy balance. Nat. Med. 15: 741-745.

Kingston, R. E., Chen, C. A., Okayama, H. 2003. Calcium phosphate transfection. Curr. Protoc. Cell Biol. Chapter 20: Unit 20. 3.

Kiss-Toth, E., Dower, S. K., Sayers, J. R. 2000. A method for enhancing transfection efficiency of minipreps obtained from plasmid cDNA libaries. Anal. Biochem. 288: 230-232.

Kleywegt, G., Jones, T. 1994. Detection, delineation, measurement and display of cavities in macromolecular structures. Acta Cryst. D50: 178-185.

Krahn, J., Kim, J., Burns, M., Parry, R., Zalkin, H., Smith, J. 1997. Coupled formation of an amidotransferase interdomain ammonia channel and a phosphoribosyltransferase active site. Biochemistry 36: 11061-11068.

Kurokawa, K., Yorifuji, T., Kawai, M., Momoi, T., Nagasaka, H., Takayanagi, M., Kobayashi, K., Yoshino, M., Kosho, T., Adachi, M., Otsuka, H., Yamamoto, S., Murata, T., Suenaga, A., Ishii, T., Terada, K., Shimura, N., Kiwaki, K., Shintaku, H., Yamakawa, M., Nakabayashi, H., Wakutani, Y., Nakahata, T. 2007. Molecular and clinical analyses of Japanese patients with carbamoyl phosphate synthetase I (CPS1) deficiency. J. Hum. Genet. 52: 349-354.

Laemmli, U. K. 1970. Cleavage of structural proteins during the assembly of the head of bacteriophage T4. Nature 227: 680–685.

Laskowski, R. A., Rullmannn, J. A., MacArthur, M. W., Kaptein, R., Thornton, J. M. 1996. AQUA and PROCHECK-NMR: programs for checking the quality of protein structures solved by NMR. J. Biomol. NMR 8: 477-86.

Lehninger, A. L., Nelson, D. L., Cox, M. M. 2005. Lehninger Principles of Biochemistry (4th Ed.): W H Freeman & Co.

Leonard, J., Platt, M., Morris, A. 2008. Hypothesis: proposals for the management of a neonate at risk of hyperammonemia due to a urea cycle disorder. Eur. J. Pediatr. 167: 305-309.

Lim, A. L., Powers-Lee, S. G. 1996. Requirement for the carboxyl-terminal domain of Saccharomyces cerevisiae carbamoyl-phosphate synthetase. J. Biol. Chem. 271: 11400-9.

Lim, A., Powers-Lee, S. G. 1997. Critical roles for arginine 1061/1060 and tyrosine 1057 in *Saccharomyces cerevisiae* arginine-specific carbamoyl-phosphate synthetase. Arch. Biochem. Biophys. 339: 344-352.

Liu, X., Guy, H. I., Evans D. R. 1994. Identification of the regulatory domain of the mammalian multifunctional protein CAD by the construction of an *Escherichia coli* hamster hybrid carbamyl-phosphate synthetase. J. Biol. Chem. 269: 27747-27755.

Loscalzo, M. L., Galczynski, R. L., Hamosh, A., Summar, M. L., Chinsky, J. M., Thomas, G. H. 2004. Interstitial deletion of chromosome 2q32-34 associated with multiple congenital anomalies and urea cycle defect (CPSI deficiency). Am. J. Med. Genet. 128A: 311-315.

Lund, L., Fan, Y., Shao, Q., Gao, Y. Q., Raushel, F. M. 2010. Carbamate transport in carbamoyl phosphate synthetase: a theoretical and experimental investigation. J. Am. Chem. Soc. 132: 3870-3878.

Lusty, C. J. 1983. The molecular structure and function of carbamyl phosphate synthetase I. Trans N Y Acad Sci 41, 103-115.

Mareya, S., Raushel, F. 1994. A molecular wedge for triggering the amidotransferase activity of carbamoyl phosphate synthetase. Biochemistry 33: 2945-2950.

Mareya, S., M., Raushel, F. M. 1995. Mapping the structural domains of *E.coli* carbamoyl phosphate synthetase using limited proteolysis. Bioorg. Med. Chem. 3: 525-532.

Marshall M., Cohen P. P. 1972. Ornithine transcarbamylase from *Streptococcus faecalis* and bovine liver. I. Isolation and subunit structure. J. Biol. Chem. 247: 1641-1653.

Marshall, M., Fahien, L. A. 1988. Proteolysis as a probe of ligand-associated conformational changes in rat carbamoyl phosphate synthetase I. Arch. Biochem. Biophys. 262: 455-470.

Marshall, E. 1999. Clinical trials: Gene therapy death prompts review of adenovirus vector. Science 286: 2244-2245.

McReynolds, J. W., Crowley, B., Mahoney, M. J., Rosenberg, L. E. 1981. Autosomal recessive inheritance of human mitochondrial carbamoyl phosphate synthetase deficiency. Am. J. Hum. Genet. 33: 345-353.

Meister, A. 1989. Mechanism and regulation of the glutamine-dependent carbamoyl phosphate synthetase of *Escherichia coli*. Adv. Enzymol. Relat. Areas Mol. Biol. 62: 315-374.

Mergeay, M., Gigot, D., Beckmann, J., Glansdorff, N., Pierard, A. 1974. Physiology and genetics of carbamoylphosphate synthesis in *Escherichia coli* K-12. Mol. Gen. Genet. 133: 299-316.

Miran, S., Change, S., Raushel, F. 1991. The role of the four conserved histidine residues in the amidotransferase domain of carbamoyl phosphate synthetase. Biochemistry 30: 7901-7907.

Mitchell, S., Ellingson, C., Coyne, T., Hall, L., Neill, M., Christian, N., Higham, C., Dobrowolski, S. F., Tuchman, M., Summar, M.; Urea Cycle Disorder Consortium. 2009. Genetic variation in the urea cycle: a model resource for

investigating key candidate genes for common diseases. Hum. Mutat. 30: 56-60.

Mommsen, T. P., Walsh, P. J. 1989. Evolution of urea synthesis in vertebrates: the piscine connection. Science 243: 72-75.

Moonen, R. M., Paulussen, A. D., Souren, N. Y., Kessels, A. G., Rubio-Gozalbo, M. E., Villamor, E. 2007. Carbamoyl phosphate synthetase polymorphism as a risk factor for necrotizing enetrocolitis. Pediatr. Res. 62: 1-3.

Mora, P., Rubio, V., Fresquet, V., Cervera, J. 1999. Localization of the site for the nucleotide effectors of *Escherichia coli* carbamoyl phosphate synthetase using site-directed mutagenesis. FEBS Letters 446: 133-136.

Morizono, H., Caldovic, L., Shi, D., Tuchman, M. 2004.Mammalian N-acetylglutamate synthase. Mol. Genet. Metab. 81: S4-11.

Morrow, J. K. 2008. Optimizing transient gene expression. Gen. Eng. News. 28: online.

Moscioni, D., Morizono, H., McCarter, R. J., Stern, A., Cabrera-Luque, J., Hoang, A., Sanmiguel, J., Wu, D., Bell, P., Gao, G. P., Raper, S. E., Wilson, J. M., Batshaw, M. L. 2006. Long-term correction of ammonia metabolism and prolonged survival of ornithine transcarbamoylase-deficient mice following liver-directed treatment with adeno-associated viral vectors. Mol. Ther. 14: 25-33.

Mouilleron, S., Golinelli-Pimpaneau, B. 2007. Conformational changes in ammonia-channeling glutamine amidotransferases. Curr. Opin. Struct. Biol. 17: 653-664.

Msall, M., Batshaw, M. L., Suss, R., Brusilow, S. W., Mellits, E. D. 1984. Neurologic outcome in children with inborn errors of urea synthesis. Outcome of urea cycle enzymopathies. N. Engl. J. Med. 310: 1500-1505.

Mullins, L., Raushel, F. 1999. Channeling of ammonia through the intermolecular tunnel contained within carbamoyl phosphate synthetase. J. Am. Chem. Soc. 121: 3803-3804.

Murzin A. G. 1999. Structure classification-based assessment of CASP3 predictions for the fold recognition targets. Proteins Suppl 3: 88-103.

Nagata, N., Matsuda, I., Oyanagi, K. 1991. Estimated frequency of urea cycle enzymopathies in Japan. Am. J. Med. Genet. 39: 228-229.

Nakagawa, T., Lomb, D. J., Haigis, M. C., Guarente, L. 2009. SIRT5 Deacetylates carbamoyl phosphate synthetase 1 and regulates the urea cycle. Cell 137: 560-570.

Nara, T., Gao, G., Yamasaki, H., Nakama-Shimada, J., Aoki, T. 1998. Carbamoyl-phosphate synthetase II in kinetoplasts. Biochim. Biophys. Acta 1387: 462-468.

Nguyen, M., Argan, C., Lusty, C., Shore, G. 1986. Import and Processing of hybrid proteins by mammalian mitochondria in vitro. J. Biol. Chem. 261: 800-805.

Norenberg, M. D., Rao, K. V., Jayakumar, A. R. 2005. Mechanisms of ammonia-induced astrocyte-swelling. Metab. Brain Dis. 20: 303-318.

Nunoya, H., Lusty, C. J. 1983. The *carB* gene of *Escherichia coli*: a duplicated gene coding for a large subunit of carbamoyl-phosphate synthetase. Proc. Natl. Acad. Sci. USA 80: 4629-4633.

Nunoya H, Broglie K. E., Widgren E. E., Lusty C. J. 1985. Characterization and derivation of the gene coding for mitochondrial carbamyl phosphate synthetase I of rat. J. Biol. Chem. 260: 9346-9356.

Nuzum C. T., Snodgrass P. J. 1976. Multiple assays of the five urea-cycle enzymes in human liver homogenates. In The urea cycle (Grisolía S, Báguena R, Mayor F, eds) 325-349, John Wiley and sons, New York.

Ogita, T., Knowless, J. R. 1988. On the intermediacy of carboxyphosphate in biotin-dependent carboxylations. Biochemisrtry 27: 8028-8033.

Ono, H., Suto, T., Kinoshita, Y., Sakano, T., Furue, T., Ohta, T. 2009. A case of carbamoyl phosphate synthetase 1 deficiency presenting symptoms at one month of age. Brain. Dev. 31 : 779-781

O´Reilly D. R., Miller, L. K., Luckow, V. A. 1992. Baculovirus expression vectors: A laboratory manual (New York, NY.: WH Freeman and company).

Palmer, R. M., Ferrige, A. G., Moncada, S. 1987. Nitric oxide release accounts for the biological activity of endothelium-relaxing factor. Nature 327: 524-526.

Palmer, R. M., Ashton, D. S., Moncada, S. 1988. Vascular endothelial cells synthesize nitric oxide from L-arginine. Nature 333: 664-666.

Park, H. S., Kim, I. H., Kim, I. Y., Kim, K. I., Kim, H. J. 2000. Expression of carbamoyl phosphate synthetase I and ornithine transcarbamoylase genes in Chinese hamster ovary *dhfr*-cells decreases accumulation of ammonium ion in culture media. J. Biotechnol. 81: 129-140.

Paulus, T. J., Switzer, R. L. 1979. Synthesis and inactivation of carbamyl phosphate synthetase isozymes of Bacillus subtilis during growth and sporulation. J. Bacteriol. 140: 769-73.

Pearson, D. L., Dawling, S., Walsh, W. F., Haines, J., Christman, B., Bazyk, A., Scott, N., Summar, M. L. 2001. Neonatal pulmonary hypertension. N. Engl. J. Med. 344: 1832-1838.

Penefsky, H. S. 1977. Reversible binding of Pi by beef heart mitochondrial adenosine triphosphatase. J. Biol. Chem. 252: 2891-2899.

Pérez-Chacón, G., Astudillo, A. M., Ruipérez, V., Balboa, M. A., Balsinde, J. 2010. Signaling role for lysophosphatidylcholine acyltransferase 3 in receptor-regulated arachidonic acid reacylation reactions in human monocytes. J. Immunol. 184: 1071-1078

Perkins, D. N., Pappin, D. J. C., Creasy, D. M., Cottrell, J. S. 1999. Probability-based protein identification by searching sequence databases using mass spectrometry data. Electrophoresis 20: 3351-3367.

Pierrat, O. & Raushel, F. 2002. A functional analysis of the allosteric nucleotide monophosphate binding site of carbamoyl phosphate synthetase. Arch. Biochem. Biophys 400: 34-42.

Pierrat, O., Javied-Majd, F., Raushel, F. 2002. Dissection of the conduit for allosteric control of carbamoyl phosphate synthetase by ornithine. Arch. Biochem. Biophys 400: 26-33.

Post, L. E., Post D. J., Raushel, F. M. 1990. Dissection of the functional domains of *Escherichia coli* carbamoyl phosphate synthetase by site-directed mutagenesis. J. Biol. Chem. 265: 7742-7747.

Potter, M. D., Powers-Lee, S. G. 1992.Location of the ATP gamma-phosphate-binding sites on rat liver carbamoyl-phosphate synthetase I. Studies with the ATP analog 5'-p-fluorosulfonylbenzoyladenosine. J. Biol. Chem. 267: 2023-2031.

Potter, M., Powers-Lee, S. 1993. Direct photoaffinity labelling of rat liver carbamoyl phosphate synthetase I with ATP. Arch. Biochem. Biophys. 306: 377-382.

Powers, S. G., Meister, A. 1978. Carbonic-phosphoric anhydride (carboxy phosphate. Significance in catalysis and regulation of glutamine-dependent carbamyl phosphate synthetase. J. Biol. Chem. 253: 1258-65.

Powers-Lee, S. & Corina, K. 1986. Domain structure of rat liver carbamoyl phosphate synthetase I. J. Biol. Chem. 261: 15349-15352.

Rapp, B., Häberle, J., Linnebank, M., Wermuth; B., Marquardt, T., Harms, E., Koch, H. G. 2001. Genetic analysis of carbamoyl phosphate synthetase I and ornitine transcarbamoylase deficiency using fibroblasts. Eur. J. Pediatr. 160: 283-287.

Ratner, S. 1973. Enzymes of arginine and urea synthesis. Adv. Enzymol. Relat. Areas Mol. Biol. 39: 1-90.

Raushel, F. M., Thoden, J. B., Holden, H. M. 1999. The amidotransferase family of enzymes: molecular machines for the production and delivery of ammonia. Biochemistry 38: 7891-7899.

Rochera, L., Fresquet, V., Rubio, V., Cervera, J. 2002. Mechanism of allosteric modulation of *Esterichia coli* carbamoyl phosphate synthetase probed by site-directed mutagénesis of ornithine site residues. FEBS Letters 514: 323-328.

Rodriguez-Aparicio, L., Guadalajara, A., Rubio, V. 1989. Physical location of the site for N-acetyl-L-glutamate, the allosteric activator of carbamoyl phosphate synthetase, in the 20-kilodalton COOH-terminal domain. Biochemistry 28: 3070-3074.

Rubino, S. D., Nunoya, H., Lusty, C. J., 1986. Catalytic domains of carbamoyl phosphate synthetase. Glutamine-hydrolyzing site of *Escherichia coli* carbamoyl phosphate synthetase. J. Biol. Chem. 261: 11320-11327.

Rubio, V., Grisolia, S. 1977. Mechanism of mitochondrial carbamoyl-phosphate synthetase: synthesis and properties of active CO2, precursor of carbamoyl phosphate. Biochemistry 16: 321-329.

Rubio, V., Britton, H. G., Grisolia, S. 1979. Mechanism of carbamoyl-phosphate synthetase. Binding of ATP by the rat-liver mitochondrial enzyme. Eur. J. Biochem. 93: 245-256.

Rubio, V., Britton, H. G., Grisolia, S. 1983. Mitochondrial carbamoyl phosphate synthetase activity in the absence of N-acetyl-L-glutamate. Mechanism of activation by this cofactor. Eur. J. Biochem. 134: 337-343.

Rubio, V., Cervera, J., Lusty, C. J., Bendala, E., Britton H., G. 1991. Domain structure of the large subunit of *Escherichia coli* carbamoyl phosphate

synthetase. Location of the binding sites for the allosteric inhibitor UMP in the COOH-terminal domain. Biochemistry 30: 1068-1075.

Rubio, V. 1993. Structure activity correlations in carbamoyl phosphate synthetases. In Carbon dioxide fixation and reduction in biological and model systems (Bräden, C. I., Schneider, G., eds. 294-264. Oxford University Press. London.

Rubio, V., Cervera, J. 1995. The carbamoyl-phosphate synthetase family and carbamate kinase: structure-function studies. Biochem. Soc. Trans. 23: 879-883.

Russell, W. C. 2000. Update on adenovirus and its vectors. J. Gen. Virol. 81: 2573-2604.

Saadat, D., Harrison, D. 1999. The crystal structure of of methylglyoxal synthetase from *Escherichia coli*. Structure 7: 309-317.

Saeed-Koethe, A., Powers-Lee, S. G. 2002. Specificity determining residues in ammonia- and glutamine-dependent carbamoyl phosphate synthetases. J. Biol. Chem. 277: 7231-7238.

Saeed-Koethe, A., Powers-Lee, S. G. 2003. Gain of glutaminase function in mutants of ammonia-specific frog carbamoylphosphate synthetase. J. Biol. Chem. 278: 26722-26726.

Sali, A., Blundell, T. L. 1993. Comparative protein modelling by satisfaction of spatial restraints. J. Mol. Biol. 234: 779-815.

Sambrook, J., Fritsch, E. F., Maniatis, T., in Molecular Cloning: A Laboratory Manual. Cold Spring Harbor Laboratory Press, NY, Vol. 1, 2, 3 (1989).

Scaglia, F., Brunetti-Pierri, N., Kleppe, S., Marini, J., Carter, S., Garlick, P., Jahoor, F., O'Brien, W., Lee, B. 2004. Clinical consequences of urea cycle enzyme deficiencies and potential links to arginine and nitric oxide metabolism. J. Nutr. 134 (6 Suppl.): 1605S-1609S.

Scaglia, F., Carter, S., O'Brien, W. E., Lee, B. 2004. Effect of alternative pathway therapy on branched chain amino acid metabolism in urea cycle disorder patients. Mol. Genet. Metab. 81 (Suppl 1): S79-85.

Schevchenko, A., Jensen, O. N., Podtelejnikov, A. V., Sagliocco, F., Wilm, M., Vorm, O., Mortensen, P., Boucherie, H., Mann, M. 1996 Linking genome and proteome by mass spectrometry: large-scale identification of yeast proteins from two dimensional gels. Proc. Natl. Acad. Sci. USA 93: 14440-14445.

Serre, V., Penverne, B., Souciet, J. L., Potier, S., Guy, H., Evans, D., Vicart, P., Hervé, G. 2004. Integrated allosteric regulation in the S. cerevisiae carbamylphosphate synthetase – aspartate transcarbamylase multifunctional protein. BMC Biochem. 5: 5-6.

Simmer, J. P., Kelly, R. E., Rinker, A. G., Scully, J. L., Evans, D. R. 1990 Mammalian carbamoyl phosphate synthetase cDNA sequence and evolution of the multidomain of the Syrian hamster multifunctional protein CAD. J. Biol. Chem. 265: 10395-10402.

Simmons, C. Q., Simmons, A. J., Haubner, A., Ream, A., Davidson, J. N. 2004. Substitutions in hamster CAD carbamoyl-phosphate synthetase alter

allosteric response to 5-phosphoribosyl-alpha-pyrophosphate (PRPP) and UTP. Biochem. J. 378: 991-998.

Stapleton, M. A., Javid-Majd, F., Harmon, M. F., Hanks, B. A., Grahmann, J. L., Mullins, L. S., Raushel, F. M. Role of conserved residues within the carboxy phosphate domain of carbamoyl phosphate synthetase. Biochemistry 35: 14352-14361.

Summar, M. L., Dasouki, M. J., Schofield, P. J., Krishnamani, M. R. S., Vnenack-Jones, C., Tuchman, M., *et al*. 1995. Physical and linkage mapping of human carbamoyl phosphate synthetase I and reassignment from 2p to 2q35. Cytogenet. Cell Genet. 71: 266-267.

Summar, M. L. 1998. Molecular genetic research into carbamoyl phosphate synthetase I: molecular defects and linkage markers. J. Inherit. Metab. Dis. 2: 30-39.

Summar, M. L., Hall, L. D., Eeds, A., Hutcheson, H. B., Kuo, A. N., Willis, A. S., Rubio, V., Arvin, M. K., Schofield, J. P., Dawson, E. P. 2003. Characterization of genomic structure and polymorphisms in the human carbamoyl phosphate synthetase I gene. Gene 311: 51-57.

Summar, M. L., Hall, L., Christman, B., Barr, F., Smith, H., Kallianpur, A., Brown, N., Yadav, M., Willis, A., Eeds, A., Cermak, E., Summar, S., Wilson, A., Arvin, M., Putnam, A., Wills, M., Cunningham, G. 2004. Environmentally determined genetic expression: clinical correlates with molecular variants of carbamyl phosphate synthetase I. Mol. Genet. Metab. 81 Suppl.: 12-19.

Summar M. L., Gainer, J. V., Pretorius, M., Malave, H., Harris, S., Hall, L. D. Weisberg, A., Vaughan, D. E., Christman, B. W., Brown, N. J. 2004. Relationship between carbamoyl-phosphate synthetase genotype and systemic vascular function. Hypertension 43: 1-6.

Summers, M. D. 2006. Milestones leading to the genetic engineering of baculoviruses as expression vector systems and viral pesticides. Adv. Virus. Res. 68: 3-73.

Thoden, J. B., Holden, H. M., Wesenberg, G., Raushel, F. M., Rayment, I. 1997. Structure of carbamoyl phosphate synthetase: a journey of 96 Å from substrate to product. Biochemistry 36: 6305-6313.

Thoden, J. B., Miran, S. G., Phillips, J. C., Howard, A. J., Raushel, F. M., Holden H. M. 1998. Carbamoyl phosphate synthetase: caught in the act of glutaminase hydrolysis. Biochemistry 37: 8825-8831.

Thoden, J. B., Raushel, F. M., Benning, M., Rayment, I., Holden, H. M. 1999. The structure of carbamoyl phosphate synthetase determined to 2.1 Å resolution. Acta Cryst. D55: 8-24.

Thoden, J. B., Raushel, F. M., Wesenberg, G., Holden, H. M. 1999. The binding of inosine monophosphate to *Escherichia coli* carbamoyl phosphate synthetase. J. Biol. Chem. 274: 22502-22507.

Thoden, J. B., Wesenberg, G., Raushel, F. M, Holden, H.M. 1999. Carbamoyl phosphate synthetase: closure of the B-domain as a result of nucleotide binding. Biochemistry 38: 2347-2357.

Thoden, J., Huang, Y., Raushel, F. M., Holden, H. M 2002. Carbamoyl-phosphate synthetase: creation of an escape route for ammonia. J. Biol. Chem. 277: 39722-39727.

Thoden, J. B., Huang, X., Kim, J., Raushel, F. M., Holden, H.M. 2004. Long-range allosteric transitions in carbamoyl phosphate synthetase. Protein Sci. 13: 2398-405.

Thompson, J. D., Higgins, D. G., Gibson, T. J. 1994. CLUSTALW: improving the sensitivity of progressive multiple sequence alignments through sequence weighting, position specific gap penalities and weight matrix choice. Nucleic Acids Res. 22: 4673-4680.

Trammel, P. R., Campbell, J. W. 1970. Carbamyl phosphate synthesis in land snail *Strophocheilus oblongus*. J. Biol. Chem. 245: 6634-6641.

Trammel, P. R., Campbell, J. W. 1971. Carbamyl phosphate synthesis in invertebrates. Comp. Biochem. Physiol. 40B: 395-406.

Trotta, P., Burt, M., Haschemeyer, R., Meister, A. 1971. Reversible dissociation of carbamoyl phosphate synthetase into a regukated synthesis subunited and a subunit required for glutamine utilization. Proc. Natl. Acad. Sci. USA 68: 2599-2603.

Uchino, T., Endo, F., Matsuda, I. 1998. Neurodevelopmental outcome of long-term therapy of urea cycle disorders in Japan. J. Inherit. Metab. Dis. 21 (Suppl1): 151-159.

Vanoni, M. A., Curti, B. 2008. Structure-function studies of glutamate synthases: a class of self-regulated iron-sulfur flavoenzymes essential for nitrogen assimilation. IUBMB Life 60: 287-300.

Vaughn, J. L., Godwin, R. H., Tompkins, G. J., McCawley, P. 1977. The establishment of two cell lines from the insect Spodoptera frugiperda (Lepidoptera; Notuidae). In vitro 13: 213-217.

Verbiest, H. B., Straver, J. S., Colombo, J. B., van deer Vijver, J. C., van deer Woerkom, T. C. 1992. Carbamyl phosphate synthetase-1 deficiency discovered after valproic acid-induced coma. Acta Neurol. Scand. 86: 275-279.

Verdonk, M. L., Cole, J. C., Hartshorn, M. J., Murray, C. W., Taylor, R. D. 2003. Improved protein-ligand docking using GOLD. Proteins 52: 609-623.

Wakutani, Y., Nakayasu, H., Takeshima, T., Adachi, M., Kawataki, M., Kihira, K., Sawada, H., Bonno, M., Yamamoto, H., Nakashima, K. 2004. Mutational analysis of carbamoyl phosphate synthetase I deficiency in three Japanese patients. J. Inherit. Metab. Dis. 27: 787-788.

Waldrop, G. L., Rayment, I., Holden, H. M. 1994. Three-dimensional structure of biotin-carboxylase subunit of acetyl-CoA carboxylase. Biochemistry 33: 10249-10256.

Wallace, A. C., Laskowski, R. A., Thornton, J. M. 1995. LIGPLOT: a program to generate schematic diagrams of protein-ligand interactions. Prot. Eng. 8: 127-134.

Yefimenko, I., Fresquet, V., Marco-Marin, C., Rubio, V., Cervera, J. 2005. Understanding carbamoyl phosphate synthetase deficiency: impact of clinical mutations on enzyme functionality. J. Mol. Biol. 349: 127-141.

Zalkin, H., Smith, J. 1998. Enzymes utilizing glutamine as an amide donor. Adv. Enzymol. Rel. Areas Mol. Biol. 72: 87-144.

Zimmer, K., Bendiks, M., Mori, M., Kominami, E., Robinson, M. B., Ye, X., Wilson, J. M. 1999. Efficient mitochondrial import of newly synthesized ornithine transcarbamylase (OTC) and correction of secondary metabolic alterations in spf^{ash} mice following gene therapy of OTC deficiency. Mol. Med. 5: 244-253.

Wong, L. J., Craigen, W. E., O'Brien, W. E. 1994. Post-partum coma and death due to carbamoyl-phosphate siéntase I deficiency. Ann. Intern. Med. 120: 216-217.

ORIGINAL PAPERS

I

STRUCTURAL INSIGHT ON THE CONTROL OF UREA SYNTHESIS: IDENTIFICATION OF THE BINDING SITE FOR N-ACETYL-L-GLUTAMATE, THE ESSENTIAL ALLOSTERIC ACTIVATOR OF MITOCHONDRIAL CARBAMOYL PHOSPHATE SYNTHETASE

by

Satu Pekkala, Ana Martínez, Belén Barcelona, José Gallego, Elena Bendala, Igor Yefimenko, Vicente Rubio & Javier Cervera 2009

Biochemical Journal 424: 211-220

https://doi.org/10.1042/BJ20090888

II

UNDERSTANDING CARBAMOYL-PHOSPHATE SYNTHETASE I (CPS1) DEFICIENCY BY USING EXPRESSION STUDIES AND STRUCTURE-BASED ANALYSIS

by

Satu Pekkala, Ana Martínez, Belén Barcelona, Igor Yefimenko, Ulrich Finckh, Vicente Rubio & Javier Cervera 2010

Human Mutation 31(7): 801–808

https://doi.org/10.1002/humu.21272

III

TOWARDS UNDERSTANDING OF ALLOSTERIC SIGNAL TRANSMISSION IN CARBAMOYL PHOSPHATE SYNTHETASE I

by

Satu Pekkala, Ana Martínez, Belén Barcelona & Javier Cervera 2010

Manuscript

https://doi.org/10.1002/humu.22349